

DALHOUSIE UNIVERSITY

Identifying clast species to define the upper age-bracket of  
the Claremont conglomerate, Eastern Cobequid Highlands,  
Nova Scotia

---

B.Sc. Honours Thesis

Camille M. Malcolm

04/28/2016

## Distribution License

DalSpace requires agreement to this non-exclusive distribution license before your item can appear on DalSpace.

### NON-EXCLUSIVE DISTRIBUTION LICENSE

You (the author(s) or copyright owner) grant to Dalhousie University the non-exclusive right to reproduce and distribute your submission worldwide in any medium.

You agree that Dalhousie University may, without changing the content, reformat the submission for the purpose of preservation.

You also agree that Dalhousie University may keep more than one copy of this submission for purposes of security, back-up and preservation.

You agree that the submission is your original work, and that you have the right to grant the rights contained in this license. You also agree that your submission does not, to the best of your knowledge, infringe upon anyone's copyright.

If the submission contains material for which you do not hold copyright, you agree that you have obtained the unrestricted permission of the copyright owner to grant Dalhousie University the rights required by this license, and that such third-party owned material is clearly identified and acknowledged within the text or content of the submission.

If the submission is based upon work that has been sponsored or supported by an agency or organization other than Dalhousie University, you assert that you have fulfilled any right of review or other obligations required by such contract or agreement.

Dalhousie University will clearly identify your name(s) as the author(s) or owner(s) of the submission, and will not make any alteration to the content of the files that you have submitted.

If you have questions regarding this license please contact the repository manager at [dalspace@dal.ca](mailto:dalspace@dal.ca).

Grant the distribution license by signing and dating below.

---

Name of signatory

---

Date

## ABSTRACT

The structural complexities of the Cobequid Highlands, NS caused by the Acadian orogeny restricts the ability to date sedimentary units therein. Accurate dating requires extensive geochemical analyses or is limited to homogenous, unaltered material. The aim of this thesis is to investigate the potential of using conglomeratic clasts to bracket the age of the Claremont conglomerate in the Eastern Cobequid Highlands. This is attempted by identifying the suites of clasts present in the conglomerate using petrography and XRF geochemistry to correlate the clasts to proximal units of known age. Due to data and time limitations, this thesis focuses on the upper age-bracket of the Claremont conglomerate. The Claremont conglomerate consists of volcanic, siltstone and limestone clasts. The clasts were divided into three groups: mafic, felsic and sedimentary. These correlated with the Diamond Brook-Byers Brook Formation and Wilson Brook Formation. The presence of red siltstones, unique to the Diamond Brook Formation, determined the youngest age for the clasts:  $348 \pm 3$  Ma. The Wilson Brook Formation is the suspected source of the group of sedimentary clasts. The upper age bracket for the Claremont conglomerate is thus set to  $348 \pm 3$  Ma which is consistent with the stratigraphic constraint imposed by the Boss Point Formation (320 Ma).

## TABLE OF CONTENTS

ABSTRACT	i
LIST OF FIGURES	iv
LIST OF TABLES	v
TABLE OF MINERAL ABBREVIATIONS	vi
ACKNOWLEDGEMENTS	vii
CHAPTER 1: INTRODUCTION	
1.1 Introduction	1
CHAPTER 2: GEOLOGICAL SETTING AND STUDY AREA	
2.1 Geological Setting	4
2.2 Study Area	7
2.3 Previous Work	8
2.3.1 Descriptions of Proximal Formations	8
2.3.2 Conglomerate Age-Dating Techniques	15
CHAPTER 3: FIELD OBSERVATIONS	
3.1 Sampling Methods	18
3.2 Balmoral Mills Outcrop	19
3.3 Core	23
CHAPTER 4: PETROGRAPHY OF CONGLOMERATIC CLASTS	
4.1 Thin Sections	32
4.1.1 Methods	32
4.1.2 Results	32
4.2 Microprobe	37
4.2.1 Methods	37
4.2.2 Results	38
CHAPTER 5: GEOCHEMISTRY OF CONGLOMERATIC CLASTS	
5.1 Methods	39
5.2 Results	41
CHAPTER 6: COMPARATIVE ANALYSIS TO POSSIBLE SOURCE ROCKS	



6.1 Geochemistry	48
6.1.1 Introduction	48
6.1.2 Results and Discussion	50
6.2 Hand Sample Comparison	58
6.2.1 Introduction	58
6.2.2 Results and Discussion	58
CHAPTER 7: SYNTHESIS	
7.1 Clast Species	63
7.2 Relation to Claremont Age	66
7.3. Possible Sources of Error	67
CHAPTER 8: CONCLUSION	
8.1 Conclusion	69
8.2 Recommendations	70
REFERENCES	71
APPENDIX A- Geological Map of the Cobequid Highlands	
APPENDIX B- Petrographic Sample Descriptions	
APPENDIX C- Microprobe Parameters & Results	
APPENDIX D- XRF data and Error analysis	
APPENDIX E- Anomalous Samples	

## LIST OF FIGURES

1.1	Map of Cobequid Highlands (Pe-Piper, 2003)	1
2.1	Geological terranes of Atlantic Canada (MacHattie, 2012)	4
2.2	Location of study area in Cobequid Highlands (Pe-Piper, 2002)	7
2.3	Stratigraphic location of Claremont Formation (Ryan & Boehner, 1990)	8
2.4	Geologic map of Claremont Formation (Ryan & Boehner, 1990)	9
2.5	Geologic map of the Eastern Cobequid Highlands (MacHattie, 2014)	11
2.6	Jeffers and Bass River Block of the Cobequid Highlands (Pe-Piper, 2002)	12
3.1	Geological map with sample locations (Ryan, 1990)	18
3.2	Location of Balmoral Grist Mill Museum (Google images, 2016)	19
3.3	Outcrop location in relation to Grist Mill Museum (Google images, 2016)	20
3.4	Cobble clasts from the Eastern outcrop	21
3.5	Eastern bank of Balmoral Brook: outcrop has shallowly dipping beds	21
3.6	Cobble clasts from the Western (riverbank) outcrop	22
3.7	Carbonate patches in red siltstone clast	23
3.8	Location of core (Google images, 2016)	24
3.9	Upper portion of core	24
3.10	Mafic conglomerate clasts	25
3.11	Sketch log of core	26
3.12	Clastic mudstone interbedded with felsic conglomerate	27
3.13	Fe-staining in mafic portion	27
3.14	Carbonate patches in clasts	28
3.15	Porphyritic clast repeated throughout core	28
4.1	Cross-cutting relationship in sedimentary species	34
4.2	Calcite alteration in sample BM-4	34
4.3	Flow banding in felsic samples	35
4.4	Highly altered porphyritic felsic sample	35
4.5	Graphic texture in felsic species	35
4.6	Spherulitic texture in felsic species	36
4.7	Pilotaxitic texture signature of mafic species	36
4.8	Kink banding in mafic sample	36
5.1	Claremont data discrimination (Winchester & Floyd, 1977)	42
5.2	Related compositional fields to Winchester & Floyd discrimination	43
5.3	Claremont data discriminated by Zr-Ti-Y (Pearce & Cann, 1973)	44
5.4	Multi-element diagram for mafic species	45
5.5	Multi-element diagram for sedimentary species	46

5.6	Multi-element diagram for felsic group	46
5.7	Discrimination diagrams for rocks with granitic composition (after Pearce et al., 1984)	47
6.1	Geological map of proximal Eastern Cobequid formations (MacHattie, 2012)	48
6.2	Claremont and Cobequid geochemistry	50
6.3	Felsic species match to BB-DB Formation	51
6.4	Two-element diagrams correlates felsic species to BB-DB	52
6.5	Mafic species match BB-DB and FR Formations	53
6.6	Two-element diagrams correlate mafic species to BB-DB	54
6.7	Sedimentary species plotted against BB-DB Formation	55
6.8	Two-element diagrams for sedimentary species	56
6.9	Ti-Zr diagram correlates sedimentary species to Wilson Brook Formation	57
6.10	Claremont mafic species and BB samples	60
6.11	Claremont felsic compared to BB rhyolite	61
6.12	Porphyritic, felsic rock common to the Eastern Cobequids	61
6.13	Carbonate patches resemble carbonate in Wilson Brook Formation	62
7.1	Claremont sedimentary species compared to BB-DB siltstone	65

## LIST OF TABLES

2.1	Relationship of Phanerozoic Cobequid Formations (after Pe-Piper 2002)	12
2.2	Known ages of Formations(from Murphy et al 2000, Papoutsas, 2015)	13
3.1	Sample classification from field observations	29
4.1	Sample classification from petrography	33
4.2	List of minerals identified by microprobe	38
5.1	List of representative elements per sample groups	40
5.2	XRF results for mafic species	41
5.3	XRF results for felsic species	41
5.4	XRF results for sedimentary species	41
5.5	Samples associated with felsic sub-species	47
6.1	Claremont samples matched to DNR hand samples	58
7.1	Summary of results for each analytical method	64

**MINERAL ABBREVIATIONS**

<b>Mineral</b>	<b>Abbreviation</b>
Aegerine	agr
Amphibole	amph
Biotite	bt
Calcite	Ca
Chlorite	chl
Epidote	ept
Felspar	flds
K-Feldspar	kfs
Hematite	ht
Ilmenite	ilm
Magnetite	mgt
Muscovite	musc
Plagioclase	plg
Quartz	qtz
Sanidine	snd
Sericite	ser
Serpentine	spt
Zircon	zr

## ACKNOWLEDGEMENTS

I would like to thank Trevor MacHattie for his invaluable counsel and giving me access to his data on the Eastern Cobequids. Thank you to the Department of Natural Resources for the use of their portable XRF and to Rob Ryan for his instruction and aid. I would like to thank Dr. Richard Cox for his critiques as well as Glenn Chapman and Ryan Kressal for lending me their expertise in the lab. Thanks also go to the Scotia Exploration Research Committee without whom this research would not have been possible. I would also like to acknowledge the contributions of Dr. Dan McDonald and Gordon Brown at Dalhousie University for their technical support as well as Mick O'Neill for access to the core at the Stellarton coreshack. Thanks to Dr. Lawrence Plug for his recommendations and for giving us the 411 on thesis writing as well as Dr. Rebecca Jamieson for her thorough notes and words of wisdom. Lastly, I would like to thank my supervisor, Dr. Anne-Marie Ryan, for her persistence and patience throughout the year.

There are no words that can express the gratitude I have for my friends and family's support and encouragement these past months. Thanks especially to Corin, Dana and Erin for their help and advice and to my roommate for her inexhaustible optimism.

## CHAPTER 1: Introduction

### 1.1 INTRODUCTION

Sedimentary rocks common throughout the Appalachians are difficult to date due to their polyolithic composition and the effects of weathering and diagenesis. The central mainland of Nova Scotia, Canada is transected by the Cobequid Highlands (Pe-Piper, 2003: Fig. 1.1). Belonging to the Acadian orogeny, the Highlands are associated with the Appalachian orogeny in Eastern North America. Given the structural complexity and the lack of fossil-bearing strata, the ages of most sedimentary units in the Cobequids are not tightly constrained. This thesis investigates a relative age-bracketing technique based on the identification of clast species present in a conglomerate.

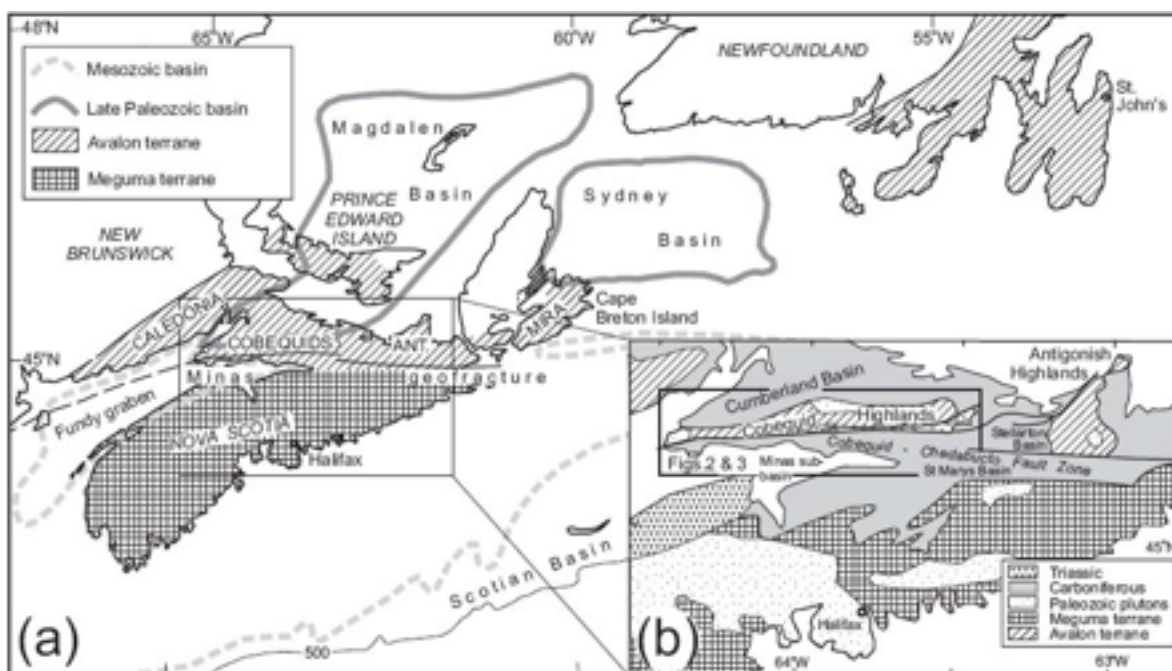


Figure 1.1 A) Nova Scotia is transected by Cobequid-Chedabucto (C-C) Fault, marking the contact between Avalon and Meguma terranes. B) Cobequid Highlands are located North of the Minas geofracture which consists primarily of the C-C Fault (Pe-Piper, 2003).

The Cobequid Highlands are located on the southern boundary of the Avalon terrane. The collision with the Meguma terrane in the late Silurian-early Devonian caused deformation and

thickening which created the Cobequid-Chedabucto Fault (Murphy, 1998). The Cobequids are characterized by a series of volcanic and sedimentary rocks that have undergone considerable deformation (MacHattie, 2012; Papoutsas, 2015; Pe-Piper, 2002).

In the Eastern Cobequids, these units eroded northwards into the Magdalen Basin creating a series of clastic sedimentary deposits (Murphy, 1998) including the Claremont conglomerate. The Claremont conglomerate is a clastic sequence 50 - 1500 m thick composed of volcanic, igneous and sedimentary clasts (Ryan & Boehner, 1986). This study attempts to bracket the age of the Claremont by identifying the clast species present in the conglomerate and correlating them to proximal units of known ages.

The correlation of clast species to proximal units of known age constrains the maximum age bracket of the conglomerate (Fralick, 1997). The reliability of this method can be tested by known stratigraphic constraints on the Claremont. The upper age bracket of the conglomerate is restricted to the Pennsylvanian (320 Ma) by the overlying Boss Point Formation (Ryan & Boehner, 1986). The underlying late Visean Middleborough Formation controls the lower age-bracket of the conglomerate (Pe-Piper, 2004; Ryan & Boehner, 1986).

Petrographic and geochemical analyses are used to identify clast species in the Claremont conglomerate. Since X-ray fluorescence (XRF) geochemical data from proximal Cobequid units are available through T. MacHattie (Department of Natural Resources; pers. comm.), this thesis uses the same method in order to obtain comparable geochemical data. MacHattie's data from the Eastern Cobequids represent potential source rocks for the clasts of the Claremont conglomerate.

The Claremont conglomerate offers an excellent opportunity to test the feasibility of using clasts to bracket the age of a conglomerate unit since it is stratigraphically constrained in

the Eastern Cobequids. The coarse pebble, polymict nature of the Claremont conglomerate offers the chance to analyze a variety of clast species and correlate them with proximal units. The known ages of these correlated units supply age-brackets for the Claremont. If successful correlation proves possible, this approach may serve to help determine ages for other conglomerate units where stratigraphic constraints are indefinite.



## CHAPTER 2: Geologic Setting & Study Area

### 2.1 GEOLOGIC SETTING

The geology of Nova Scotia in the Palaeozoic was characterized by continent-continent collisions of peri-Gondwanan terranes with Laurentia associated with the accretion of the Appalachians. Atlantic Canada is composed of four peri-Gondwanan terranes: Meguma, Avalonia, Ganderia and peri-Gondwanan arcs (Satkoski, 2010; Fig. 2.1). In the late Ordovician-early Silurian, Avalonia collided with Laurentia forming the Acadian orogen (420-360 Ma) (McClellan, 2014). Later collision of the Meguma and Avalonia terranes formed the Cobequid Highlands (Olsen, 1990).

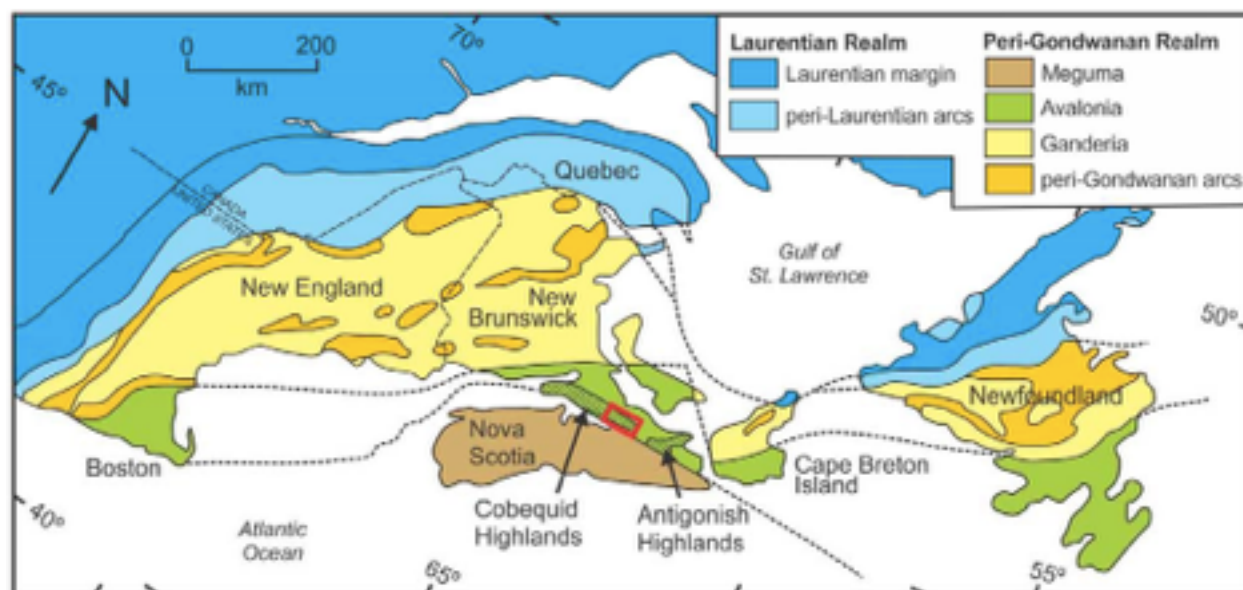


Fig. 2.1 Geological terranes of Atlantic Canada and USA. Cobequid Highlands are present north of the Meguma-Avalonia terrane contact. The Eastern Cobequids are outlined by box (from MacHattie, 2012).

The exact timing of the collision between the Avalonia and Meguma terranes is unknown (Murphy, 1998). The Avalon terrane originated as an arc-related terrane along the periphery of Gondwana in the Neo-proterozoic and evolved by calc-alkalic volcanism and co-genetic plutonism (Murphy, 1998). The Avalonian sequence consists of intracontinental volcanic rocks

interbedded with red clastic sediments and disconformably overlain by a sequence of shallow marine (fossiliferous) siliciclastic rocks (Murphy, 2005). The geochemistry of mafic rocks in the area are characteristic of magmatic plumes (Pe-Piper, 2002).

The Meguma terrane consists of Cambrian-Ordovician submarine fan deposits unconformably overlain by a mid-Ordovician- Silurian succession of bimodal within-plate volcanic and siliciclastic rocks (Murphy, 1998). The Devonian Meguma sequence is thought to have derived from the Avalonian basement (Keppie et al., 1997). Rapid uplift and erosion in the late Devonian exposed metamorphic rocks of the Meguma terrane (Samuel, 2011).

The boundary between the Meguma and Avalon terranes was “overstepped” by the deposition of the Horton Group (Murphy, 1998). These clastic units from the early Viséan (Ryan & Boehner, 1990) were deposited along the southern boundary of the Magdalen Basin just north of the Eastern Cobequid Highlands (Murphy, 1998).

The Cobequid Highlands are the result of the collision between the Meguma and Avalonia terranes. The Highlands are transected by the Cobequid-Chedabucto Fault (CCF) which marks the current contact between these terranes. Part of the Minas Fault Zone, the CCF was reactivated by dextral motion in the Late Carboniferous (Murphy, 1998). The extent of the CCF displacement is debated, but lithostratigraphy can be traced from the Annapolis Valley into Cape Breton Island (Murphy, 1998). Distinctive Ordovician-early Devonian volcanic and sedimentary rocks in both the Avalon and Meguma terranes form a continuous NE-trending belt across this region (Murphy, 1998).

The Magdalen is likely not a rift or pull-apart basin as previously thought, but rather a low topographic area within a mountain belt formed by rapid uplift in the mid-Devonian: “an example of basin formation associated with transpression, uplift and relaxation following collision” (Murphy, 1998). Subsequent slip and subsidence in and around the mountain belt created small, deep basins resulting in a “mosaic geography of interconnected mountains and basins” (Olsen, 1990).

During the Mesozoic, the Fundy Basin experienced two major episodes of deformation:

- 1) a series of normal faults, forming the northwestern boundary faults of the Chignecto and Fundy sub-basins (Withjack, 1995), displaced beds over 10km and the subsiding basins were subsequently filled by eolian sand deposits (Olsen, 1990).
- 2) a NW-SE compression, created NE- and E-trending anticlines and synclines (Withjack, 1995).

This history is vital to bracketing the age of the Claremont conglomerate. Understanding the depositional environment will enable the discrimination of possible source rocks and the youngest clast species will provide an upper age-bracket for the conglomerate.

## **2.2 STUDY AREA**

The conglomerate outcrops examined for this study are located in Balmoral Mills, Nova Scotia proximal to the Balmoral Grist Mill Museum (45°64'35" N, 63°19'34" W) (Fig. 2.2). The TF-86-1 core was drilled by the Department of Natural Resources (DNR) about 4 km NW of Balmoral Grist Mill Museum (45°38'53"N, 63°15'9"W).

The Claremont conglomerate is the geologic subject of this study. It belongs to the Claremont Formation of the Cumberland Group (Ryan & Boehner, 1990). This formation was

referred to as the Falls Formation by Pe-Piper (2002). The Claremont Formation is folded by the Tatamagouche syncline (Fig. 2.3). It consists of poorly sorted conglomerate and red sandstone.

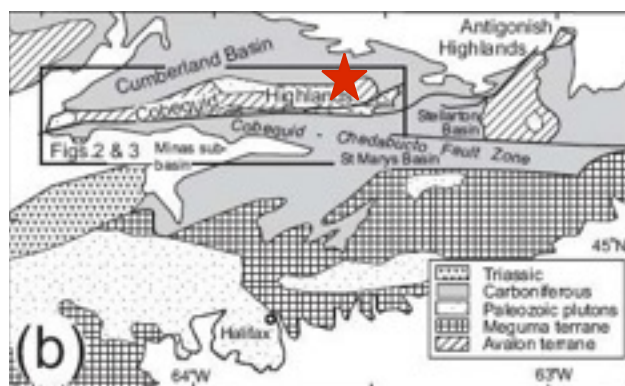


Fig. 2.2 Study area marked by star on the Eastern boundary of the Cobequid Highlands. (Map from Pe-Piper, 2002).

The Claremont Formation unconformably overlies the Middleborough Formation and is disconformable to the overlying, early-Westphalian Boss Point Formation (Ryan & Boehner, 1990).

It should also be noted that The tectonic and stratigraphic evolution of the area is dominated by salt withdrawal and resulting subsidence (Waldron, 2013). Deposition of a thick continuous evaporite layer was followed by early minibasin development in the Tatamagouche syncline area where terrestrial sediment eroded from extensional fault block (Waldron, 2013). Thus, the development of this study area was greatly affected by salt tectonics.

The Claremont Formation is located just beyond the northeastern-most boundary of the Cobequid Highlands (Fig. 2.5). Weathering and erosion of the Highlands northwards into the Magdalen basin resulted in the deposition of the Claremont conglomerate unit (Murphy, 1998). The formations from the Highlands that are proximal to the Claremont conglomerate are

considered as potential source units for the Claremont clasts and are described in the next section.

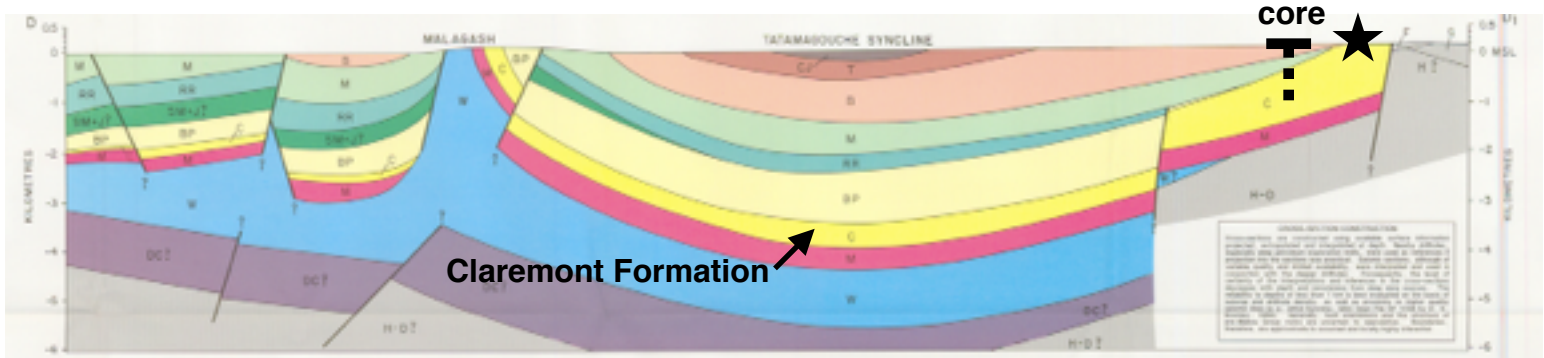


Fig. 2.3 Claremont Formation is folded by the Tatamagouche syncline (Mesozoic). The Claremont Formation is constrained between the Middleborough (M) Formation (Mabou Group) and overlying Boss Point (BP) Formation (Cumberland Group). Approximate core and outcrop (star) location superimposed onto cross section (actual location and cross section line shown in Fig. 2.4). (Modified from Ryan & Boehner, 1990).

## 2.3 PREVIOUS WORK

### 2.3.1 Descriptions of Proximal Formations

Geologic formations proximal to the Claremont conglomerate are shown in Fig. 2.5.

These rock units are divided into the Jeffers and Bass River Blocks (Fig. 2.6).

The stratigraphic sequence of the Eastern Cobequids is disputed. With regards to this thesis, the Claremont Formation is part of the Cumberland Group outside of the Cobequids (as per Ryan & Boehner, 1990). Alternatively, the Falls Formation might belong to the Jeffers Block and overlies unconformably the Diamond Brook Formation (Pe-Piper, 2002). The relationships between blocks and time are shown in Table 2.1. Known ages of proximal units are shown in Table 2.2.

It should be noted that unit names are tentative since the mapping of the Cobequid Highlands is ongoing (MacHattie, pers. comm.). Further, only the formations for which data was available are described below.

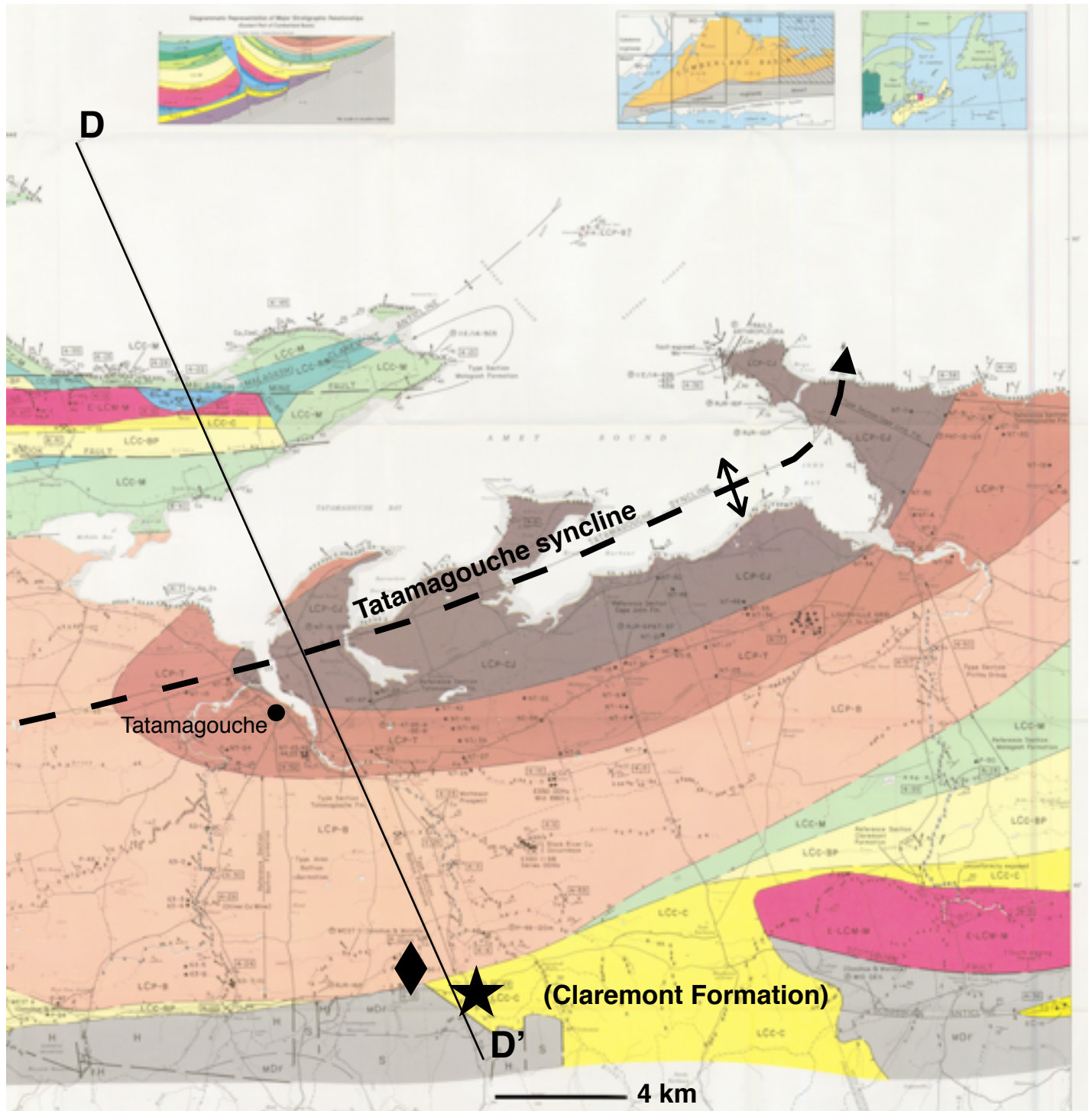


Fig. 2.4 The Claremont Formation is exposed at the northeastern-most boundary of the Cobequid Highlands by the Tatamagouche syncline. Study areas are shown by diamond (core) and star (outcrop) symbols. Cross section (Fig. 2.3) is outlined. (Modified from Ryan & Boehner, 1990).





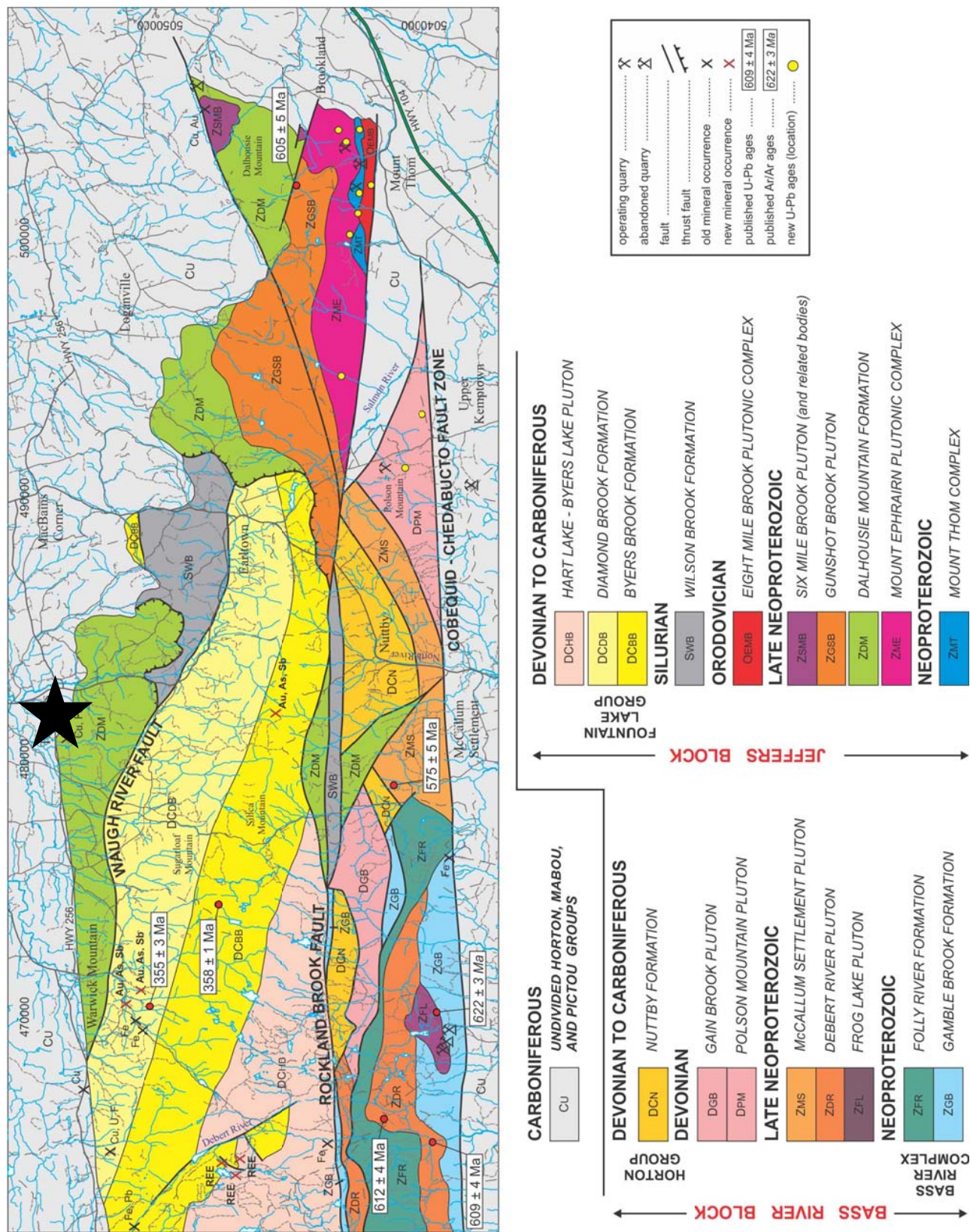


Fig. 2.5 Geologic map of the Eastern Cobecoquids. Dalhousie Mountain, Wilson, Diamond Brook, Byers Brook and Gunshot Pluton are most proximal to study area (black star on Balmoral Mills outcrop site). Cobecoquid-Chedabucto and Rockland Brook Faults cut and transpose units. Note ages of Byers Brook (356 ± 1 Ma) and Diamond Brook (355 ± 3 Ma) formations (Map modified from MacHattie, 2014).



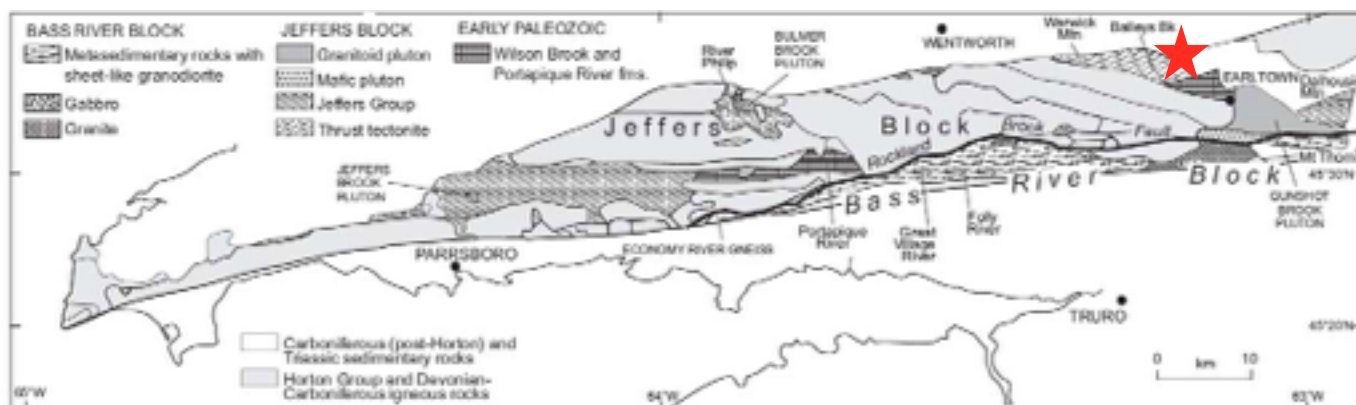


Fig. 2.6 The Cobequid Highlands comprised units from the Jeffers and Bass River Blocks. The Rockland Brook Fault thrusts the Jeffers Block over the Bass River Block. Study area is marked by red star. (Map from Pe-Piper, 2002).

**Table 2.1:** Stratigraphic Relationships of the Cobequid Formations

Time	Jeffers Block	Bass River Block
e. Carboniferous	Falls Formation	Diamond Brook
Late Devonian	Nuttby	Byers Brook -Undivided-
Mid Devonian	Murphy Brook	
Early Devonian		Portapique River
Silurian		Wilson Brook
Cambrian- Ordovician		
Late Neoproterozoic	-Undivided- Cranberry Lake Gilbert Hills Dalhousie Mountain	
Middle Neoproterozoic		Folly River Gamble Brook

*\*table after Pe-Piper 2002*

Table 2.2

Geological Unit	Age (Ma)	Method	Reference
<b>Byers Brook Formation (upper)</b>	358 ± 1	U-Pb (zircon)	Dunning et al. (2002)
<b>Diamond Brook Formation (Upper)</b>	348 ± 3	palynology	Menning et al. (2006)
<b>Diamond Brook Formation (Mid)</b>	353 ± 3	U-Pb (zircon)	Dunning et al. (2002)
<b>Diamond Brook Formation (Mid-Low)</b>	359 ± 2	palynology	Martel et al. (1993)
<b>Fountain Lake (young) Volcanics</b>	341 ± 4	Rb-Sr	Cormier (1982); Pe-Piper et al. (1989)
<b>Fountain Lake (old) Volcanics</b>	387 ± 2	Rb-Sr	Cormier (1982); Pe-Piper et al. (1989)

*\*Modified from tables in Murphy et al., 2000 and Papoutsas, 2015*

### **Dalhousie Mountain Formation:**

The Dalhousie Mountain Formation is the oldest and most proximal unit to the study site. It belongs to the Jeffers Block and is in faulted contact with adjacent units except at its northern and eastern extents where it unconformably overlain by late Carboniferous sedimentary rocks (MacHattie, 2012). Dalhousie Mountain consists of lower greenschist facies rocks, including dacitic to andesitic tuff, felsic ignimbrites, lapilli tuff, amygdaloidal basalt flows and laminated cherty siltstone with preserved graded beds and cross-laminations (Murphy et al., 2001; MacHattie, 2012; Pe-Piper 2002). It was intruded by the Gunshot Pluton and the 6-Mile Pluton. A distal submarine fan was likely the depositional environment for this unit (Murphy, 2001). Age is unknown.

### **Wilson Brook Formation:**

The Wilson Brook Formation was cropped out in a fault sliver by the Rockland Brook Fault (MacHattie, 2012). It consists of grey-black micaceous siltstone and shales, minor quartz-

arenite and fossiliferous limestones. Limestones are Silurian (Murphy et al., 2000). The Wilson Brook Formation is distinct in the region due to the lack of deformation and the lack of volcanic rocks (only one mafic dyke was noted; MacHattie, 2012).

### **Fountain Lake Group:**

The Fountain Lake Group is part of the Bass River Block. The group is characterized by rapid changes in facies from conglomerate and lacustrine deposits to a bimodal volcanic suite. The Byers Brook ( $358 \pm 1$  Ma) Formation consists of orange-brown rhyolitic flows and ignimbrites interlayered with dacitic flows, crystal tuffs and greenish-grey siltstone and sandstone (MacHattie, 2012).

The Diamond Brook ( $355 \pm 3$  Ma) conformably overlies the Byers Brook Formation and is composed of basaltic flows interbedded with red sandstone and siltstone (MacHattie, 2012). Rhyolites are also interbedded in the flows (Pe-Piper, 2002).

### **Folly River Formation:**

The Folly River Formation resides in the core of the Bass River Block (MacHattie, 2012). It is composed of dark green-grey basaltic lapilli tuff, amygdaloidal basaltic flows, tuffaceous siltstone, sandstone and rare quartzite (MacHattie, 2012). The extent the Folly River Formation is disputed. To be consistent, this thesis adopts the interpretation by MacHattie and White (2012) that the Folly River is related to the Gamble Brook Formation.

### **Boss Point Formation:**

The Boss Point Formation (320-318.5 Ma) is part of the Cumberland Group. It consists of sandstone, grey-green shale, limestones and calcareous mud-chip conglomerate (Ryan &

Boehner, 1990). The Boss Point succeeds the Claremont Formation disconformably (Ryan & Boehner, 1990).

### **2.3.2 Conglomerate Dating Techniques**

This next section describes current methods used to date conglomerate or siliclastic rocks. The provenance of fine-grained sediments is difficult to determine due to chemical and physical modification of the source material during weathering, erosion, transportation and deposition (Fralick, 1997). Moreover, multiple age populations are often associated with conglomerate rocks due to their polyolithic nature. The lack of age populations in a conglomerate may be due to: a) crust of this age did not exist in the particular drainage basin, b) rocks of this age were not exposed to erosion when the sediments were deposited (Samuel, 2011).

The ages of sedimentary rock are currently constrained globally using a number of indirect dating techniques including: the dating of contemporaneous volcanic rocks, bracketing relationships of igneous and metamorphic rocks and dating detrital diagenetic material (Rasmussen, 2005). However, stratigraphic relationships are rarely able to constrain the age of successions to better than hundred million years and detrital minerals only yield maximum ages (Rasmussen, 2005). Nevertheless, these methods record information on the composition of the continental crust, the chemical evolution of the hydrosphere and atmosphere, changes in climate (Manzotti et al., 2015). Clastic sediment rocks can provide material for unravelling orogenic evolution (Kotkova et al., 2007). Thus, rapid and simple age-dating techniques for conglomerate rocks are of interest to multiple geologic applications.

Radiometric dating can yield precise and stratigraphically-meaningful maximum ages. This technique uses K-Ar,  $^{40}\text{Ar}$ - $^{39}\text{Ar}$ , Rb-Sr or U-Pb (Rasmussen, 2005; Li et al., 2015). Unaltered volcanic rocks from interbedded volcanic and sedimentary sequences are ideal for radiometric dating.

The radiogenic method most often used to date sedimentary rocks is U-Pb geochronology of detrital zircon minerals. Several problems arise from radiogenic U-Pb dating.

First, the maximum age of the rock is determined from the youngest zircon (Rasmussen, 2005). A major uncertainty lies in the limitations of the sample site: the confidence that minerals from the youngest population have been sampled (Grange, 2009). Internal complexities of the zircon further increase the uncertainty of results and may include: zoning, cross-cutting features and patchy recrystallization patterns (Grange, 2009). Also, zircon are affected by hand-picking sampling bias (Slama et al., 2012).

Furthermore, many zircons are recycled from pre-existing quartz-rich sedimentary rocks rather than primary magmatic or metamorphic hosts (Grange, 2009). This can explain the presence of numerous age populations in one rock: old zircons are recycled into new rocks where new zircons are crystallizing. Possible explanations for multiple ages include: multiple periods of sedimentation, tectonic interleaving of different-aged sedimentary rocks, unknown lapse time between mineralization and sedimentation (Grange, 2009) and/or magmatic activity (Samuel, 2011). The “spectrum” of age populations is advantageous in that it can discriminate the stages of genesis including provenance, orogenesis, palaeogeography and sediment dispersal patterns (Rasmussen, 2005).

Finally, high-U zircons rarely survive the extensive transportation and reworking prerequisite for lithification and are thus absent from mature sediments (Rasmussen, 2005).

A different approach to dating conglomerate rocks in particular uses conglomeratic clasts to identify the sources of a conglomerate. A study by Zaroni et al. (2010) is similar in nature to this thesis. Zaroni et al. used microstructural analyses and thermo-barometric estimates from metamorphic pebbles to distinguish the basement sources of conglomerates in the Southalpine Orobic Alps. The relative chronology of fabrics and mineral assemblages was inferred from microstructural analysis for each of the 39 pebbles selected to represent the diversity of clasts in the conglomerate. The pebbles were grouped by lithological affinity and relative chronology and potential sources were assessed by comparing the specific metamorphic evolution of each pebble group to those of the surrounding metamorphic units. The study claimed success and showed that the integrated analytical method has further advantages; namely that conglomerates preserve geological records, thus providing unique information regarding geologic history. Zaroni concluded that pebble identification is necessary to restrict the thermal signature of the potential source basement and that grains from single mineral species cannot alone distinguish source material.

This thesis will provide an additional test to Zaroni's hypothesis. This research examines the clasts of the Claremont conglomerate to test whether it is possible to establish age-brackets by correlating the clast species to proximal source rocks.

## CHAPTER 3: Field Observations

### 3.1 SAMPLING METHOD

Forty-four samples were collected on the northeastern boundary of the Cobequid Highlands around the Balmoral Mills area (Fig. 3.1) from outcrop and core locations in the fall of 2015. Samples were selected based on the following criteria: visible compositional diversity, minimal weathering and in particular, of large enough size to be thin-sectioned ( $> 4$  cm). Samples of apparently similar composition along the length of the core were collected to account for possible chemical variation or to confirm consistency with depth. Due to limited outcrops and field data, this thesis examines only the vertical variation in the Claremont conglomerate.

All hand samples collected from field sites were characterized qualitatively based on textural features. Clasts were subdivided based on these preliminary observations. Petrographical

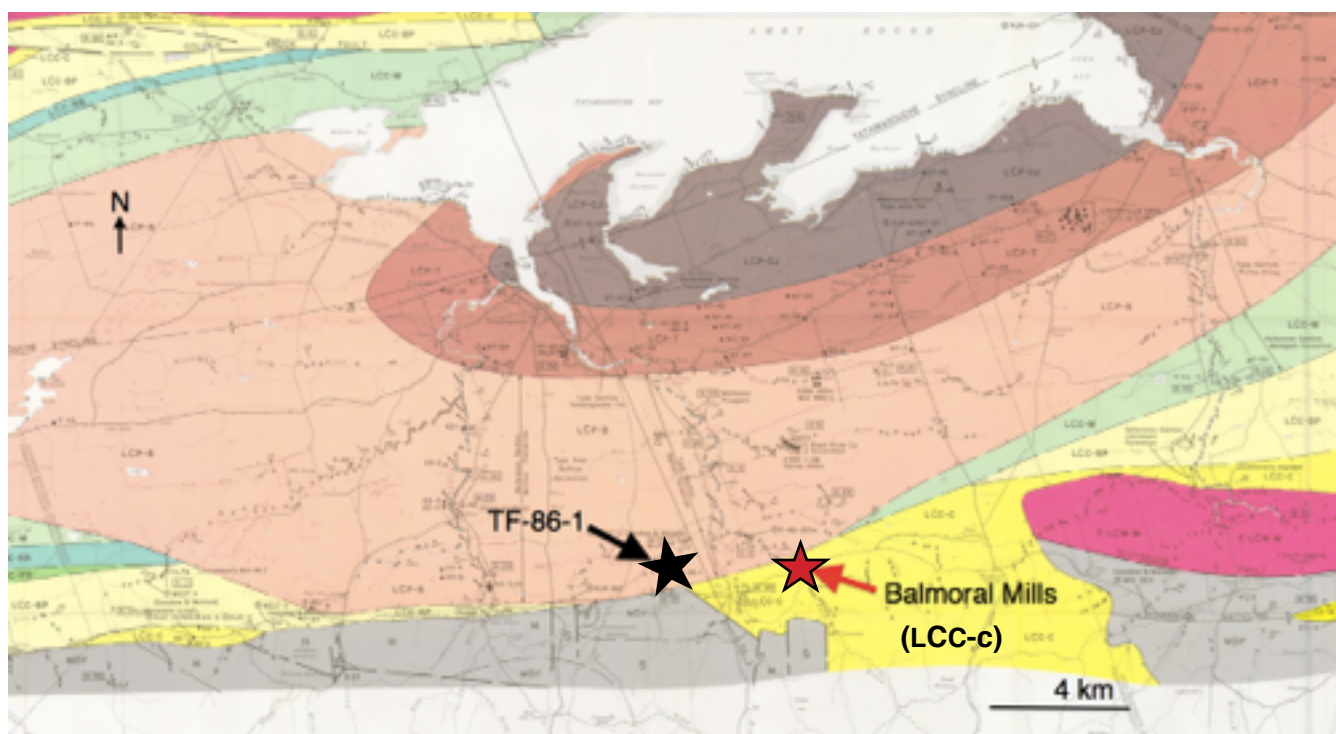


Figure 3.1 Geologic map of Colchester county showing Claremont Formation (bright yellow: LCC-C) as well as core (black arrow) and outcrop (red arrow) sample sites. (Map from Ryan & Boehner, 1990) \*See Fig. 2.5 for legend.

descriptions for 21 samples and XRF elemental analysis for 20 samples was completed. Those results are discussed later (see chapter 5).

### 3.2 BALMORAL MILLS OUTCROP

The main conglomerate outcrops examined for this study are located at the Balmoral Grist Mill Museum, mainland Nova Scotia ( $45^{\circ}38'14''\text{N}$ ,  $63^{\circ}11'10''\text{W}$ ). Observations were also made at a small roadside outcrops located within 1 km of the main site along Balmoral Road (Fig. 3.2).



Fig. 3.2 Location of Balmoral outcrop at the Grist Mill Museum (labelled on maps). Roadside outcrop location marked by red star. (Google images 2016)

The two main outcrop sites are proximal to the Grist Mill Museum. The first outcrop is 20 m x 2 m and about 5 m due east of the Museum (Fig. 3.3). The outcrop has well-sorted conglomeratic beds dipping shallowly NW with thicknesses on the cm-scale and a red, coarse sandstone to mud-dominated matrix. Overall grain size coarsens down-section (SE). Clasts are subangular to sub-rounded cobbles and dominantly sedimentary; mainly grey limestone and arkose (Fig. 3.4). The outcrop detail is partially obscured by weathering and erosion (Fig. 3.5).





Fig. 3.3 Outcrop locations shown in relation to Grist Mill Museum: Eastern outcrop outlined in red, NW outcrop outlined in blue. Black dotted line traces Balmoral Brook. (Google image 2016)

The second outcrop is about 20 m northeast of the Museum along the eastern bank of Balmoral Brook (Fig. 3.3). It is about 4-5 m high and 10 m wide (at this location, the outcrop continues the length of the brook but is inaccessible on foot). Poorly sorted beds (m-scale) dip gently to the NW and contain sub-angular and sub-rounded clasts in a red, mud-dominated matrix. Clasts are easily pulled out or knocked out of the rock with a rock hammer. The following lithologies represent the clasts in order of abundance: grey siltstone, limestone (red limestone and fossiliferous limestone), red siltstone (Fig. 3.6). Calcite veins in the clasts are common, especially in limestone clasts. Some red siltstones have irregular carbonate patches (Fig. 3.7).

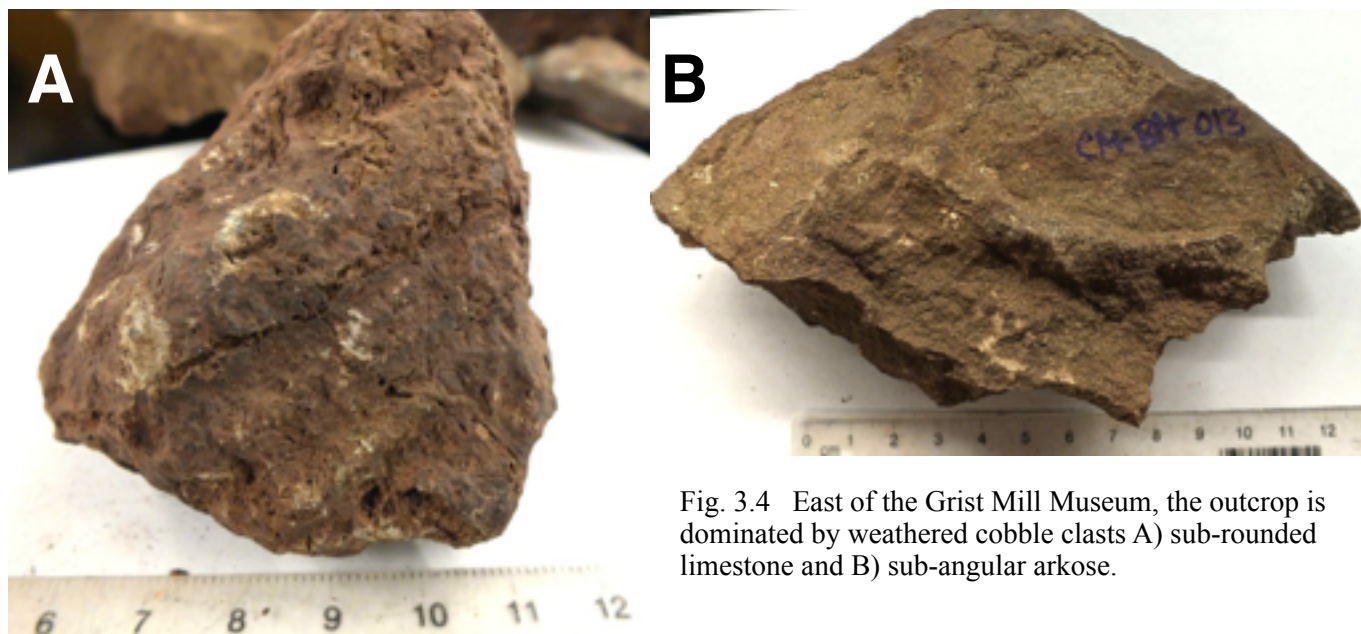


Fig. 3.4 East of the Grist Mill Museum, the outcrop is dominated by weathered cobble clasts A) sub-rounded limestone and B) sub-angular arkose.



Fig. 3.5 Along the eastern bank of Balmoral Brook, beds dip shallowly to the NW. Beds are about 20-60 cm thick and consist of poorly sorted, sub-angular clasts embedded in a red fine-sand matrix with mud lenses. Outcrop is obscured by mud. (Photo by A.Ryan 2015)

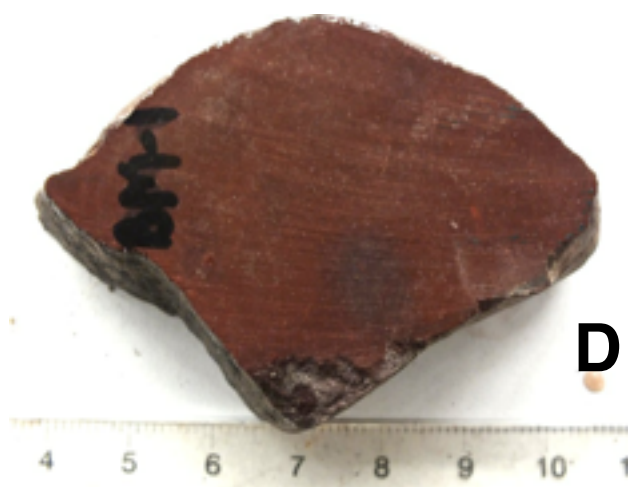
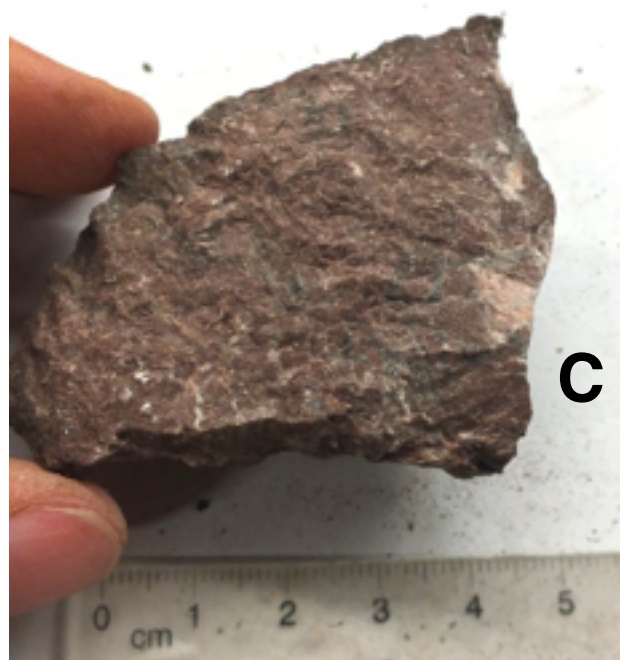
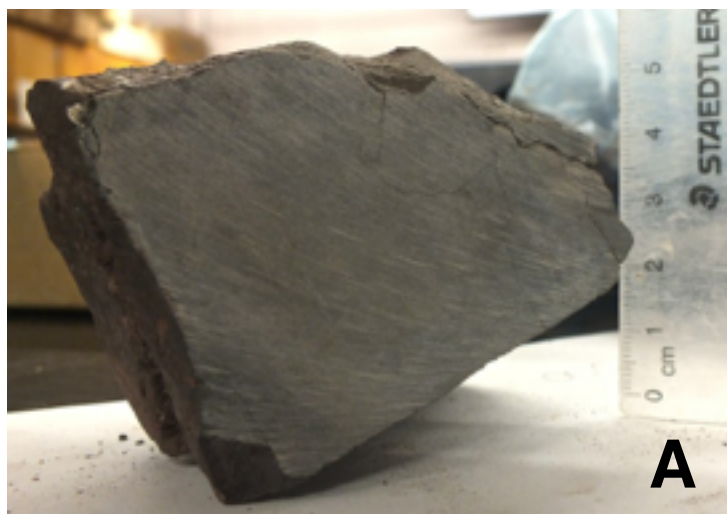


Fig. 3.6 Cobble clasts of the riverbank outcrop. Main lithologies shown in order of abundance A) Grey siltstone B, C) Red limestones D) Red siltstone



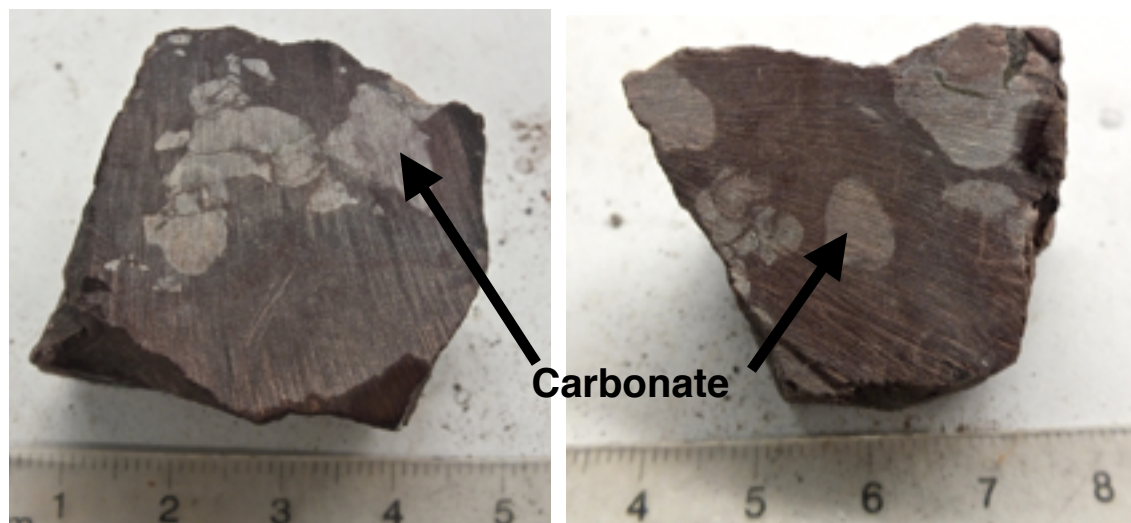


Fig. 3.7 Carbonate “patches” in red siltstone sample BM-4.

### 3.3 CORE

The TF-86-1 core was drilled in 1986 by the DNR about 4 km NNW of Balmoral Mills (Fig. 3.8). It is held by the Department of Natural Resources (DNR) at the coreshack in Stellarton, NS. The core is 750 m long and was retrieved using a N.S.D.M.E. No. 20 drill. R.J. Ryan (DNR) completed a geological log of the core shortly after drilling. Samples were collected at depths ranging from 356-783 metres (1170-2568 ft) in the core. Note: Imperial units are included to be consistent with the core and all depths are relative to the top of the core (0 ft). Short pieces of the core were sampled and individual clasts subsequently hammered out.

Qualitative observations of the core note a progressive shift in bulk clast composition from predominantly felsic to predominantly mafic around 400 m (1310 ft) (Fig. 3.9).

Considering the core did not penetrate through the bottom of the unit and that the purpose of the



Fig. 3.8 Location of TF-86-1 core (red star) with relation to Grist Mill Museum (black star) (Google images, 2016).

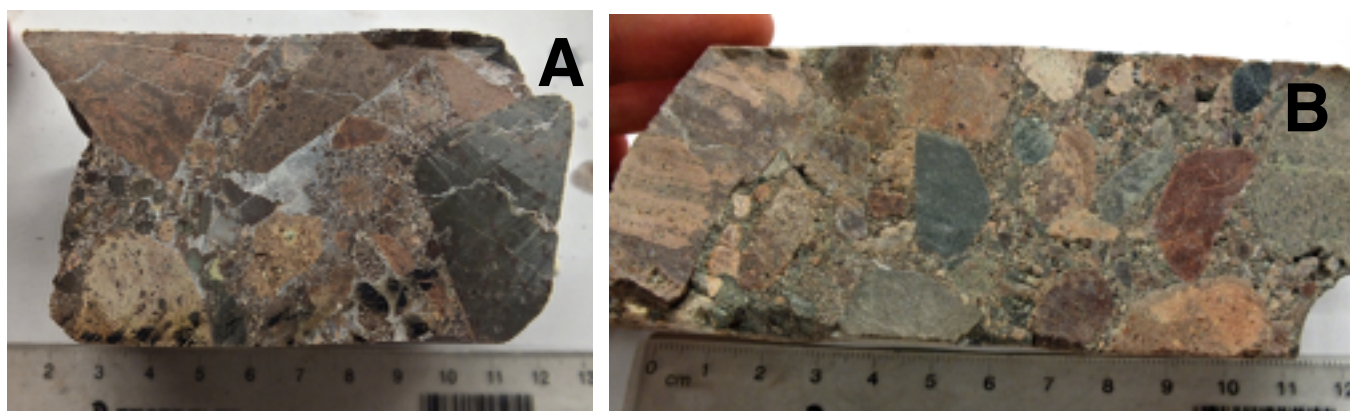
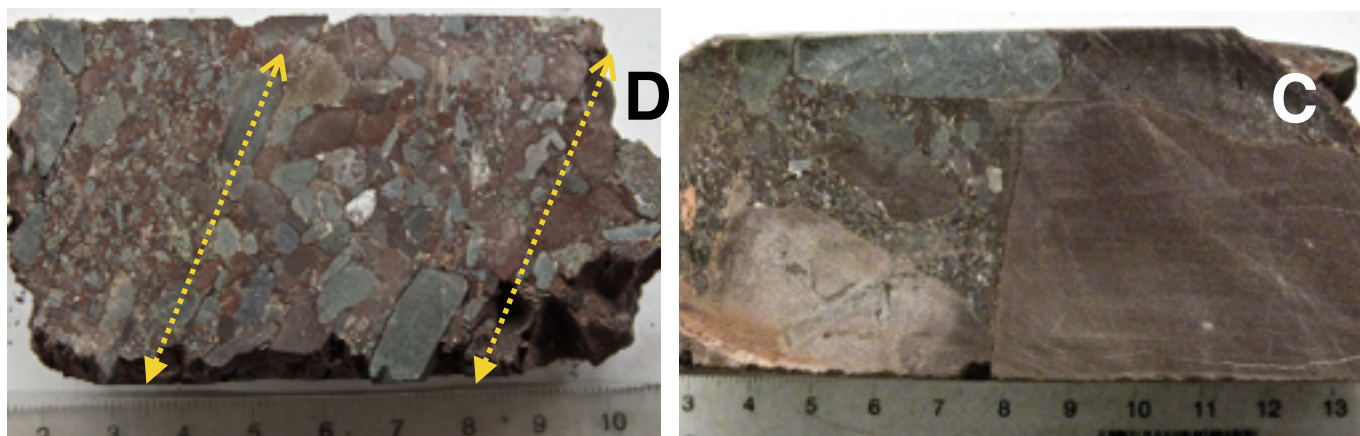


Fig. 3.9 Felsic section of core (A,B) in contrast to more mafic section located deeper in the core (C,D). The division is made around 400 m into the Claremont unit. A) 382.5 m (1255 ft), B) 356.6 m (1170 ft), C) 627.9 m (2060 ft), D) 554.4 m (1812 ft). In the mafic section, the size difference between clasts and matrix becomes more pronounced with depth (C). In the shallow mafic, grains are aligned along c-axis (D).



study is to bracket the age of the conglomerate, the focus will be on the defining the upper age bracket of the Claremont conglomerate.

Overall, the core consists of fine pebble to large cobble poly lithic clasts with varying degrees of roundness and sorting set in a red mud f. sand matrix. Despite the mixed composition of clasts, there are visible patterns throughout the core. Due to the shift in the dominant clast species around 400 m, the following observations are organized based on “upper” (<400 m) and “lower” (>400 m) section of the core (Fig. 3.11).

In the lower section, the conglomerate is unsorted and contains sub-angular, pebble-cobble clasts set in a coarse sandstone to fine pebble matrix. The matrix and clasts appear to have similar compositions and the grain size difference between them increases with depth. Three major lithologies are present: siltstone, limestone and mafic igneous clasts (Fig. 3.10). Their size varies from fine pebble to small cobbles. The pebbles are occasionally aligned along the c-axis (Fig. 3.9d). Abundant Fe-staining is present and carbonate alteration is abundant in the clasts (Fig 3.13).

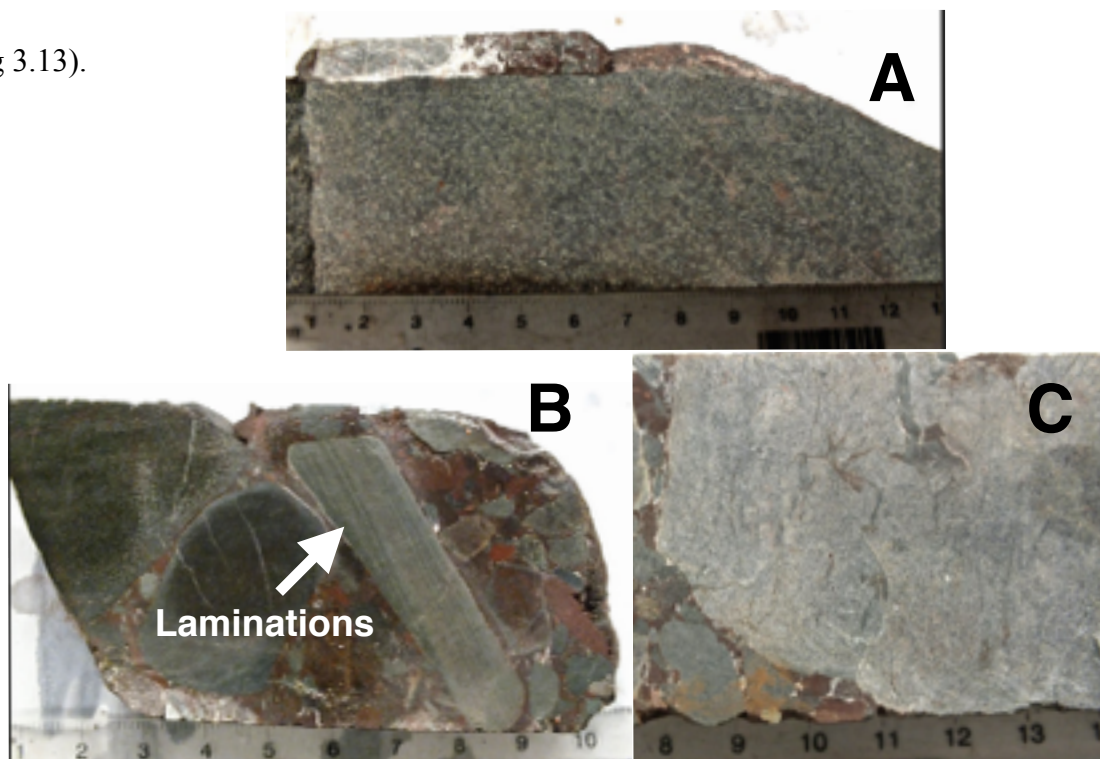


Fig. 3.10 “Mafic” conglomerate clasts: A) Igneous B) Siltstone, with preserved sedimentary laminations (arrow), C) Biomicritic limestone with fossil fragments

In the upper section, the conglomerate is interbedded with clastic mudstone (Fig. 3.12). The conglomerate is unsorted and composed of sub-rounded and sub-angular poly lithic clasts set in a mud to very fine matrix. A felsic clast species is identified by colour and flow banding within clasts. This felsic species dominated the upper section of the core with sparse sedimentary clasts. Carbonate alteration and veining are abundant in the matrix. Pebbly lenses (about 5 cm thick) occur occasionally in the mud beds. Mean grain size increases with depth.

Some siltstones from 397.8 m (1305 ft), 429.5 m (1409ft) and 772 m (2532 ft) show irregular carbonate patches similar to outcrop sample BM-4 (Fig. 3.14). A porphyritic basalt with coarse grained, idiomorphic feldspar phenocrysts is present at 740.1 m (2428 ft). This porphyritic texture and composition is also present at depth 377 m (1237 ft) in the felsic section (Fig. 3.15).

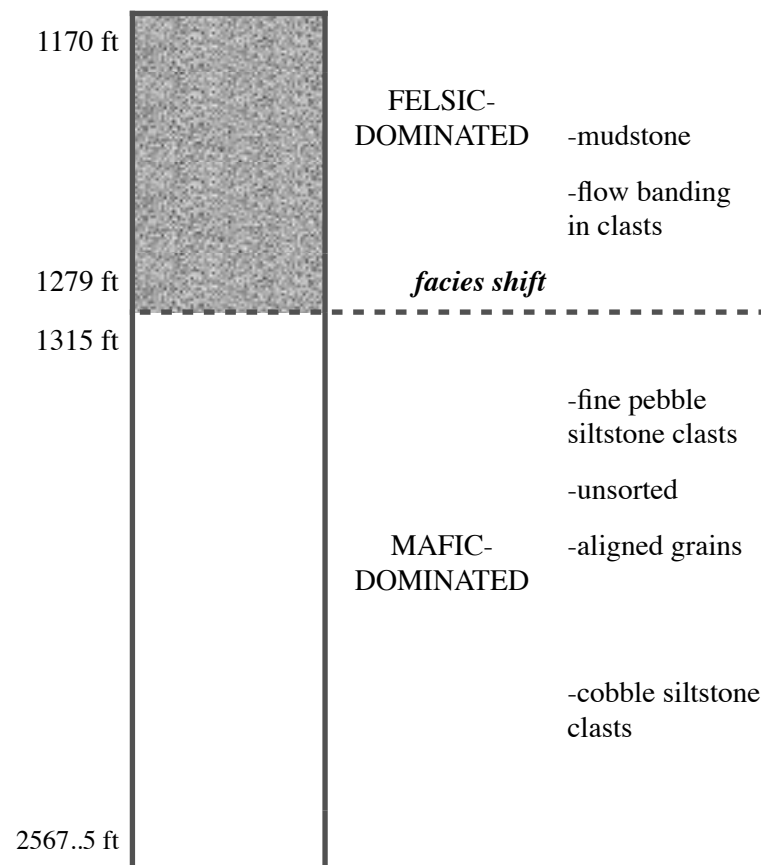


Fig. 3.11 Sketch log of core. Felsic clasts dominate the upper portion while mafic clasts dominate the lower portion of the core. Main features for each facies are listed. Depths are labelled in feet to show sample correlation to core log. Facies shift is estimated around 400 m.



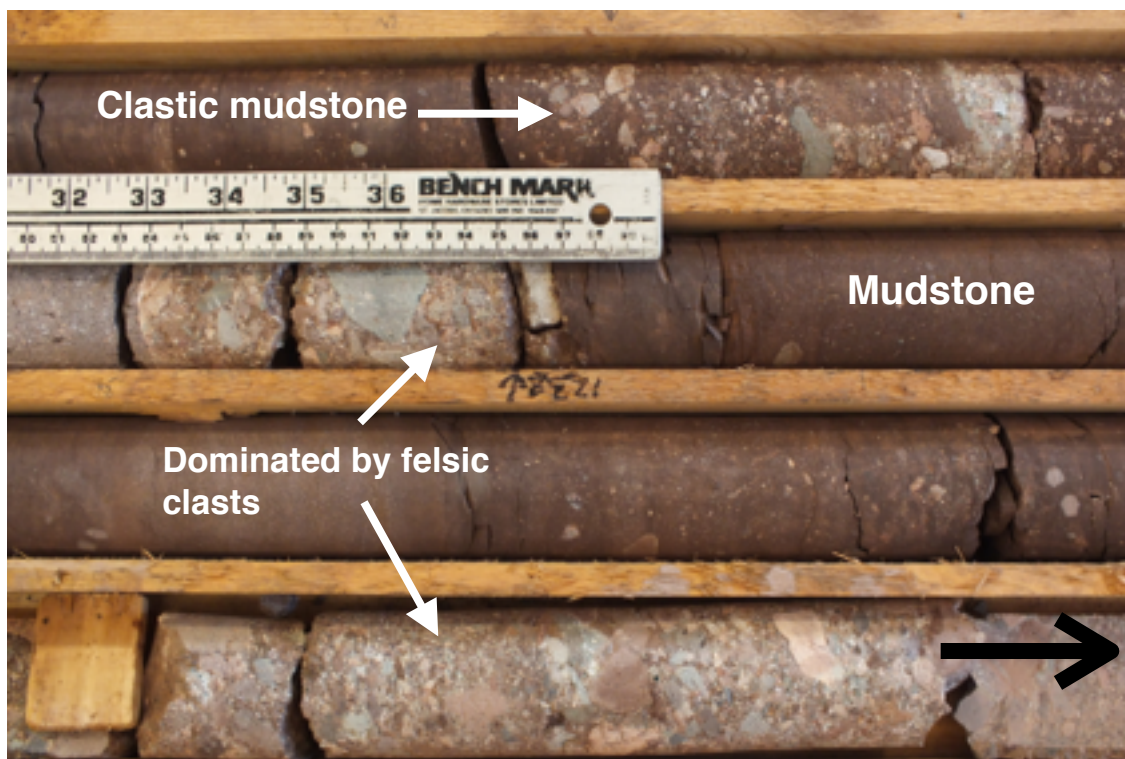


Fig. 3.12 Core around 375.5 m (1232 ft): “Felsic section” is composed of a sequence of clastic mudstone, mudstone, unsorted conglomerate with v.c. sand to f. pebble matrix. (Black arrow indicates downsection)



Fig. 3.13 Core around 401 m (1317 ft): transition zone/top of “mafic section” has larger clasts. Clasts are more rounded and sorting increases with depth. Abundant Fe-staining. (Black arrow indicates downsection).



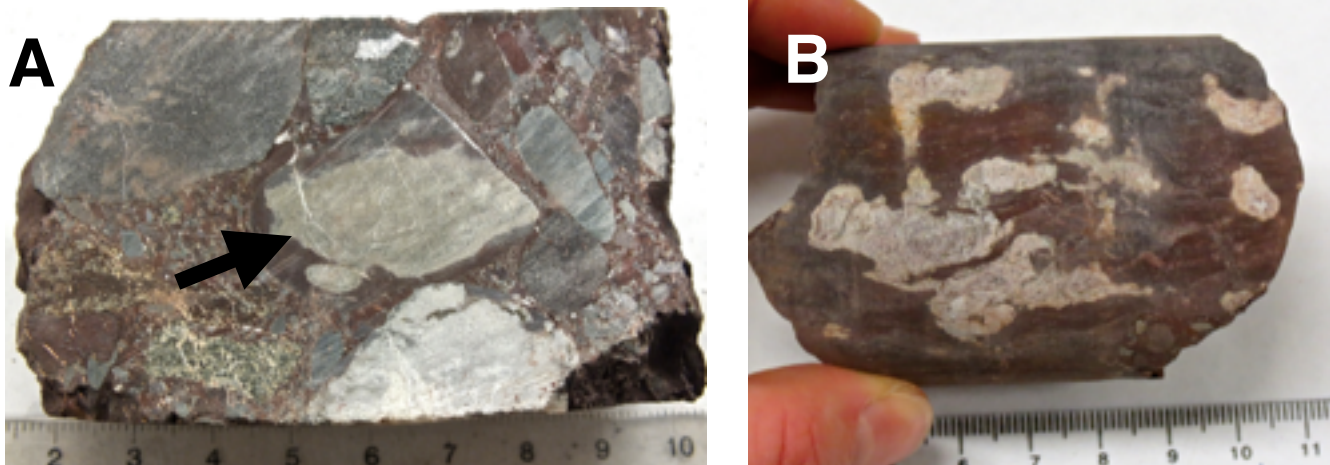


Fig. 3.14 Carbonate patches in clasts: A) 429.5 m (1409 ft), B) 397.8 m (1305.5 ft).

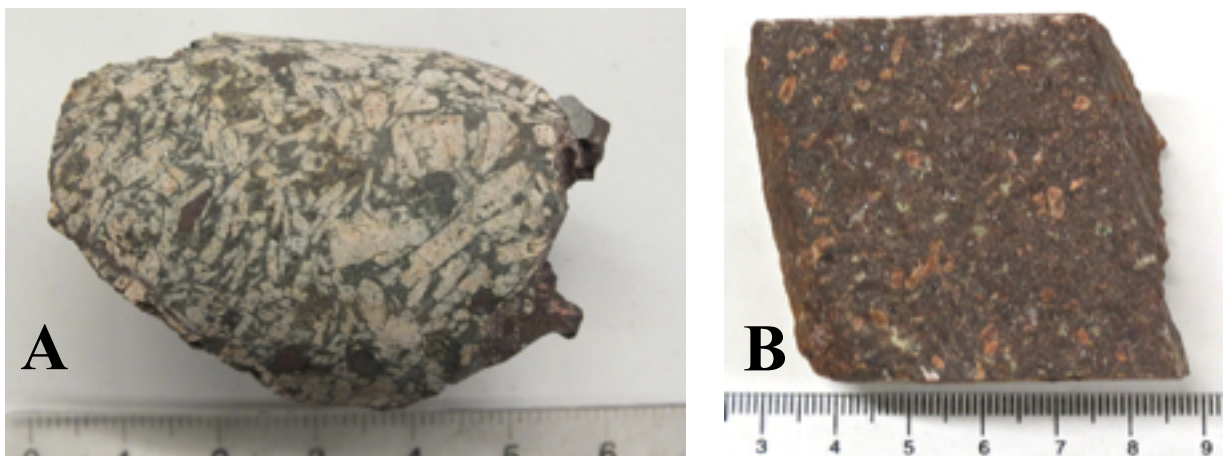


Fig. 3.15 A) Porphyritic unit at 740.1 m (2428 ft) has coarse grained, euhedral feldspar phenocrysts, B) m.-f. grained felds phenocrysts in a clast from 377 m (1237 ft).

Based on these observations, samples were classified into the following groups: sedimentary, mafic, felsic (Table 3.1). Several samples from each group were selected for petrographic description. Limestones are considered separately as they were sent to R. Ryan (DNR) for analysis. They are not included with the sedimentary species. Preliminary results show limestones are biomicrites (R. Ryan pers. comm.). Fossils are present but fragmented. Pieces of orthid articulate brachiopods and algal pisoliths are present (R. Ryan pers. comm.).

**Table 3.1:** Hand samples collected from Balmoral outcrops (o/c) and core. Sample names for core correspond to their depths in the core. (Y) indicates that said analysis was completed.

<b>Sample</b>	<b>Location</b>	<b>Clast Description</b>	<b>Group</b>	<b>Thin Section</b>	<b>Geo-chemistry</b>
<b>CM-BM-003</b>	o/c	red siltstone, sub-rounded small cobble	Sedimentary	Y	Y
<b>CM-BM-004</b>	o/c	grey limestone, sub-angular coarse pebble	Limestone		
<b>CM-BM-005</b>	o/c	grey shale, angular small cobble	Sedimentary		
<b>CM-BM-005E</b>	o/c	grey limestone, coarse pebble	Limestone		
<b>BM-3M</b>	o/c	grey siltstone, sub-rounded coarse pebble	Sedimentary	Y	Y
<b>CM-BM-011</b>	o/c	limestone, fossiliferous, sub-rounded small cobble	Limestone		
<b>CM-BM-006</b>	o/c	grey limestone, m. pebble	Limestone		
<b>CM-BM-007</b>	o/c	grey shale, angular small cobble	Sedimentary		
<b>CM-BM-003B</b>	o/c	red limestone, angular coarse pebble	Limestone		
<b>BM-1</b>	o/c	grey limestone, coarse pebble	Limestone		
<b>BM-4</b>	o/c	red siltstone, leucocratic inclusion	Sedimentary	Y	Y
<b>BM-2M</b>	o/c	grey siltstone, sub-rounded coarse pebble	Sedimentary		Y
<b>CM-BM-013</b>	o/c	arkose, sub-angular large cobble	Sedimentary		
<b>CM-BM-009</b>	o/c	limestone, sub-angular small cobble	Limestone		
<b>CM-BM-010</b>	o/c	limestone, sub-angular small cobble			
<b>2547</b>	core	grey siltstone	Sedimentary		
<b>2535.5</b>	core	red siltstone	Sedimentary		
<b>2515</b>	core	red siltstone	Sedimentary		
<b>1305.5</b>	core	red siltstone with leucocratic inclusions	Sedimentary		
<b>1170A</b>	core	pink-purple bands, red phenocrysts, sub-angular m. pebble	Felsic	Y	Y

<b>1232a</b>	core	pink and purple chaotic flow bands, c. pebble	Felsic	Y	Y
<b>1232b</b>	core	purple chaotic flow bands, red phenocrysts, c. pebble	Felsic	Y	Y
<b>1228</b>	core	porphyritic	Felsic	Y	Y
<b>1315</b>	core	red siltstone	Sedimentary		
<b>1237</b>	core	kfs phenocrysts in purple groundmass	Felsic	Y	Y
<b>1245</b>	core	red siltstone, calcite alterations, pebble	Sedimentary		
<b>1255</b>	core	flow banded volcanic	Felsic		
<b>1256.2</b>	core	flow banded pink m. pebble	Felsic	Y	
<b>1180.5</b>	core	pyroclastic	Felsic	Y	Y
<b>1247</b>	core	kfs phenocrysts	Felsic		
<b>1279</b>	core	Purple phenocrysts in pink groundmass	Felsic	Y	Y
<b>1315.5</b>	core	equigranular, small cobble	Mafic	Y	Y
<b>1819</b>	core	equigranular, large cobble	Mafic	Y	Y
<b>2234</b>	core	porphyritic igneous, small cobble	Mafic	Y	Y
<b>2236.5</b>	core	porphyritic igneous, small cobble	Mafic	Y	Y
<b>2513</b>	core	equigranular,			Y
<b>2549</b>	core	c. grained equigranular, small cobble	Mafic	Y	Y
<b>2060c</b>	core	red siltstone, rounded cobble	Mafic	Y	Y
<b>2567</b>	core	c. grained equigranular, small cobble	Mafic	Y	Y
<b>2567.5</b>	core	c. grained equigranular, small cobble	Mafic	Y	Y
<b>2428</b>	core	v.c kfs phenocrysts, pebble	Mafic		
<b>1336</b>	core	equigranular, calcite alt., large cobble	Mafic		
<b>1409</b>	core	red siltstone with leucocratic inclusions, pebble	Sedimentary		

<b>1407</b>	core	equigranular, large cobble	Mafic		
<b>1821</b>	core	equigranular with calcite amygdules, large cobble	Mafic		
<b>1895</b>	core	limestone, fossiliferous, large cobble	Limestone		
<b>2529</b>	core	grey siltstone, cobble	Sedimentary		
<b>2537</b>	core	concretion			
<b>2540</b>	core	equigranular, small cobble	Mafic		
<b>CM-BM-002</b>	o/c	Fossiliferous red-stained limestone, parallel calcite veins, small cobble	Limestone		

## **CHAPTER 4: Petrography of Conglomeratic Clasts**

### **4.1 THIN SECTIONS**

#### **4.1.1 METHODS**

Twenty-one samples were described using a petrographic microscope with reference to Nesse (2012) for mineralogy. Photomicrographs were taken for reference and to compare clast samples. Thin sections were prepared by G. Brown at Dalhousie University. Samples were selected for thin sectioning from preliminary specie groups based on hand-sample observations (Table 3.1). I included multiple samples from the “mafic, porphyric” species in order to reflect the range in groundmass size throughout this species. Size permitting, unique clasts were also selected for thin sectioning (greater than 4 x 3 cm). Due to the fine-grain size, high weathering and alteration effects, this section is not a comprehensive petrographic analysis. Instead, the petrography is used as a basis for correlation with possible source rocks.

#### **4.1.2 RESULTS**

Samples can be divided into three species based on mineralogy and textural features: felsic, mafic and sedimentary (Table 4.1). The petrography of individual Claremont clasts is described in Appendix B.

Sedimentary clasts are fine-medium grained and well-sorted silt-sandstones. Laminations and some cross-bedding is present (Fig. 4.1). Grains are angular and consist mostly of quartz, plagioclase and opaque minerals. Chlorite replacement is common and zircon is present. Calcite veins cut oblique to laminations. Irregular carbonate patches present in sample BM-4 (Fig. 4.2) as seen on hand sample.

Felsic clast samples are porphyritic and hypocrySTALLINE (Fig 4.3-6). Many show flow banding (Fig. 4.3) and graphic texture (Fig. 4.5). Phenocrysts are generally fine-medium grained (Fig. 4.4). Composition is mainly: quartz, plagioclase, feldspar, Fe-oxide. Calcite and chlorite are common secondary minerals. Spherulitic and recrystallization textures are abundant (Fig 4.6). Compositional banding, lithic fragments are among other features present in some clasts.

**Table 4.1**

<b>Sample id.</b>	<b>Location</b>	<b>Description</b>	<b>Group</b>
BM-003	o/c	red siltstone	Sedimentary
BM-3M	o/c	grey siltstone	Sedimentary
BM-4	o/c	red siltstone with carbonate patches	Sedimentary
1170A	core	banded rhyolite	Felsic
1180.5	core	lithic arenite?	Anomalous
1228	core	rhyolitic with flds phenocrysts	Felsic
1232a	core	highly altered porphyritic rhyolite	Felsic
1232b	core	altered, flow-banded rhyolite	Felsic
1237	core	porphyritic, pink phenocrysts	Felsic
1255	core	porphyritic rhyolite	Felsic
1256.2	core	altered, brecciated	Anomalous
1279	core	graphic, hypocrySTALLINE	Felsic
1315.5	core	altered basalt	Anomalous
1819	core	hyalo-ophitic basalt	Mafic
2060c	core	red siltstone	Sedimentary
2234	core	vesicular basalt	Mafic
2236.5	core	dyke?	Anomalous
2513	core	pilotaxitic basalt	Mafic
2549	core	holocrySTALLINE basalt	Mafic
2567	core	pilotaxitic basalt	Mafic
2567.5	core	inequigranular basalt	Mafic

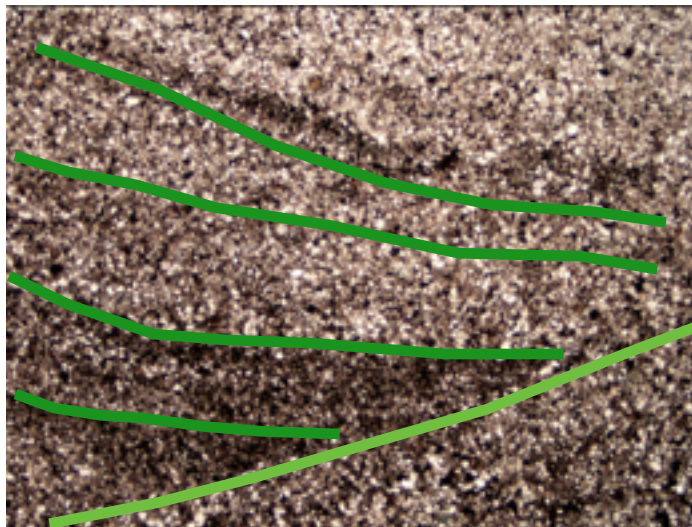


Fig. 4.1 Cross-bedding relationship in sedimentary pebble (sample BM-003) PPL. FOV: 10.5 mm

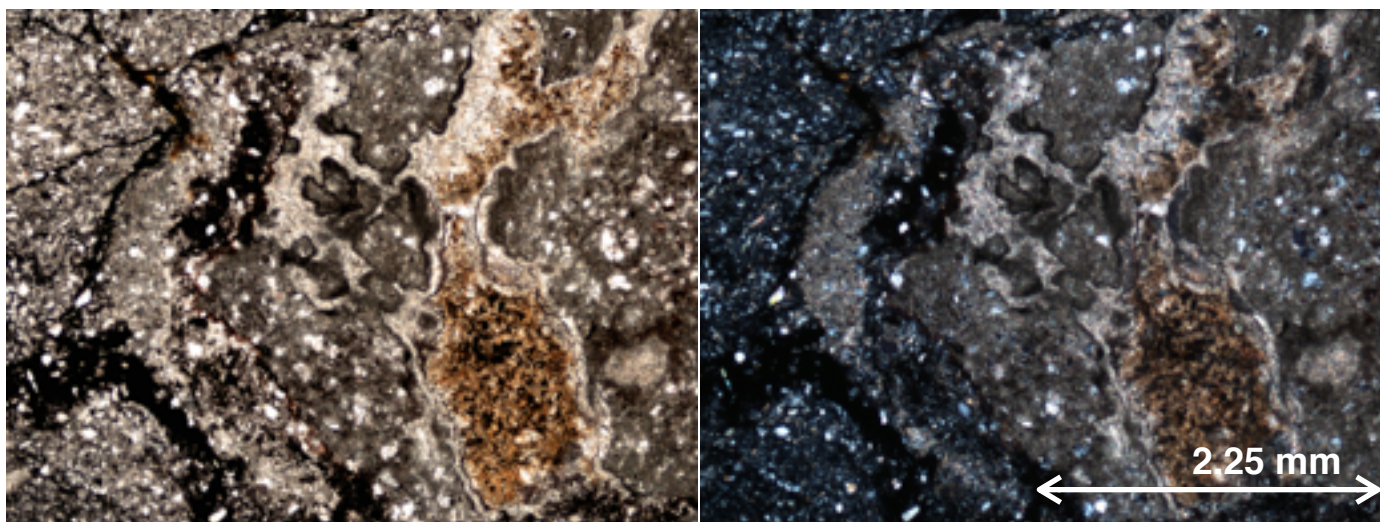


Fig. 4.2 Sedimentary sample BM-4: irregular calcite patch with orange alteration in fine-grained matrix. (PPL, XPL)

Mafic clast samples are fine-medium grained with a plagioclase, pyroxene and Fe-oxide primary composition (Fig. 4.7-8). Clasts are commonly porphyritic with a fine-grained, pilotaxitic groundmass. Coarse, subidiomorphic feldspar phenocrysts display poikilitic texture. Most clasts have Fe-staining.



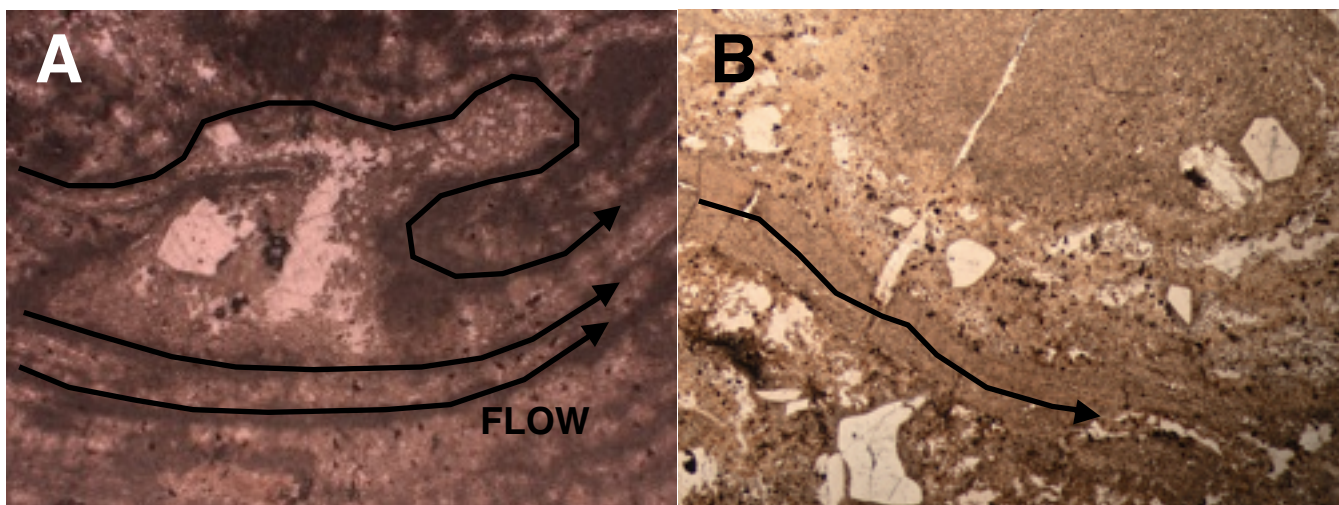


Fig. 4.3 Flow banding in felsic samples 1232b (A) and 1228 (B). PPL; FOV 10.5 mm

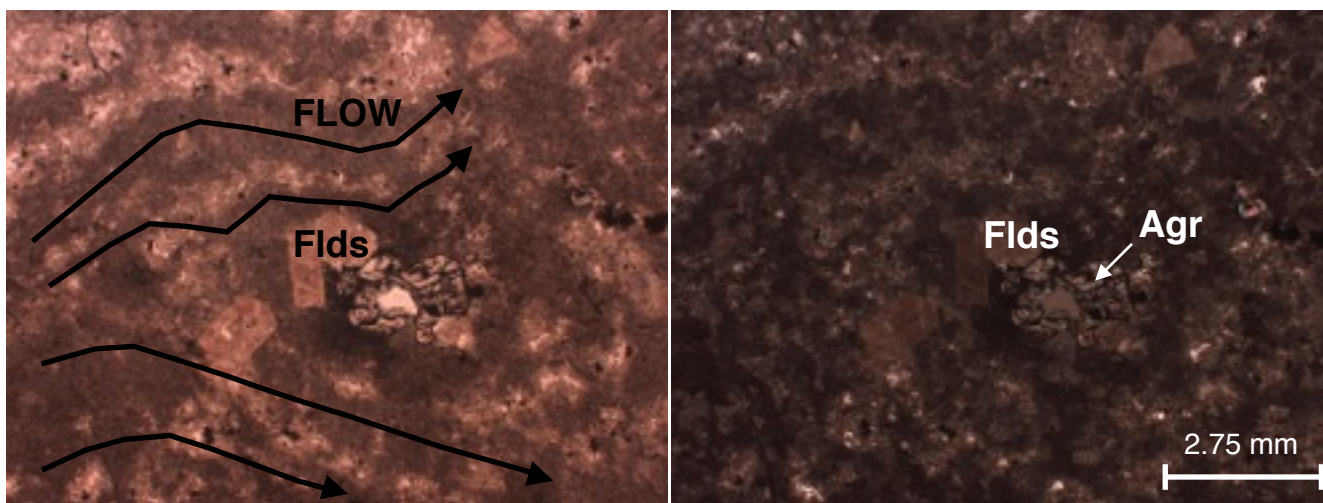


Fig. 4.4 Felsic sample 1232b: Phenocrysts (possibly aegerine) highly altered by Fe-rich oxide. Kfs phenocrysts in a flow banded groundmass. (PPL, XPL)

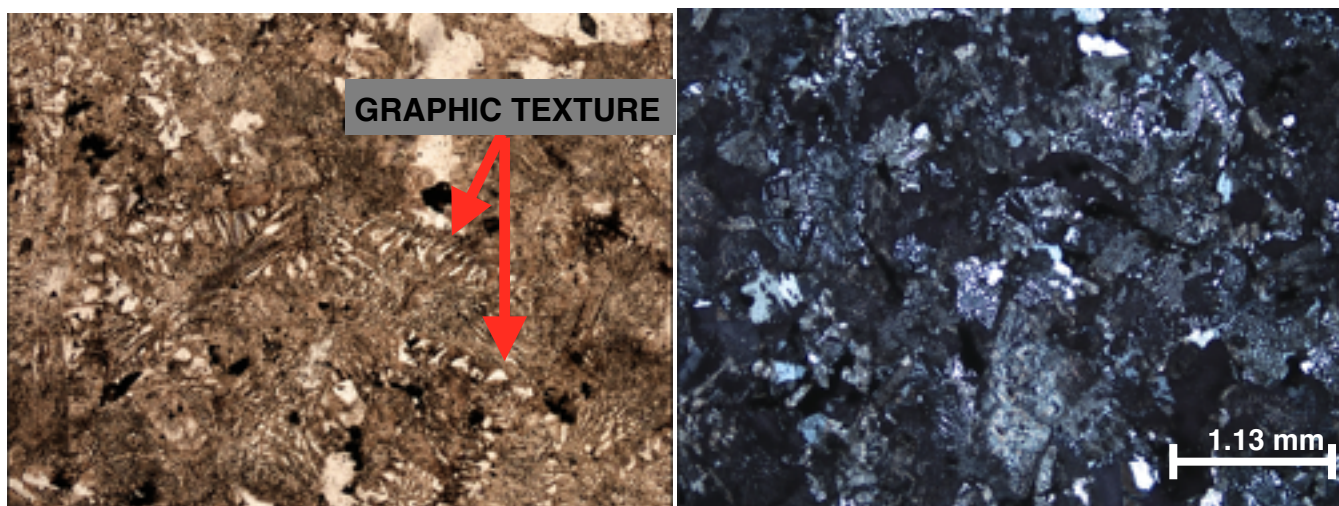


Fig. 4.5 Graphic texture in felsic sample 1279. (PPL, XPL)



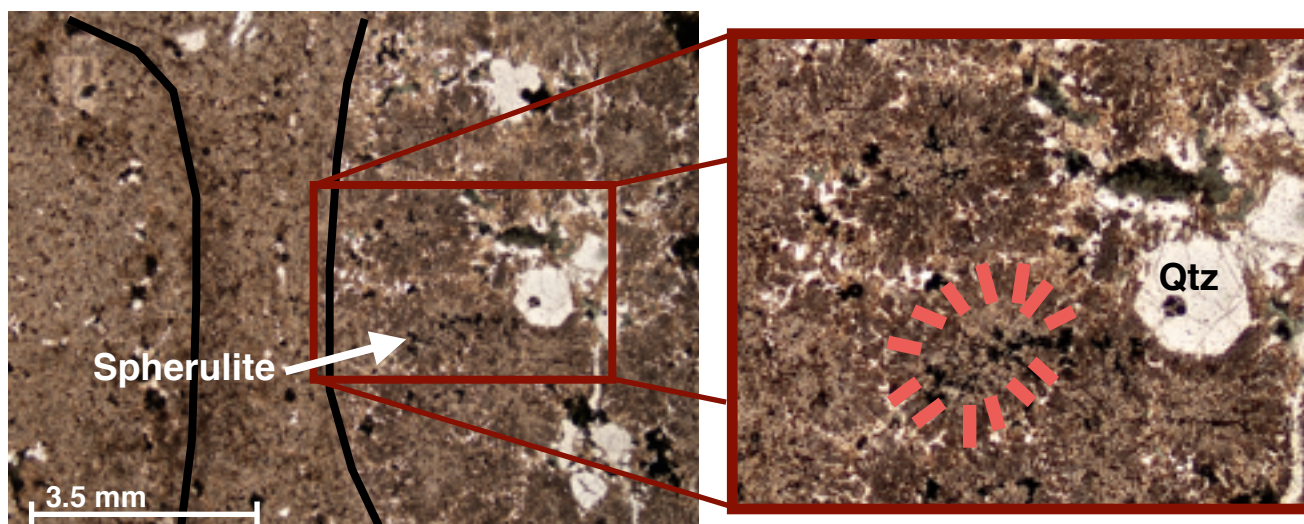


Fig. 4.6 Spherulitic texture in felsic sample 1170a. Black lines trace compositional bands. Right image shows closer view of radial crystal growth (outlined in red). (PPL)

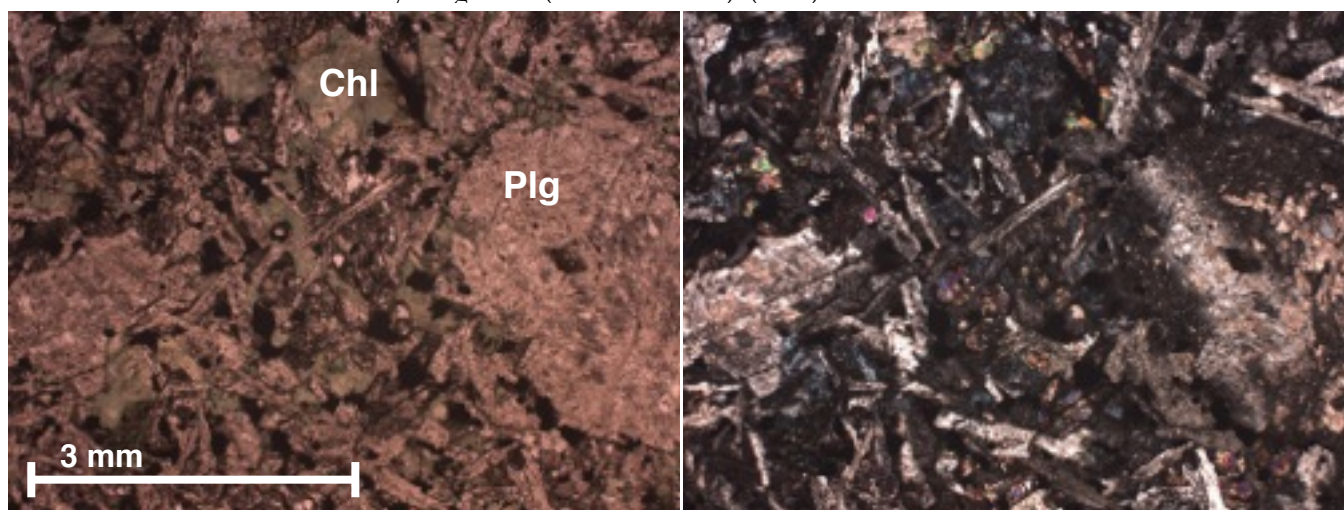


Fig 4.7 Mafic sample 2234: Poikilitic plg phenocrysts (Ca-alt inclusions) in pilotaxitic groundmass (plg, px, olv). Chl amygdules. (PPL, XPL)

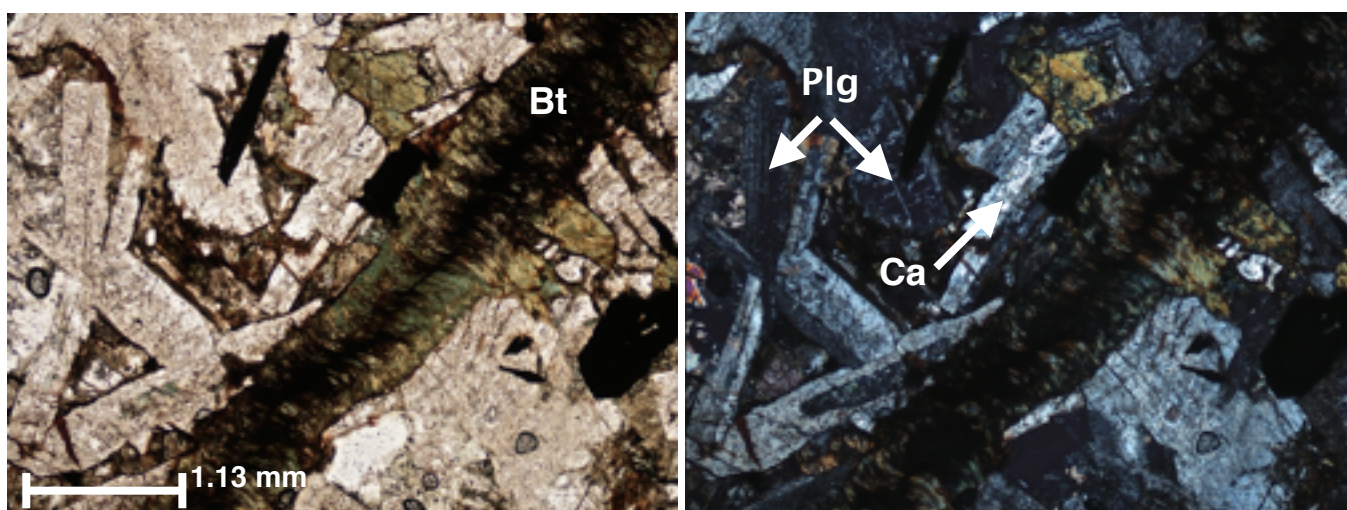


Fig. 4.8 Bt kink bands in pilotaxitic groundmass. Ca alteration on plg crystals (sample 2567.5). (PPL, XPL)

Four clast samples were anomalous due to unique features. These clasts have been included in Table 4.1 as an “anomalous” species and were excluded from further analysis. Brief descriptions for these clasts are found in Appendix E.

## **4.2 MICROPROBE**

Microprobe analysis was conducted to identify opaque minerals in Claremont samples. Preliminary results were inconclusive so no further analysis were done.

### **4.2.1 METHODS**

Microprobe analysis was completed at the Robert M. MacKay Electron Microprobe Laboratory at Dalhousie University using a JOEL 8200 Superprobe. Polished sections of 3 rhyolite and 2 basalt samples were prepared by G. Brown at Dalhousie University. The sections were carbon coated by D. MacDonald (Dalhousie University) prior to probe analysis. Block 53 was used for calibration. It includes the following mineral standards: sanidine (K, Al, Si), garnet (Fe), chromite (Cr), Jadeite (Na), Pyrolusite (Mn) and kaersutite (Ca, Ti, Mg). Analytical parameters are presented in Appendix C.

The purpose of microprobe analysis was for mineral identification. Point analysis in grain cores was used to identify opaque minerals. Pictures of the analyzed grains are available in

Appendix C. The fine grain size and abundance of alterations in Claremont samples resulted in low totals for most samples. Fresh spots were difficult to find in thin sections.

#### 4.2.2 RESULTS

Inferred minerals listed per sample (Table 4.2). Further analysis was not completed due to the high level of alteration and weathering in the Claremont samples. Analytical results for the preliminary analysis are in Appendix C.

**Table 4.2**

<b>Sample</b>	<b>Inferred Minerals present</b>
1237	Fe-oxide Ilm Titanite
1279	alt biotite musc
1228	Ti-Fe oxide
2567	Fe-oxide plg (albite)
2234	Amph (high Al) Fe-oxide

## CHAPTER 5: Geochemistry of Conglomeratic Clasts

The geochemistry of the Claremont clasts was determined by XRF analysis. These results were combined with petrographic findings to reveal the species present in the Claremont conglomerate.

### 5.1 METHODS

The geochemistry of selected clasts was determined using a portable bench-top X-ray fluorescence analyzer. The XRF method was chosen because it is the same method used by T. MacHattie on his samples from the Eastern Cobequids. Since the ultimate aim of this study is to find source rocks by comparative analysis, using the same instrument increases the reliability of the comparison. In total, hand samples of 21 pebbles were analyzed using the same portable XRF as T. MacHattie at the Department of Natural Resources (Halifax).

In-house basalt (09-TM054) and rhyolite (A09-TM-165A) standards were used to calibrate the data from the Claremont clasts with pre-existing data from the Eastern Cobequids (data obtained from T. MacHattie pers. comm). The composition of these standards has been calibrated to external lithological standards by T. MacHattie (pers. comm.). Peak intensities of the data were calibrated using an external standard: international standard no.316 (metal puck). A calculated correction for certain elements based on internal instrumental error was applied by T. MacHattie; the same calculation was made on his Cobequid data (T. MacHattie pers. comm.).

After the first XRF run, uneven surfaces on some clasts were identified as a potential cause for error. For the second run, a flat surface was cut using a rock saw on the clasts in question. The clasts were then wiped clean and left to dry. A second XRF analysis was carried

out for the cut samples and for clasts that had yielded poor results (high standard deviations). The same rhyolite and puck standards were used and same methods were followed.

The mean elemental results of both runs are used to characterize the species of Claremont clasts. Some clasts, which were not included in the re-run due to good standard deviation from initial results, are based solely on the results from the first run. The statistical value of each element is determined by calculating the standard deviation (Appendix D). Elements that have a standard deviation  $< 10\%$  are considered for analysis. Elements with good standard deviation for each sample within a clast species are representative for that particular species. These representative elements varied for each group (Table 5.1).

The Claremont conglomerate data are plotted on several discrimination diagrams to confirm working species groupings (from hand samples and petrography) or show variations thereof. Only discrimination diagrams involving representative elements from Table 5.1 are used. Discrimination diagrams using immobile elements were preferred due to the altered and weathered nature of the Claremont clasts. Since the aim of this section is to identify the different groups of clasts present in the Claremont conglomerate, these diagrams were used for comparative and classification purposes and not as a means of tectonic discrimination.

Complete results and statistical error calculations are presented in Appendix D.

**Table 5.1**

<b>Specie Group</b>	<b>Representative Elements</b>
Mafic	Ca, Ti, V, Mn, Zn, Sr, Y, Zr, Nb
Felsic	K, Fe, Zn, As, Rb, Sr, Y, Zr, Nb, Ba, Th
Sedimentary	K, Ti, V, Mn, Fe, Zn, Sr, Y, Zr, Nb, Ba

Table 5.1 List of representative elements per clast species group. Included elements deviate from individual sample mean by  $< 10\%$  for each sample within the species group. (See Appendix D).

## 5.2 RESULTS

The XRF data identified three distinct clast species. The mean results for the representative elements of each group are presented below: mafic (Table 5.2), felsic (Table 5.3) and sedimentary (Table 5.4). Results for anomalous clasts are included in Appendix D.

Table 5.2: Concentrations of elements (ppm) in mafic group clasts

Sample	Ca	Ti	V	Mn	Zn	Sr	Y	Zr	Nb
<b>2234.0</b>	60836	10694	155	1874	93	608	33	100	12
<b>2513.0</b>	36182	20644	216	1913	133	498	62	200	25
<b>2549.0</b>	54607	6017	88	1614	68	909	17	52	6
<b>2567.0</b>	61403	11124	137	2682	121	695	36	114	12
<b>2567.5</b>	68563	20301	296	2297	116	1027	59	172	20
<b>1819.0</b>	56610	17598	191	1655	96	513	49	164	22

Table 5.3: Concentrations of elements (ppm) in felsic group clasts

Sample	K	Fe	Zn	As	Rb	Sr	Y	Zr	Nb	Ba	Th
<b>1170a</b>	35876	10408	96	12	216	53	176	1037	72	68	24
<b>1237.0</b>	29485	19802	74	11	171	25	200	829	86	42	22
<b>1228.0</b>	13954	13225	89	10	86	67	46	296	87	59	21
<b>1232a</b>	27963	10403	61	10	123	55	77	227	80	80	22
<b>1232b</b>	13937	14796	60	10	100	118	44	272	77	169	20
<b>1279.0</b>	25260	18374	113	14	147	94	53	368	52	437	22

Table 5.4: Concentrations of elements (ppm) in sedimentary group clasts

Sample	K	Ti	V	Mn	Fe	Zn	Sr	Y	Zr	Nb	Ba
<b>BM-003</b>	8585	4301	51	403	21766	54	68	31	320	13	192
<b>BM-3M</b>	6843	4961	65	447	49749	84	66	51	244	16	170
<b>BM-2M</b>	13450	3192	48	777	21255	55	289	49	175	11	227
<b>BM-4M</b>	14315	3069	60	1336	22794	118	162	35	136	11	316
<b>2060c</b>	14364	4155	68	608	34466	73	85	26	139	14	311

Claremont data plotted on  $Zr/TiO_2$  vs  $Nb/Y$  discrimination diagram shows distinct clusters (Fig. 5.1). The data from mafic species form a tight cluster in the sub-alkaline field (Fig. 5.2). The felsic species group shows a more variable composition: plotting in two clusters roughly in the comendite-pantellerite - trachyte fields (Fig. 5.2). The felsic data are divided into sub-species 'A' and 'B'. The sedimentary species is included to show relative clustering from felsic and mafic species. The former plots at an intermediate composition between the felsic and mafic species. A separate discrimination (Pearce & Cann, 1973) shows similar discrimination among the Claremont clasts (Fig. 5.3).

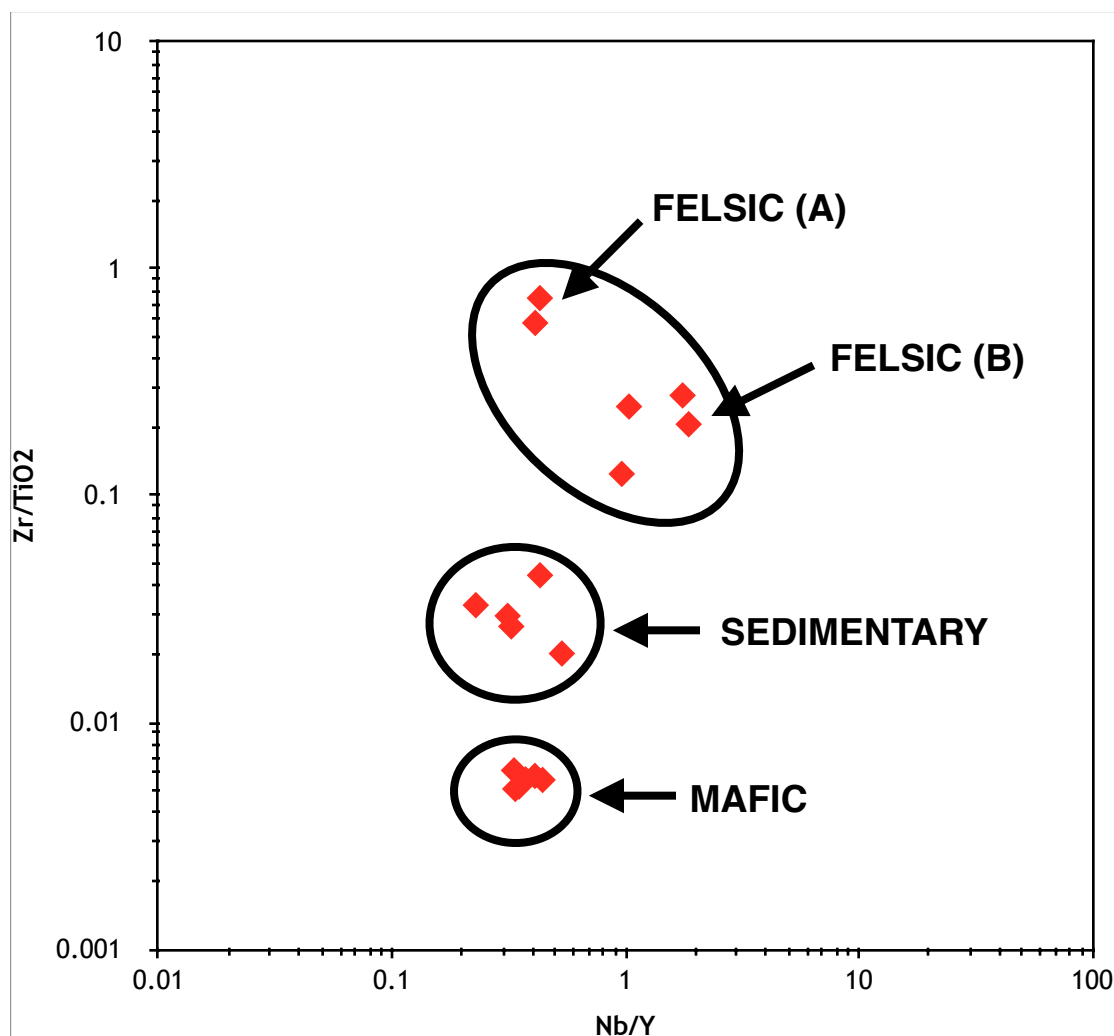


Fig. 5.1 Claremont species groups outlined. Felsic species can be sub-divided: data plot in distinct clusters. These sub-species are referred to as Felsic (A) and Felsic (B). (Discrimination based on Winchester and Floyd, 1977).



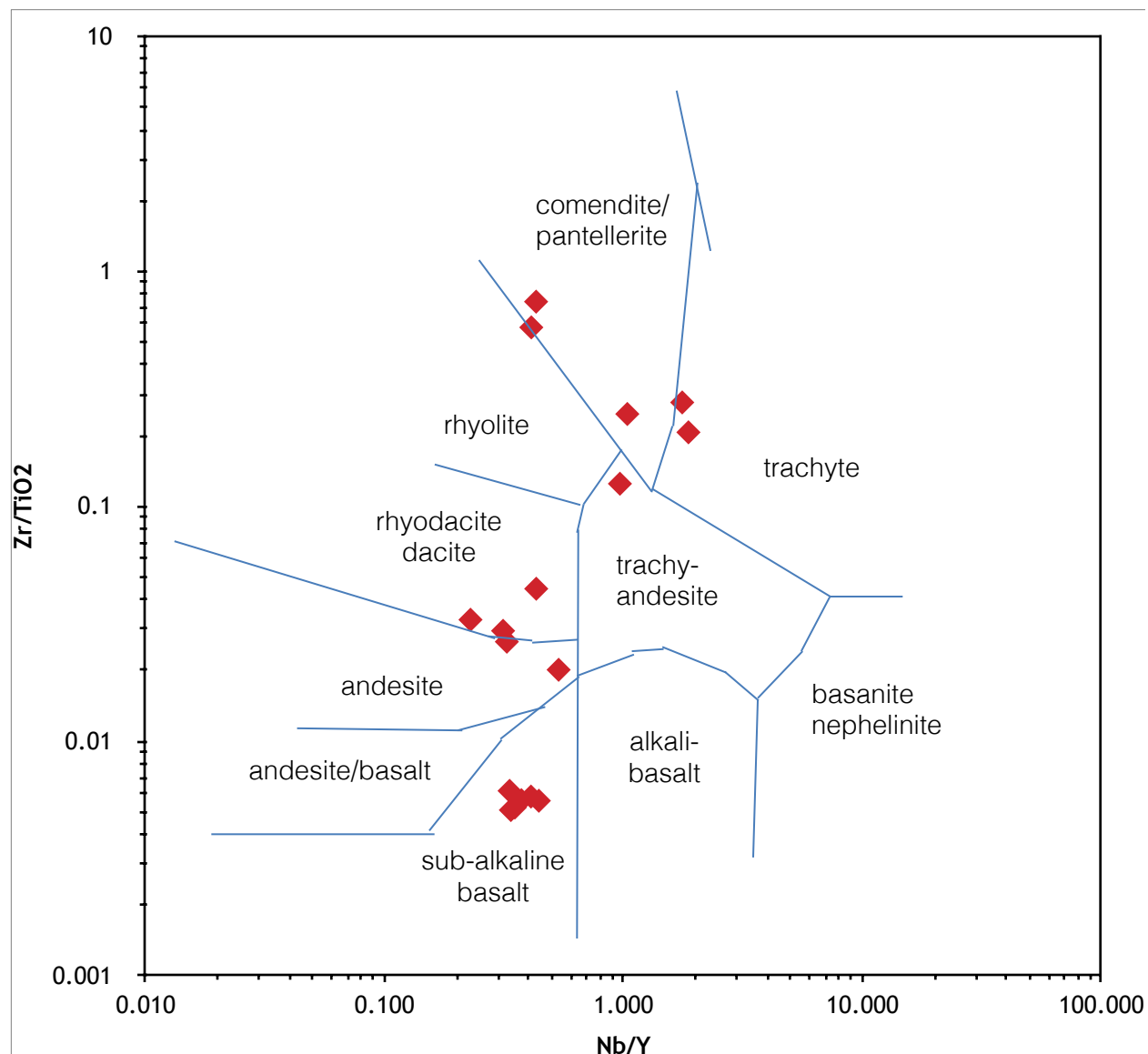


Fig. 5.2 Claremont data (red) clusters into three distinct species. Composition fields characterize the mafic species as sub-alkaline basalt while the felsic species is trachyte and comendite/pantellerite. (Fields are modified from Winchester & Floyd, 1977)

It should be noted that two samples plotted highly peraluminous and are distinct in the comendite/pantellerite field (Fig. 5.2). Due to the fact that there were only two samples and that the felsic group showed considerable variation, these were not treated separately.



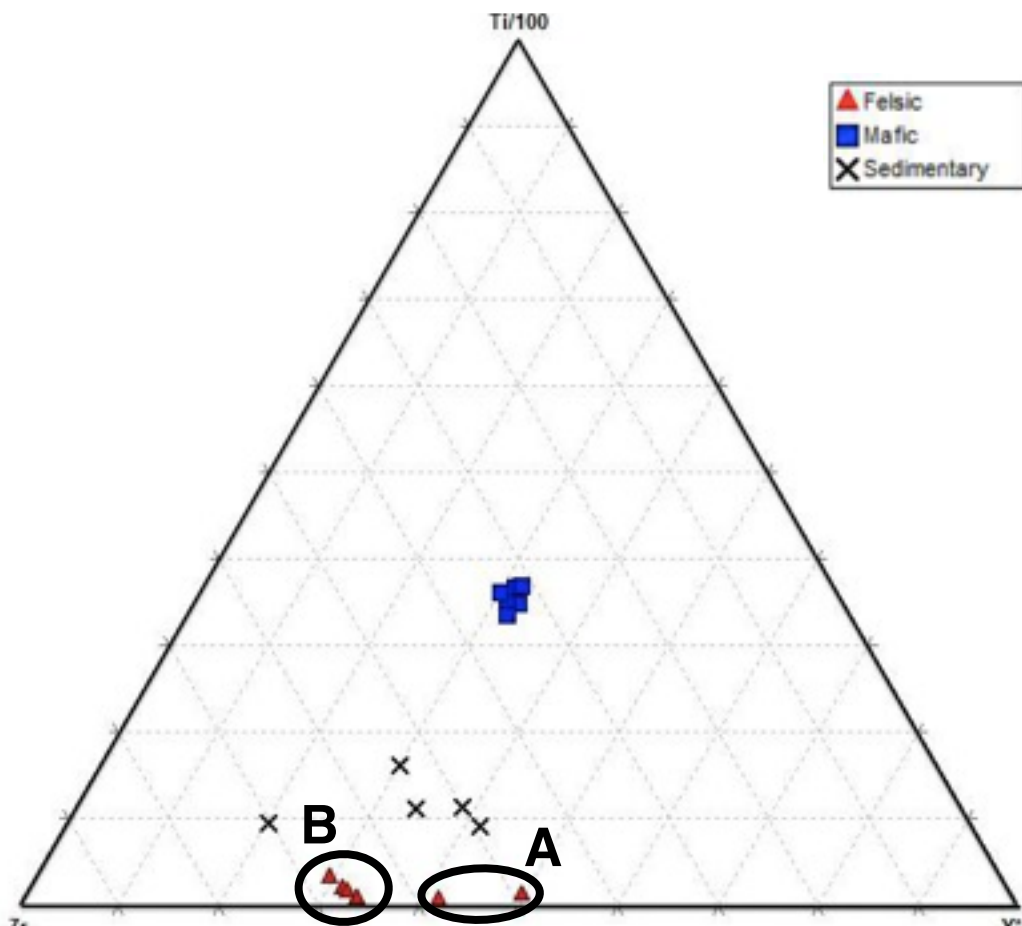


Fig. 5.3 Division of Claremont data based on discrimination diagram by Pearce and Cann (1973) is concordant with Winchester species groupings (Fig. 5.1). Felsic, mafic and sedimentary species groups plot distinctly. Division of felsic species is repeated. Sedimentary species included to show relative distinction between all three Claremont species.

Multi-element diagrams were used to investigate further the trends of trace element. The mafic species group show almost identical element behaviour with a greater concentration range observed for elements Ti, Y, Zr and Nb (Fig. 5.4). The mafic data forms a tight cluster which plots as sub-alkaline according to Winchester & Floyd (1977).

The sedimentary species clusters at a composition intermediate between the felsic and mafic groups (Fig. 5.2). The multi-element diagram for the sedimentary species shows all

## Multi-Element Diagram: Mafic Species

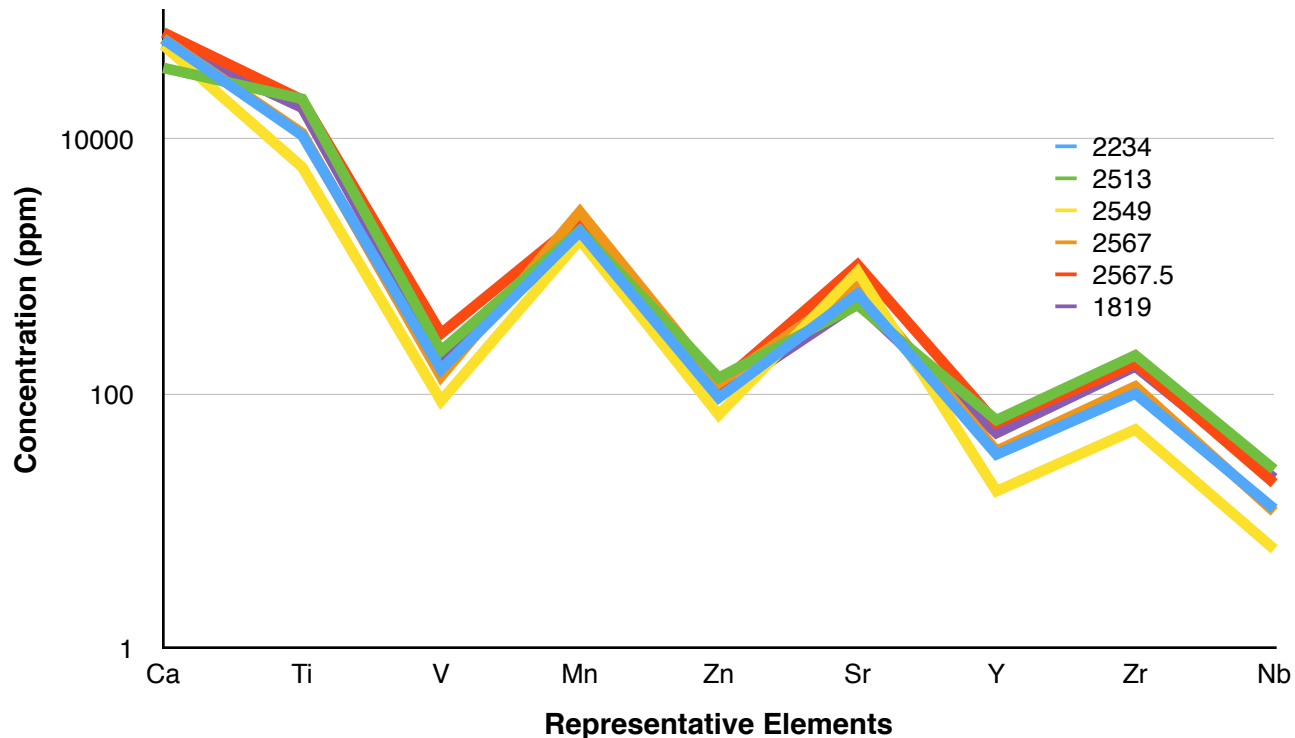


Fig. 5.4 Multi-element diagrams for mafic species group show identical relationship between samples for representative elements (Table 5.1). Some variability with Ti, Y, Zr and Nb. Concentration in log

components have a similar element trends and a tight compositional range (Fig. 5.5). Slight range in concentration is observed in clast samples BM-2M and BM-4 for elements Mn and Sr.

The felsic species shows the greatest elemental range. Sub-species A and B plot within the commendite/pantellerite (CP) or trachyte fields respectively (Fig. 5.2: Winchester & Floyd, 1977). Claremont samples comprising sub-species 'A' and 'B' are listed in Table 5.5. The multi-element diagram for the felsic species shows similar concentration within the sub-species (Fig. 5.6). Sub-species A is distinguished by Sr and Zr concentrations but otherwise has a similar trend to the rest of the species (Fig. 5.6). The distinction between the felsic sub-species is replicated in

## Multi-Element Diagram: Sedimentary Species

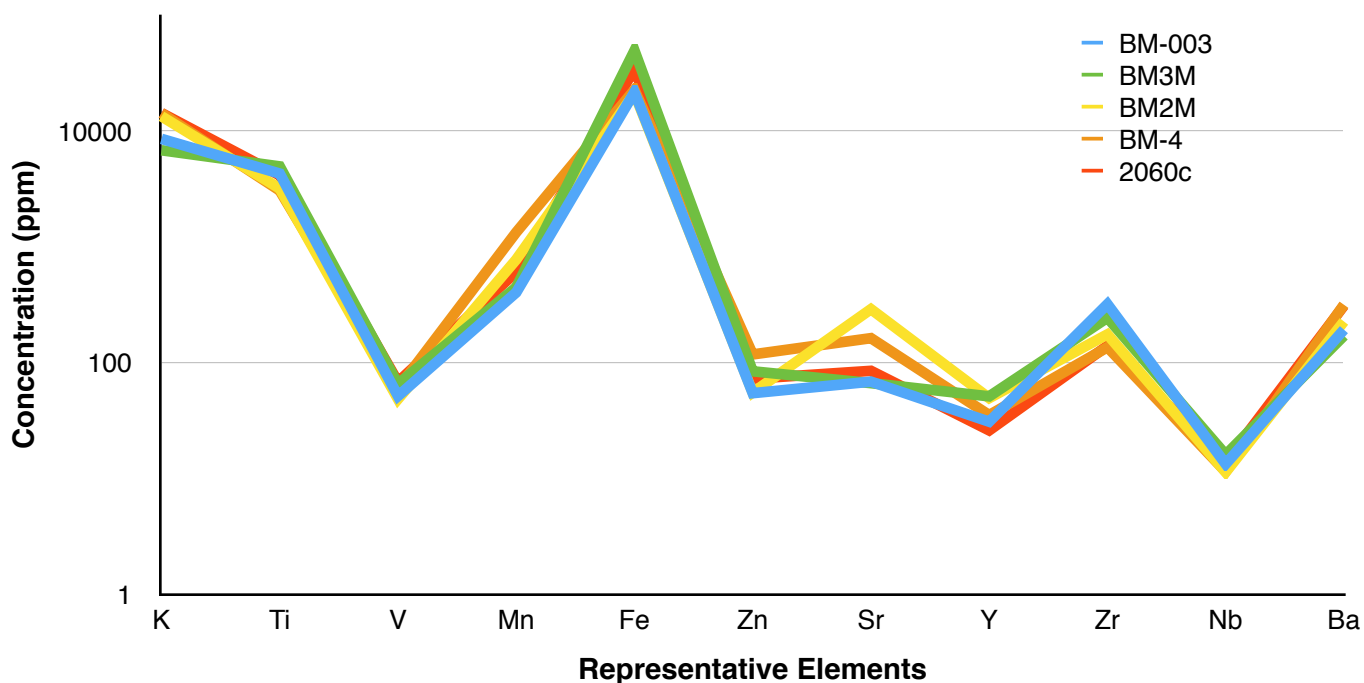


Fig. 5.5 Multi-element diagram with representative elements for the sedimentary group. All elements except for Sr show similar concentrations. Sedimentary samples BM-2M and BM-4 are enriched in Sr relative to the rest of the species group. Concentration in log scale.

## Multi-Element Diagram: Felsic Species

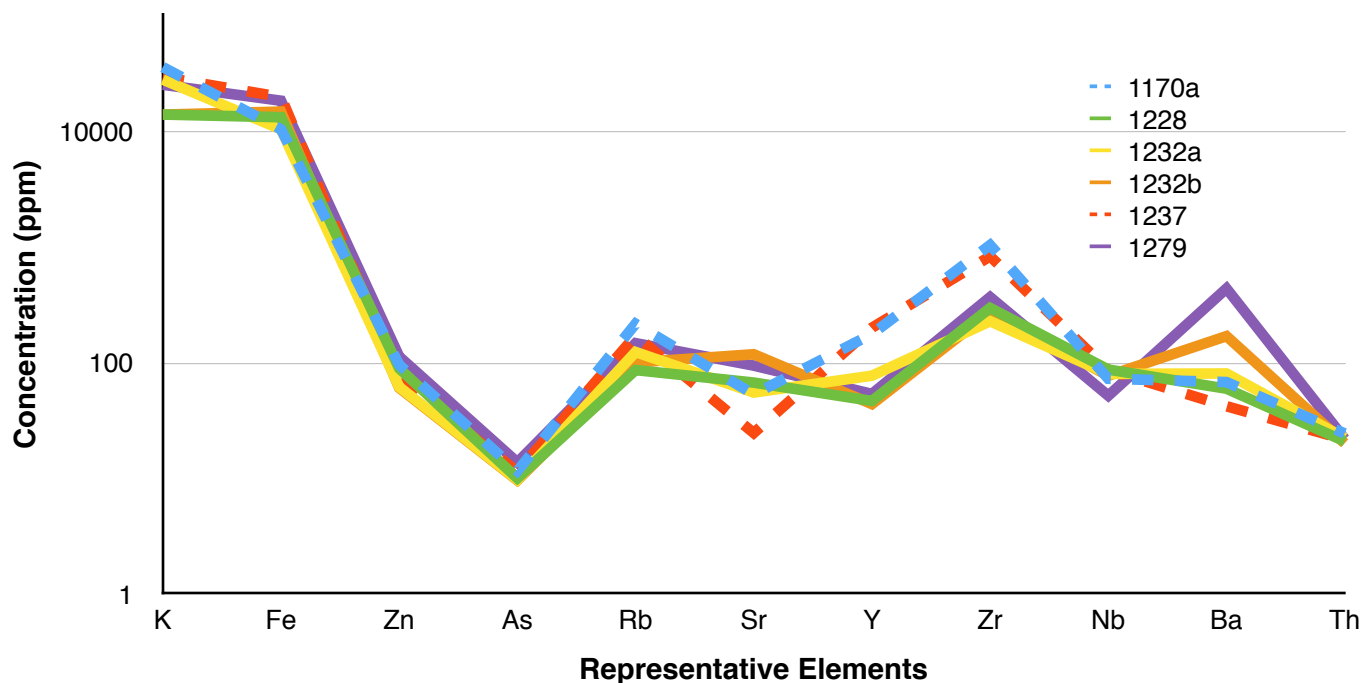


Fig. 5.6 Multi-element diagrams for felsic species group is the most variable. Considerable variation of Sr, Zr and Ba is contrasted by very similar concentrations of Fe, Zn and As in the species group. The variability of elemental range is diminished when considering only sub-species (sub-species A is represented by dotted lines).

a granite discrimination diagram (Fig. 5.7).

**Table 5.5 Felsic sub-species:**

A	B
1170	1228
1237	1232a
	1232b
	1279

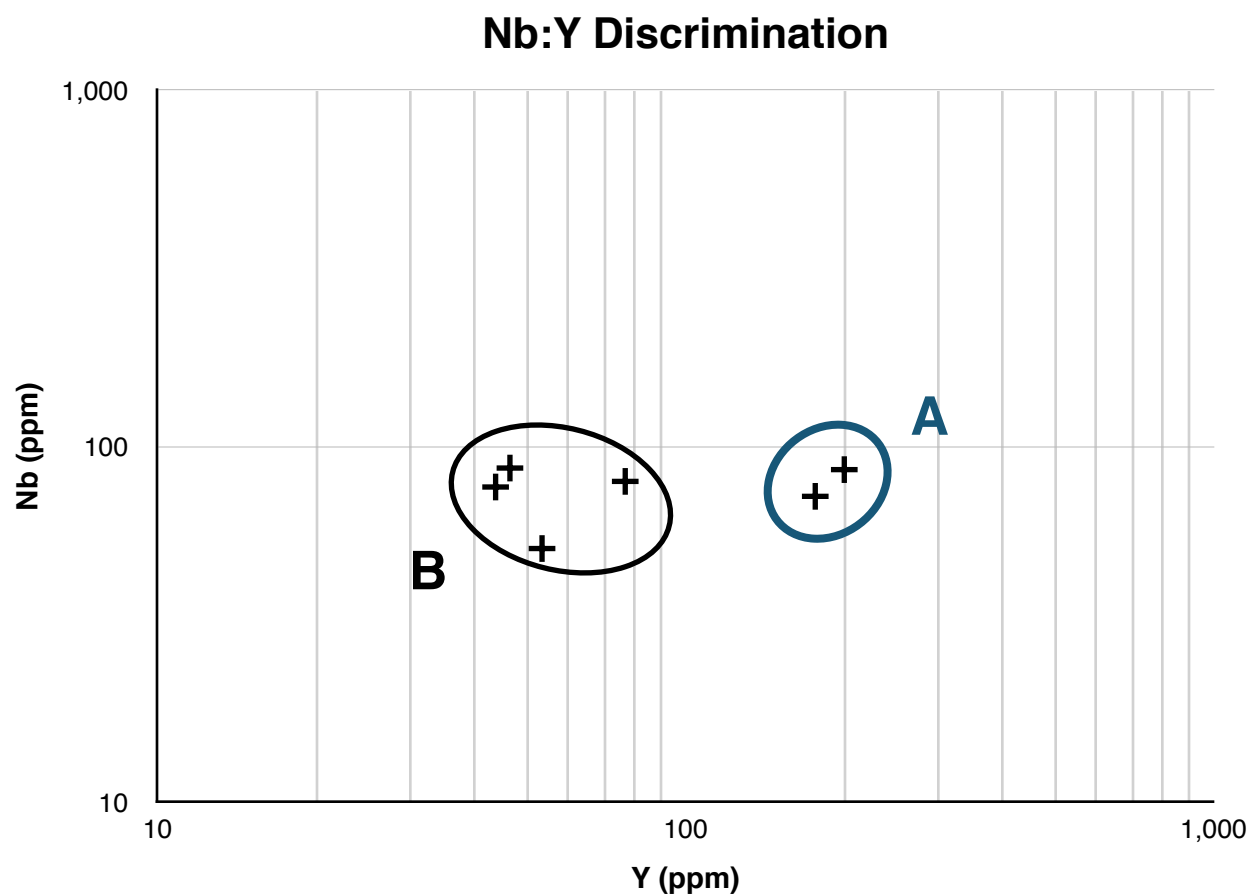


Fig. 5.7 Data from felsic species form distinct clusters and also divide the group into sub-species A and B. (Pearce et al., 1984)

## CHAPTER 6: Comparative Analysis to Possible Source Rocks

### 6.1 GEOCHEMISTRY

Results from XRF geochemistry are used to compare clast compositions with those of possible source rocks for each of the clast species in the Claremont conglomerate.

#### 6.1.1 INTRODUCTION

The Claremont clast samples are compared to hand samples and the geochemical data of proximal units in the Eastern Cobequids. At the time of research for this thesis, data were available from the Byers Brook, Dalhousie Mountain, Wilson Brook and Folly River Formations

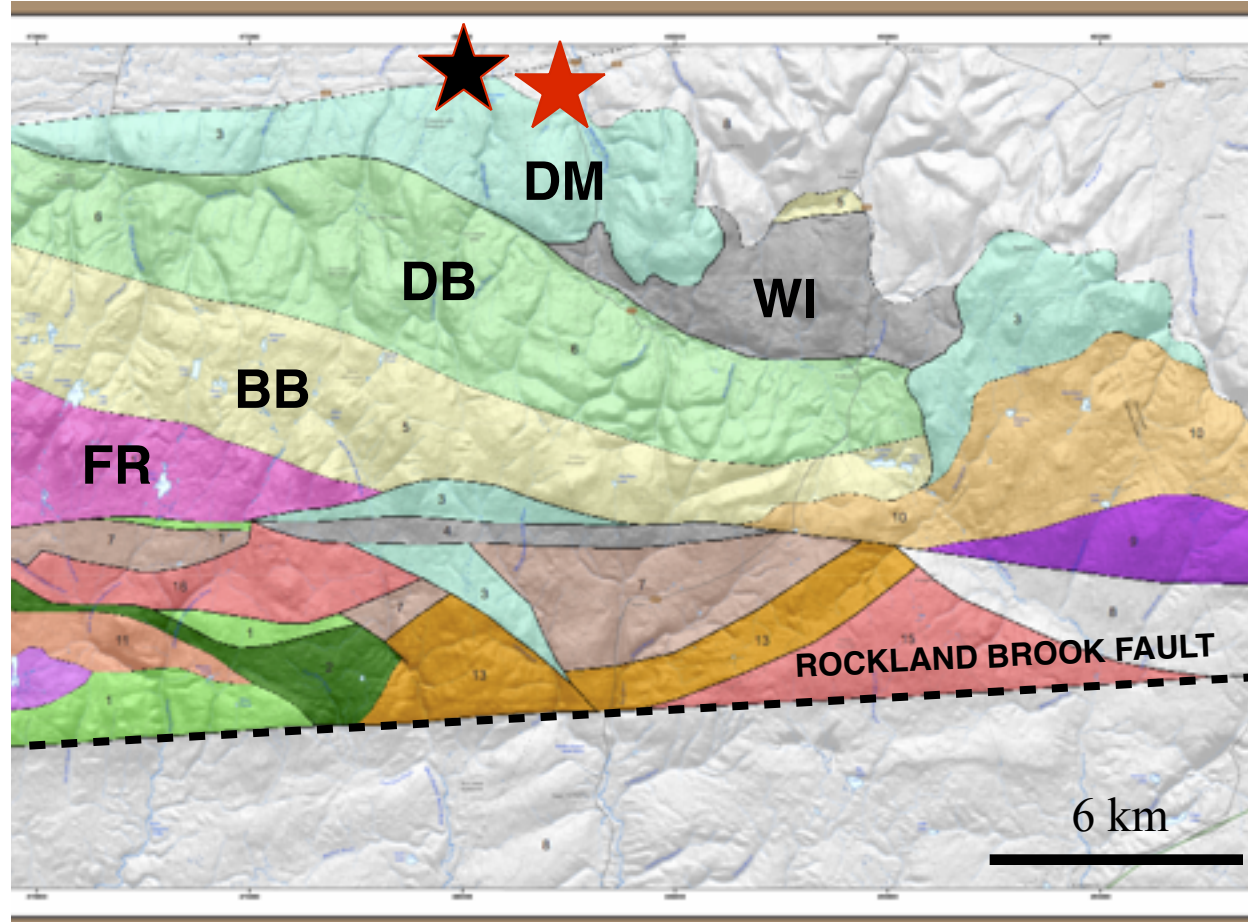


Fig. 6.1 Geological map of the Eastern Cobequids. Sampling locations indicated by stars (core is black, outcrop in red). Proximal formations to the Claremont conglomerate are (in order of proximity): Dalhousie Mountain (DM), Diamond Brook (DB), Wilson Group (WI), Byers Brook (BB) and Folly River (FR). Southern units are cut by the Rockland Brook Fault. Map modified from MacHattie (2012).

through T. MacHattie (DNR) (pers. comm.) who worked in this area of the Cobequids between 2009-2012 (MacHattie, 2012; 2013; 2014). T. MacHattie's data from proximal units in the Eastern Cobequids are hereafter referred to as "Eastern Cobequid data". These Cobequid units form a sequence of adjacent formations and are located south of the Claremont conglomerate (Fig. 6.1).

The Eastern Cobequid data have been analyzed and classified into working groups defined by formation and rock type of the sample (T. MacHattie pers. comm.):

Data for the Dalhousie Mountain Formation (DM) consist of 65 samples of siltstone, basalt, chert, dacitic tuff and rhyolite rocks. Twenty-six samples from the Wilson Formation (WI) data include siltstones, Silurian siltstones and tuffs. The data from the Byers Brook-Diamond Brook (BB-DB) Formation includes basalts, rhyolites, siltstones and volcaniclastics (over 750 samples). Though they are mapped as separate units, the data from the Diamond Brook and Byers Brook Formations are merged due to the disputed nature of the contact between them (T. MacHattie, 2012; Piper, 2002).

Due to the comparative nature of this study, the Claremont data was plotted against like-type clasts. Tentative unit correlations are made from comparing both hand samples and XRF geochemistry.



### 6.1.2 RESULTS & DISCUSSION

The Claremont clasts plot within the range of the Eastern Cobequid data points (Fig. 6.2). The mafic group plots well within the range for both the Byers Brook-Diamond Brook and Folly River Formations (Fig. 6.2). Both the felsic Claremont sub-species matches the Byers Brook-Diamond Brook Formation despite a slight deviation from the mean Nb/Y ratio for the sub-species B (Fig. 6.2).

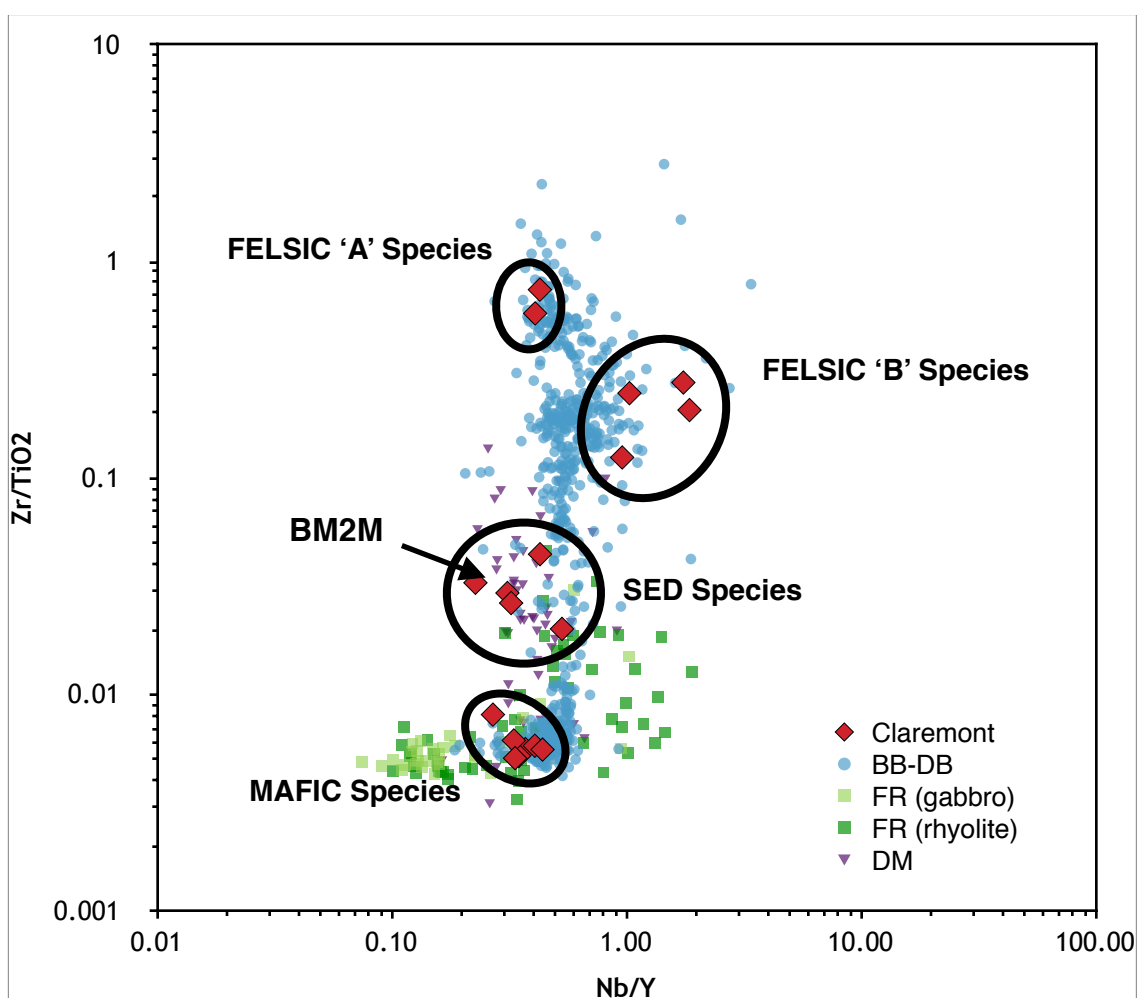


Fig. 6.2 Claremont data (red) plot within the compositional range of Eastern Cobequid units. Sedimentary clast BM2M and the felsic sub-species B lie slightly off mean trends. (Eastern Cobequid data from T. MacHattie, pers. comm.).

The Claremont geochemistry as a whole roughly reflects the bimodal character of the Byers Brook-Diamond Brook data (Fig. 6.3). Both Claremont felsic sub-species correlate exclusively to the BB-DB Formations (Fig. 6.3). Two-element diagrams show similar trace element signatures for the Claremont felsic species and BB-DB rhyolites (Fig. 6.4). Slight discrepancies are present due to higher strontium concentrations in the Claremont clast samples.

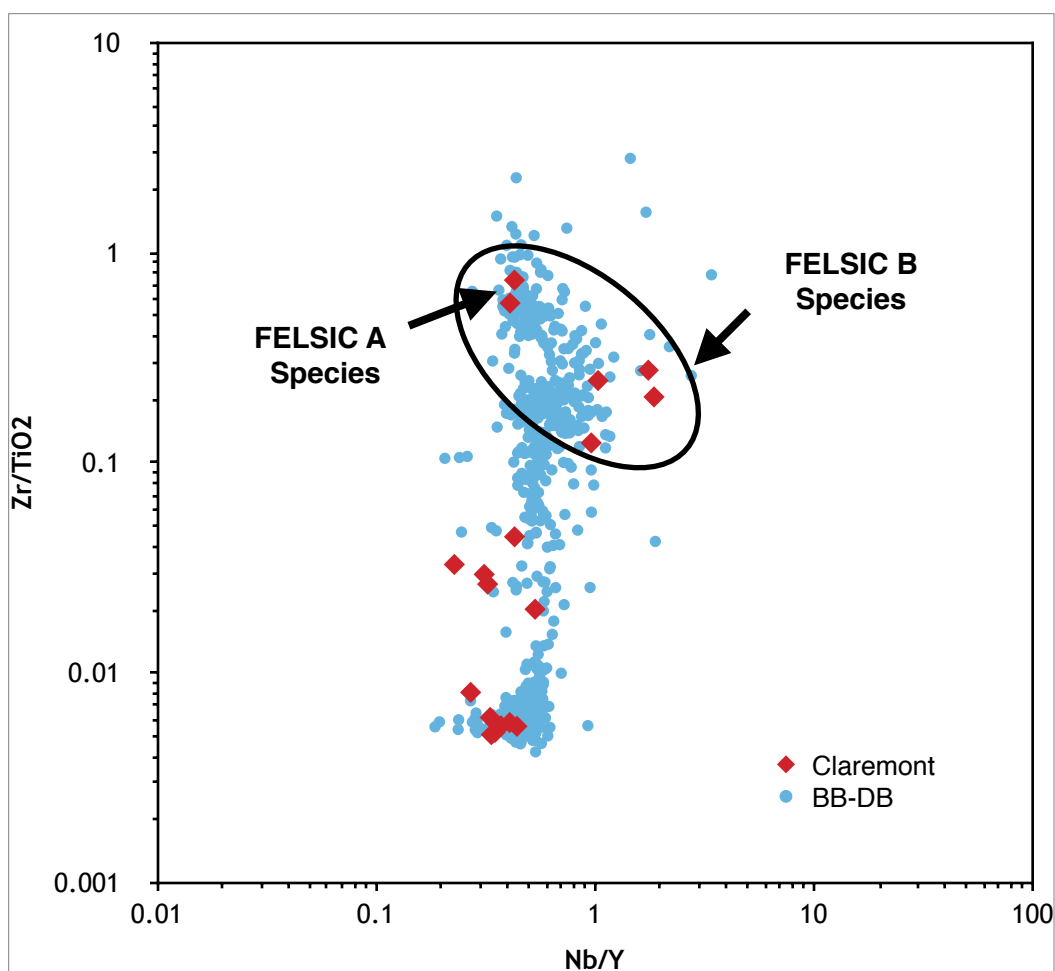


Fig. 6.3 Felsic species (outlined) plots around composition of BB-DB Formation only (compare to Fig 6.2). Bimodal distribution of Claremont clasts as a whole is reflected by BB-DB Formation. (BB-DB data from T. MacHattie).

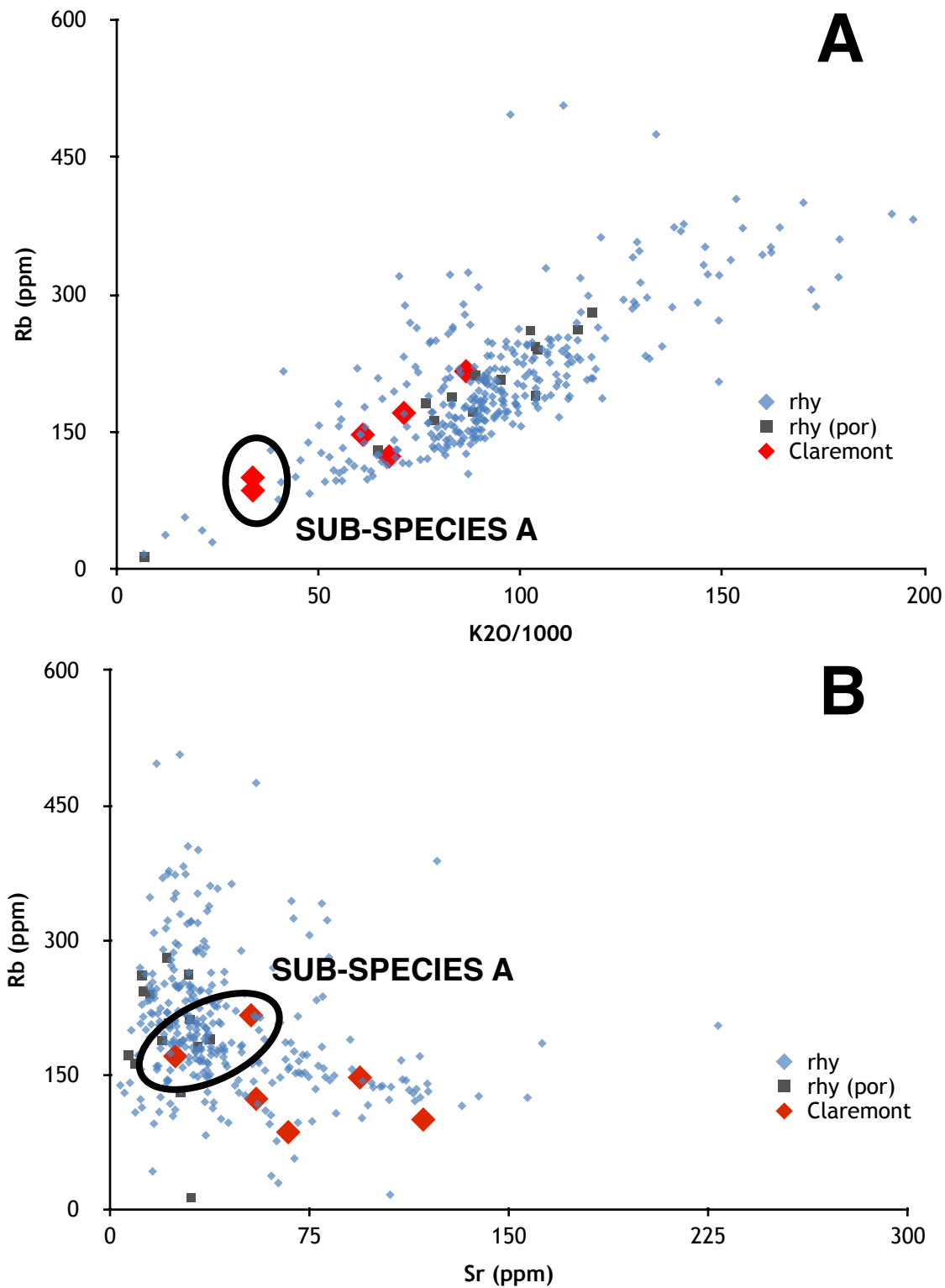


Fig. 6.4 Element diagrams show similar trend between Claremont felsics and BB-DB rhyolites. Claremont data show Sr enrichment. Sub-species are distinguishable (felsic sub-species B left unmarked). BB-DB rock types plotted are rhyolites (rhy) and porphyritic rhyolites (rhy-por).

The Claremont mafic species data share similar composition to both the BB-DB and Folly River Formations according to the Winchester & Floyd discrimination (Fig. 6.5). However, two-element diagrams show better correlation to Byers Brook - Diamond Brook basalts (Fig. 6.6). The Claremont mafic clasts also show elevated concentrations of Sr relative to the Eastern Cobequid data (Fig. 6.6c, f).

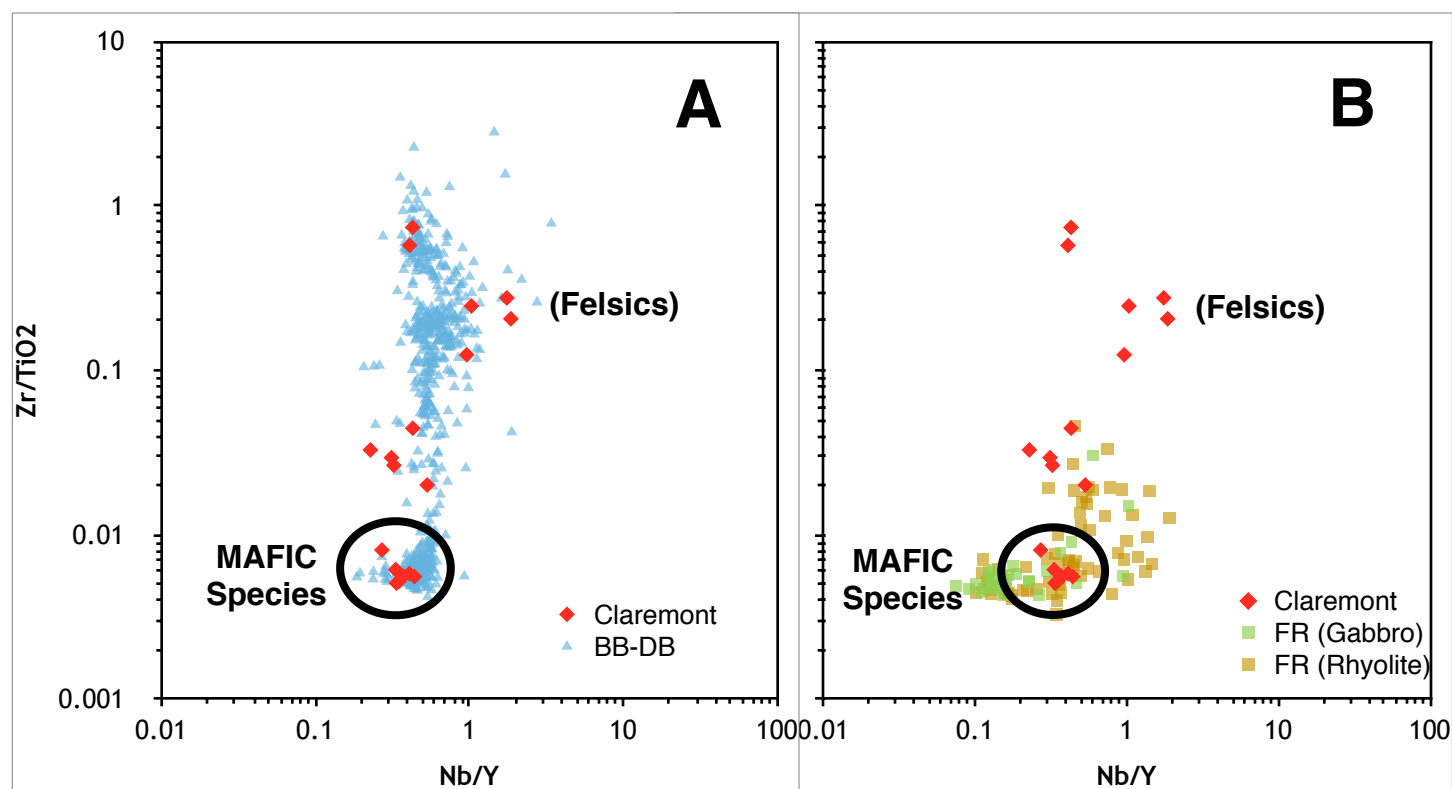


Fig. 6.5 Claremont mafic group shows same compositional range as both Byers-Diamond basalts (A) and Folly River volcanics (B). Bimodal distribution of entire Claremont suite is reflected by Byers-Diamond Brook Formation.

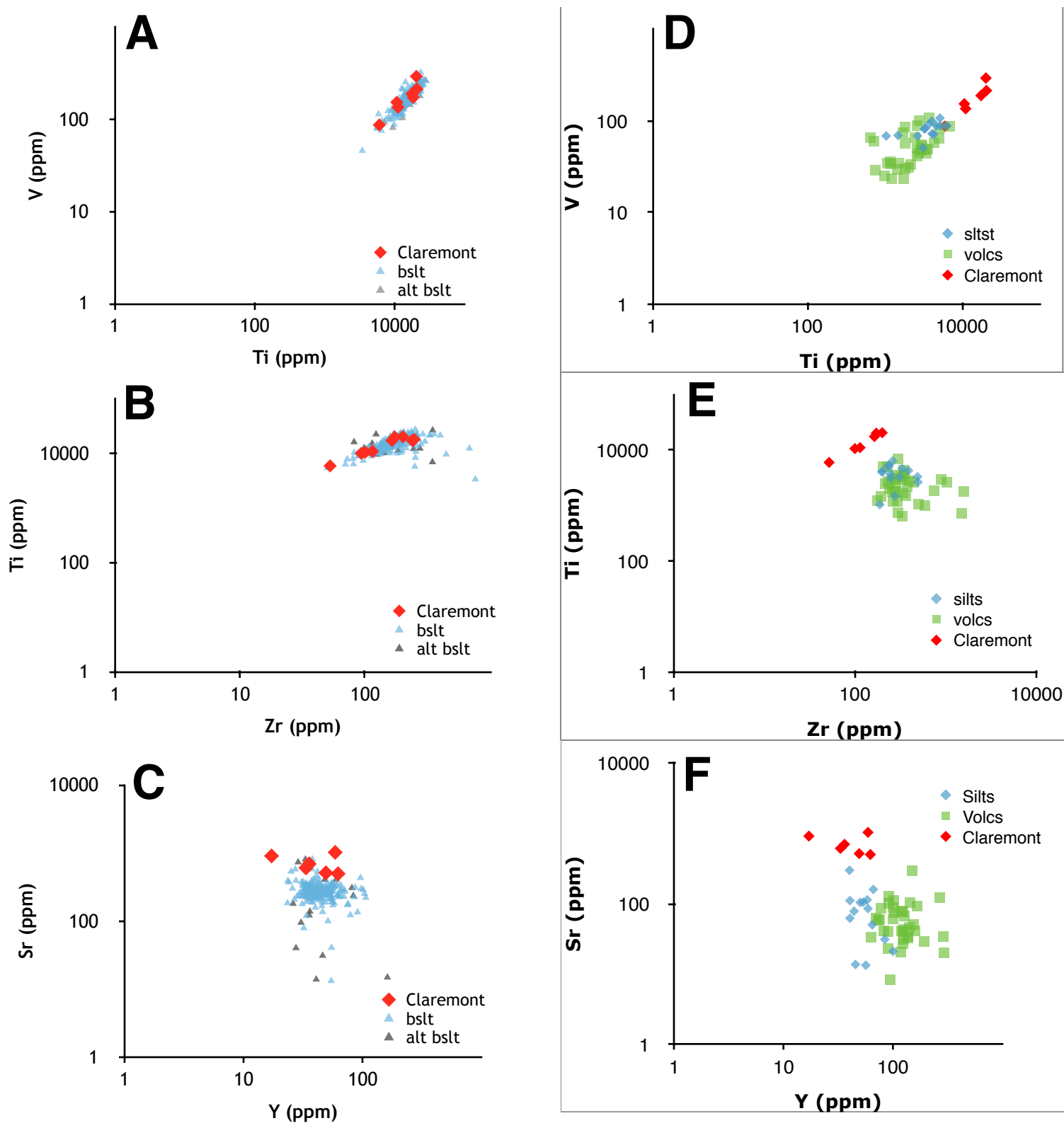


Fig. 6.6 Two-element diagrams show Claremont mafic species is more tightly clustered to BB-DB Formation (A-C) than the Folly River Formation (D-F). High concentration of Sr in Claremont mafic samples are uncommon but present in BB-DB samples (C). Log scale used throughout.

The sedimentary Claremont species plots at an intermediate between the bimodal (igneous) populations of the BB-DB Formation (Fig. 6.7). Two-element diagrams compare the sedimentary species to the BB-DB and to the Wilson Brook Formation (Fig. 6.8-9).

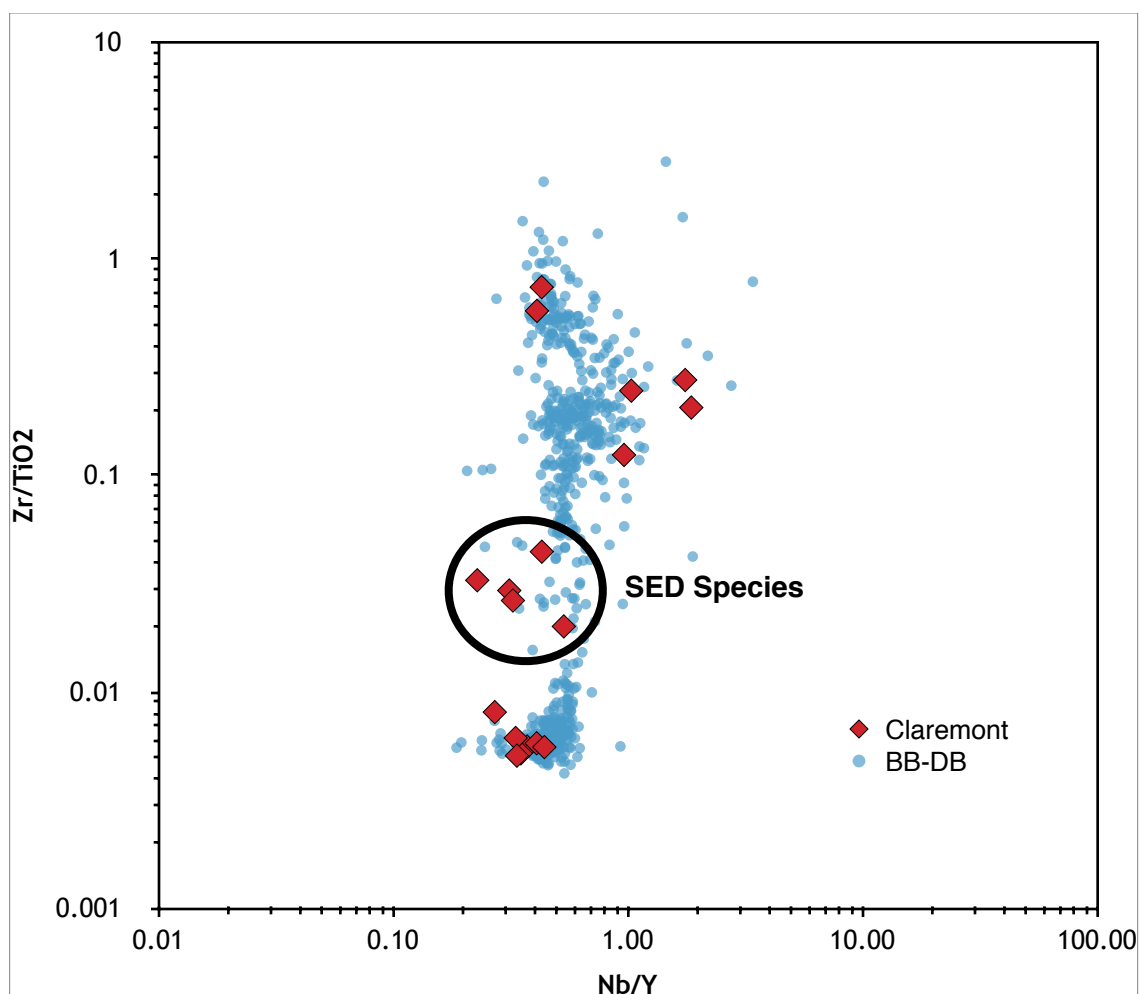


Fig. 6.7 Claremont sedimentary species plots at an intermediate between the bimodal igneous populations of the BB-DB. (Wilson Brook Formation data not included due to poor Nb results).

The Wilson Brook Formation was considered for comparison since it contains Silurian-aged siltstones and since preliminary observations of the Claremont limestone clasts suggested Silurian age (R. Ryan, pers. comm.). The sediment species shows a similar degree of correlation to the Wilson Brook and BB-DB Formations (Fig. 6.8-10). However, Ti-Zr diagram shows a



higher degree of correlation between the Claremont sediment species and the Wilson Brook Formation (Fig. 6.9).

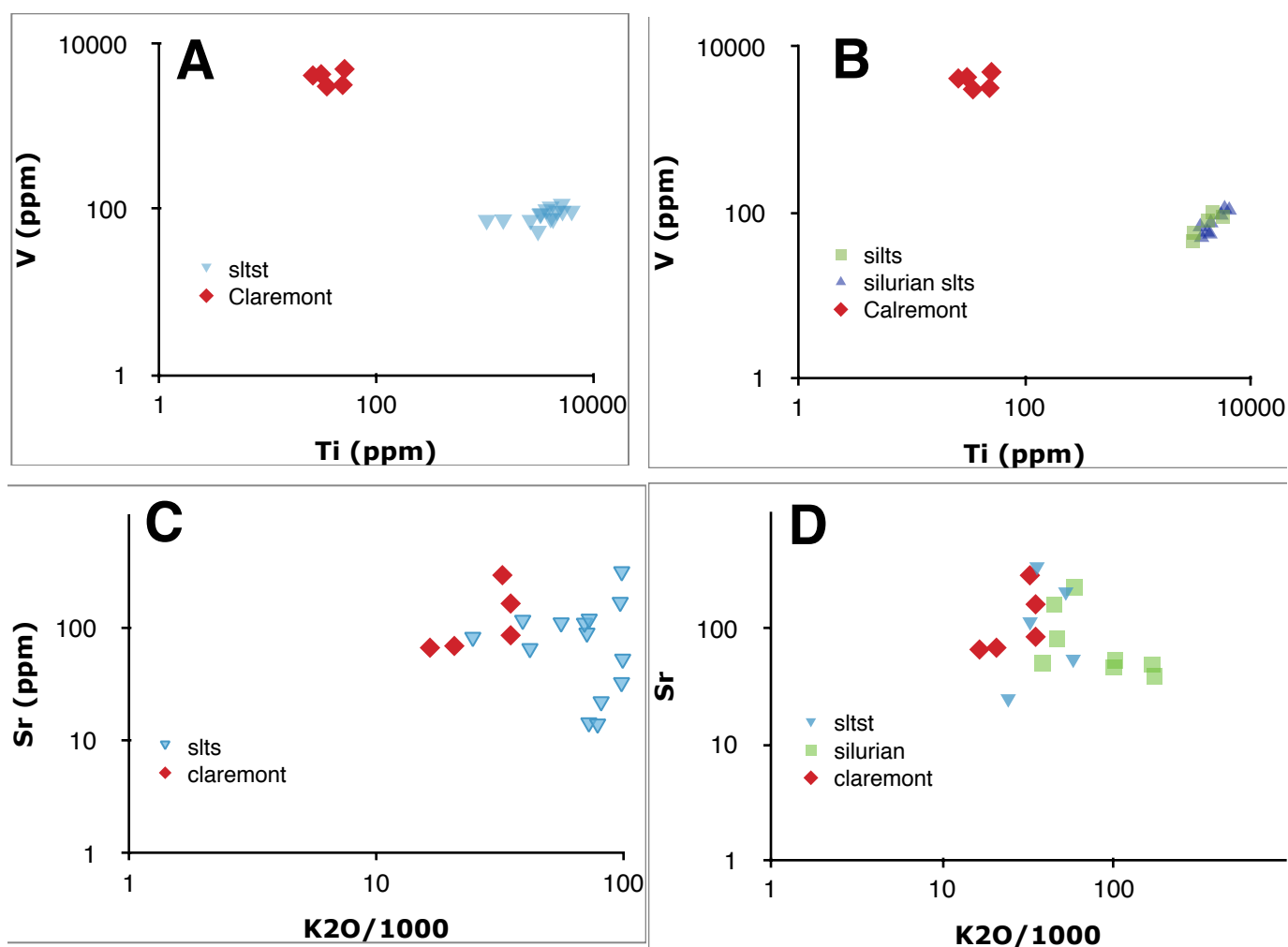


Fig. 6.8 A, C) Claremont sedimentary species against BB-DM siltstones: Mobile element compositions are comparable (C) while more immobile elements are distinct (A). B, D) Claremont sedimentary species against Wilson Formation shows same distinction as with BB-DM Formation. “siltst”: siltstone (rock types identified by T. MacHattie). Log scale used.

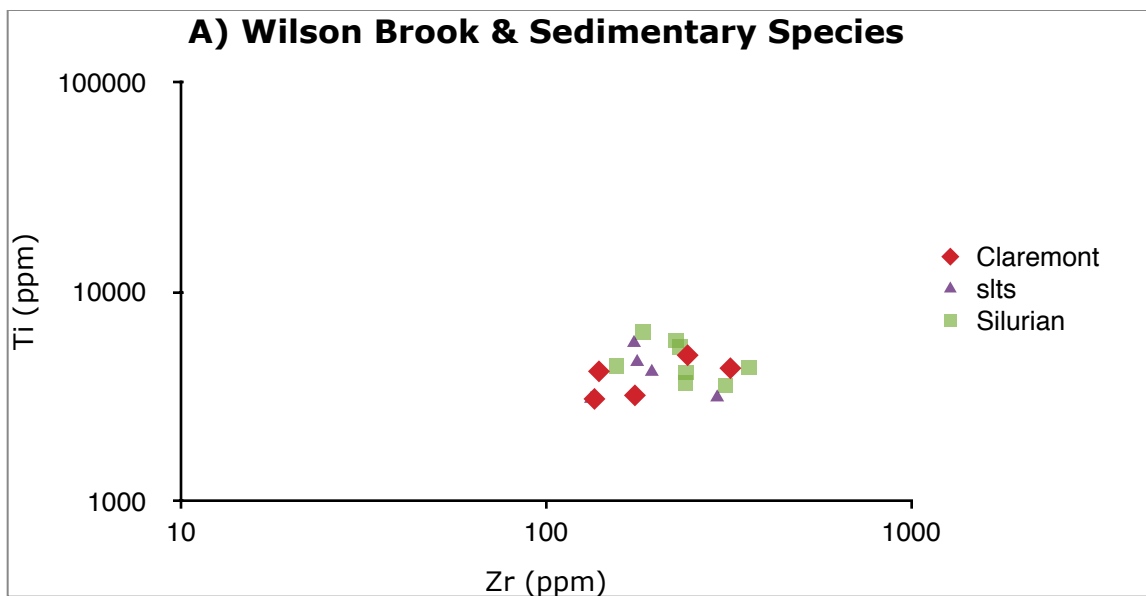
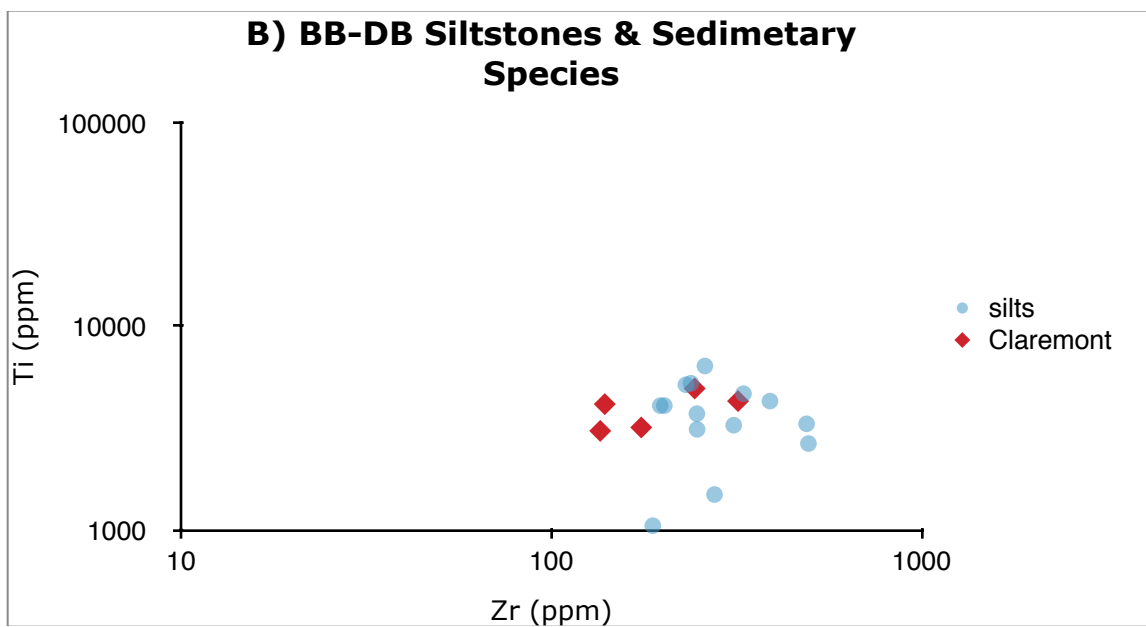


Fig. 6.9 Claremont seds have comparable compositions with Wilson Brook and Byers Brook-Diamond Brook siltstones (A, B). Ti-Zr elements chosen for immobility. Sedimentary group correlate best with Wilson Formation (A). (rock type identified by T. MacHattie).



## 6.2 HAND SAMPLE COMPARISON

### 6.2.1 INTRODUCTION

To complement the geochemical comparison, a brief observation of hand samples from the Eastern Cobequids was conducted to determine whether hand samples with unique petrologic features could reflect the unit correlations established by XRF geochemistry. Hand samples from T. MacHattie were visually compared to the Claremont clasts.

Eastern Cobequid samples were collected by T. MacHattie between 2009-2014. These are the same samples that were used to obtain XRF geochemical data from the Eastern Cobequids (used in previous sections).

### 6.2.2 RESULTS & DISCUSSION

The results are summarized in Table 6.1.

**Table 6.1:**

Correlating Claremont clasts to Eastern Cobequid Formations by comparing hand samples. Note: BB=BB-DM Basalt; BR=BB-DM Rhyolite (Rock type determined by T. MacHattie). \*Question mark denotes Cobequid samples with unknown Formation (no conclusive correlation)

Identifying Feature(s)	Claremont sample	MacHattie Sample	Formation of DNR samp
Med-grained euhedral pink phenocrysts in dark plum-coloured aphanitic matrix	1237	10TM0127 10TM0126 11TM0484 11TM0358 11TM0249 11TM0252	Porphyritic BR Porphyritic BR BR BR BR BR
Irregular carbonate inclusions	BM-4	12TM0716A 10TM0150A (vesicular)	Wilson BR
Salmon-coloured phenocrysts in phanitic pink groundmass, chaotic flow?	1232a	11TM078	BR

Grey siltstone	BM2M	10TM0244	BB*
anhedral f.-m. grained pink phenocrysts in pink groundmass	1228	12TM0351 12TM0336* 12TM0337* 12TM0352* <i>*smaller phenocrysts</i>	?
Coarse grained, leucocratic (migmatic?) with abundant green mineral	2549	12TM0655 12TM0652	?
Equigranular mafic	1819	12TM0567 12TM0585B 12TM0586 12TM0554 12TM0556 11TM0426 11TM0427 11TM0432A 11TM0431 11TM0434	?     BB BB BB BB BB
Porphyritic mafic	2234	11TM0422A	BB

The hand sample data are consistent with geochemical results. The Claremont mafic species visually match Cobequid clasts from the BB-DM Formation (Fig. 6.10). Samples 1237 and 1232a from the Claremont felsic species resemble rhyolites also from BB-DM Formation (Fig. 6.11). Rhyolite samples with medium-coarse grained pink phenocrysts are common among the DNR samples and are identical to Claremont sample 1237 which supports the interpretation that the BB-DM Formation is the source rock for this species (Fig. 6.12). The carbonate patches in sample BM-4 of the felsic species are similar to carbonate in samples from the Wilson Brook Formation (Fig. 6.13a). This feature might be related to amygdules observed in rocks from BB-DM rhyolites (Fig. 6.13b).



Fig. 6.10 Claremont sample 1819 (representative of mafic species) appears identical to DNR basalt samples 12TM0567 and 12TM0585B from the Byers Brook Formation. BIC pen for scale.

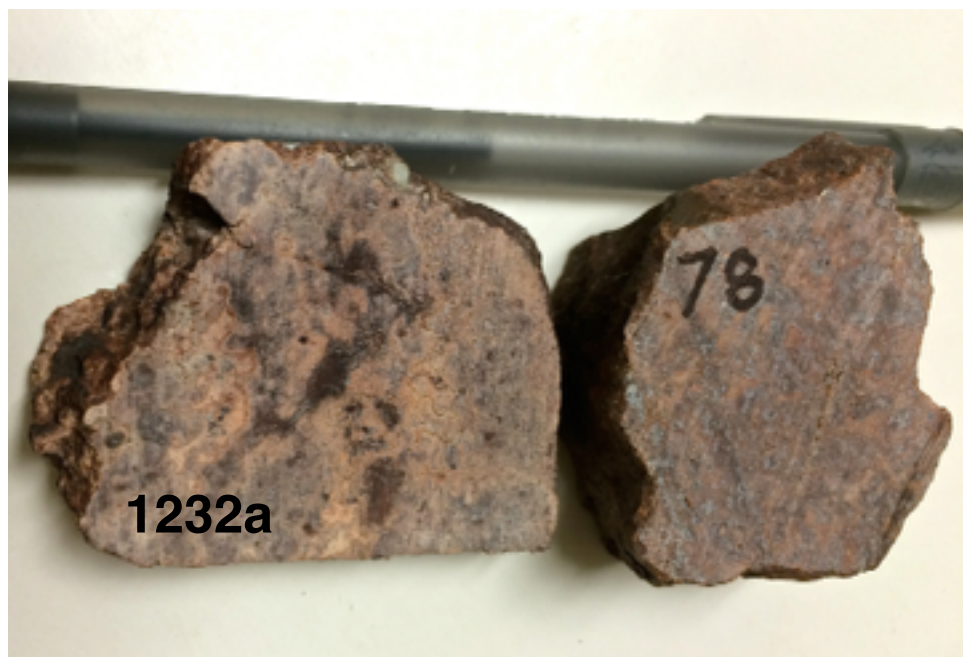


Fig. 6.11 Claremont sample 1232a is similar to Cobequid sample 11TM078, a rhyolite from the Byers Brook Formation. BIC pen for scale.

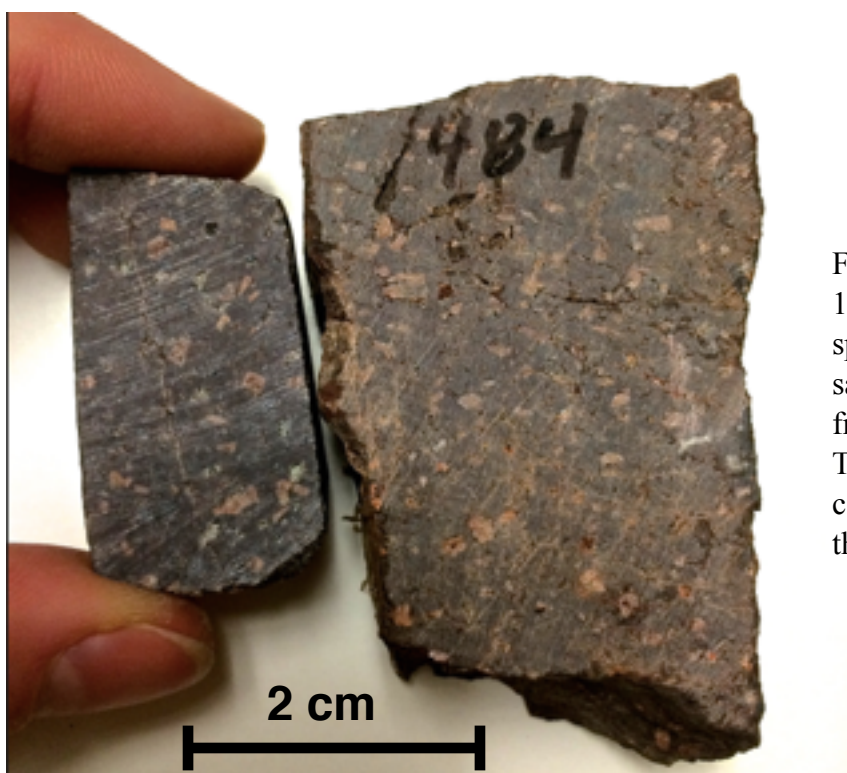


Fig. 6.12 Claremont sample 1237 (representative of felsic species) resembles Cobequid sample 11TM0484, a rhyolite from Byers Brook Formation. This porphyritic rock is common among samples from the Eastern Cobequids.



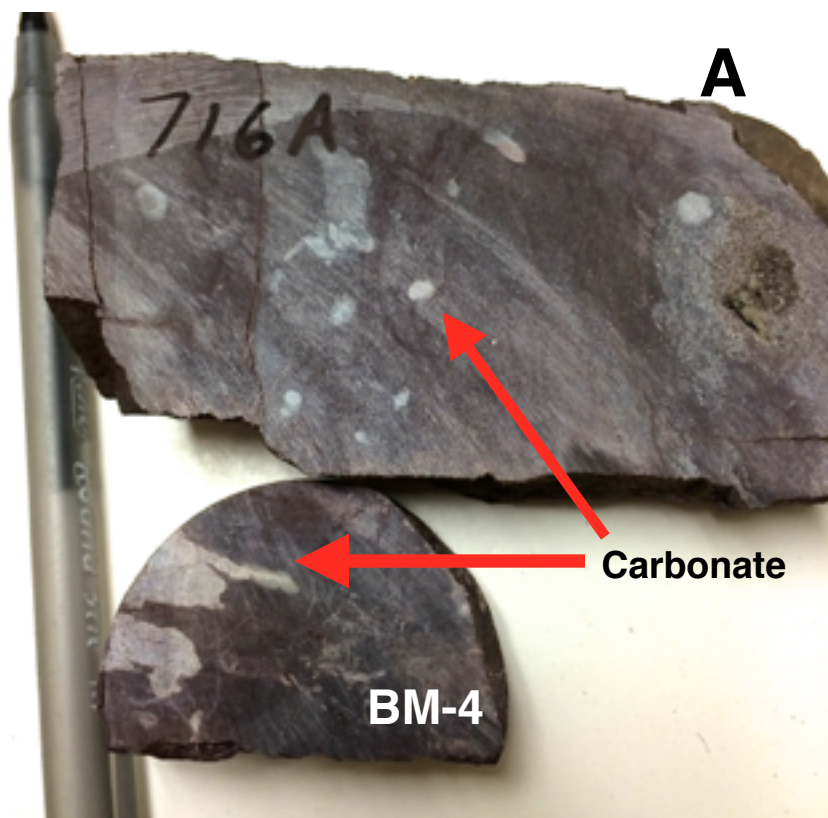
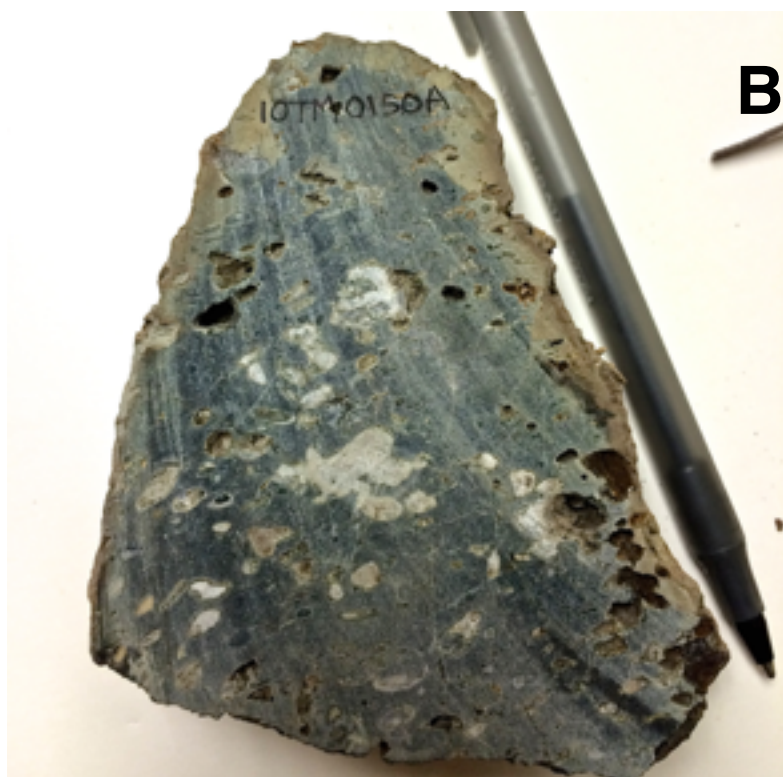


Fig. 6.13 A) Irregular carbonate patches in Claremont sample BM-4 are similar to carbonate in samples from the Wilson Brook Formation. B) Similar material in amygdules of Byers Brook Formation. BIC pen for scale.



## CHAPTER 7: Discussion

### 7.1 CLAST SPECIES

Preliminary clast groups determined by petrographic analysis are consistent with interpreted geochemical groups. The suites of clasts identified in the Claremont conglomerate consist of felsic, mafic and sedimentary species (Fig. 5.1). The Claremont clast species determined by each analytical method are summarized in Table 7.1 and discussed below.

The results for the mafic species showed the greatest congruence across analytical methods. The geochemical data for this group shows minimal compositional variation: the data form tight clusters on elemental diagrams (Fig. 5.1; 5.3). From the sub-alkaline basalt composition and comparative analysis, the mafic group correlates to the BB-DB basalts (Fig. 6.5-6).

The Claremont felsic species also shows consistent results across analytical methods. This species overlaps with the BB-DB rhyolites only (Fig. 6.3). However, the degree of geochemical variability in the felsic species is unexpected since finer-grained materials generally have less variable XRF results due to a greater grain density under the X-ray beam. The variability suggests an inherent distinction between these samples. Two separate sub-species of felsic clasts are inferred from this distinction: “sub-species A” and “sub-species B” (Fig. 6.4; Table 5.5). Discrimination diagrams reveal a good correlation between the BB-DB rhyolites and the Claremont sub-species A. Sub-species B repeatedly plots along the periphery of compositional range of the BB-DB rhyolites (Fig. 6.4). This variation, though notable, is accepted within the accepted range of the Eastern Cobequid samples. Therefore, the proposed source rock of the felsic species is the BB-DB Formation.

**Table 7.1**

Sample ID	Petrography	Geochemistry	Inferred Source	DNR hand sample
<b>1170</b>	Felsic (F)	SUB-SPECIES A	BB-DB RHY.	BB-DB RHY.
<b>1237</b>	F			
<b>1228</b>	F	SUB-SPECIES B	LIMIT OF BB-DB RHY	BB-DB RHY.
<b>1232a</b>	F			
<b>1232b</b>	F			
<b>1279</b>	F			
<b>1819</b>	M	SUB-ALKALINE BASALT	BB-DB BSLT	BB-DB BSLT
<b>2234</b>	M			BB-DB BSLT
<b>2513</b>	M			
<b>2549</b>	M			
<b>2567</b>	M			
<b>2567.5</b>	M			
<b>BM-003</b>	Sedimentary (S)	<i>Intermediate between felsic and mafic group compositions</i>	WB	
<b>BM-2M</b>	N/A			
<b>BM-3M</b>	S			
<b>BM-4</b>	S			
<b>2060c</b>	S			

Table 7.1 Summary of results for each analytical method. Geochemical compositions as per Fig. 5.2: Winchester & Floyd, 1977. Inferred source applies to entire species group. BB-DB: Byers Brook-Diamond Brook Formation, RHY: rhyolite, BSLT: basalt, WB: Wilson Brook Formation. N/A were thin sections were not available to make petrographic observations.

Given the effects of weathering and diagenetic processes, the results for the sedimentary group are largely inconclusive. These clasts are categorized as sedimentary due to characteristic structures and textures (e.g. cross-laminations: Fig. 4.1). The Nb-Y: Zr/TiO<sub>2</sub> discrimination correlates the sedimentary species with the BB-DB Formation (Fig. 6.7). Multi-element

diagrams, however, showed near identical elemental signatures between the clasts, with only weakly variable Sr within the entire species (Fig. 5.5). The Wilson Brook Formation is proposed to be the source of the sedimentary species mainly based on the presence of Silurian biomicritic limestones in the Claremont conglomerate (B. Ryan, pers. comm.). Geochemical comparison confirms overlap between the sedimentary species and the Wilson Brook Formation (Fig. 6.9). The geochemistry is thus a vital tool for correlation between clasts and source rocks.

Hand samples of the sedimentary group related to DNR samples the BB-DB Formation (Fig. 7.1). Thus, it might be that there are in fact two sedimentary species in the Claremont: some siltstones correlate to the limestones (Wilson Brook Formation) and others to the BB-DB Formation. Though more analysis is required, this correlation could help distinguish the Byers Brook and Diamond Brook Formations since Byers Brook Formation consists of rhyolitic flows, ignimbrites interlayered with dacitic flows and grey siltstones while the Diamond Brook Formation consists of basaltic flows interbedded with red sandstone and siltstone. In the lower section of the Claremont core, only red sedimentary clasts

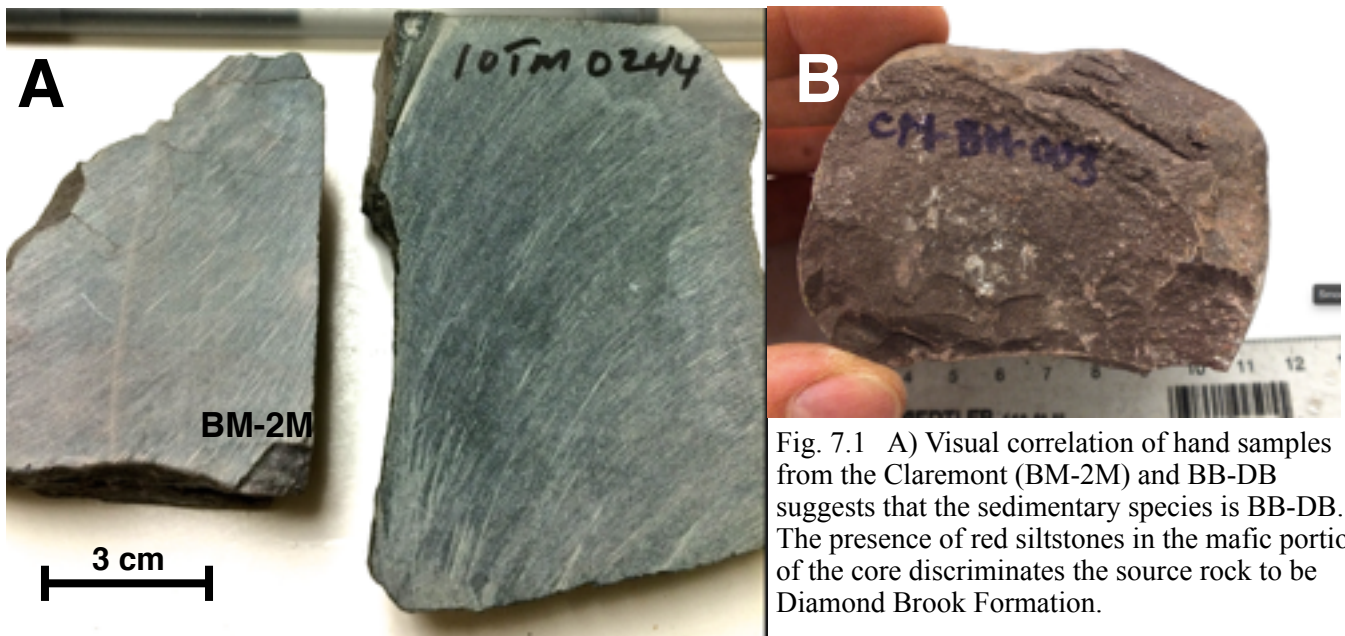


Fig. 7.1 A) Visual correlation of hand samples from the Claremont (BM-2M) and BB-DB suggests that the sedimentary species is BB-DB. B) The presence of red siltstones in the mafic portion of the core discriminates the source rock to be Diamond Brook Formation.

(sample 2060c) were found with the clasts that constitute the mafic species. The Diamond Brook Formation signature of red siltstone interbedded with basalt is thus reflected in the lower portion of the core.

This result is significant since the Diamond Brook Formation is slightly younger than the Byers Brook Formation. The proposed correlation therefore provides a tighter age-constraint on the Claremont conglomerate.

Finally, there are high levels of strontium in all clast samples from the Claremont conglomerate. Though not of direct importance to the age of the Claremont, this enrichment is notable. There are three possible explanations for this anomaly.

The first relates to sampling inconsistency. The DNR Cobequid samples were collected at the surface. These rocks were exposed to weathering which would have mobilizes Sr out of the rock. As a result, they are depleted in Sr. Since the Claremont mafic and felsic samples were collected at depth from the core, these show relative enrichment.

Another solution is sub-surface alteration. Hydrothermal fluids commonly introduce Sr into rock as it substitutes for Calcium. The abundance of calcite veins in the Claremont shows this is a likely option. Hydrothermal activity has been confirmed in this area of the Cobequids (Papoutsas, 2015).

Lastly, Sr might have been introduced by brines escaping the Wilson Group. The Wilson Group strata underlie the Claremont conglomerate in the Magdalen Basin and consists of evaporites and carbonates. Leaching of brines would escape upwards into overlying strata (including the Claremont). These brines likely contain high concentrations of Strontium which would have substituted into the Claremont. This would explain the consistency of Sr-enrichment

throughout the conglomerate and explain why the mafic group show greater enrichment than the felsic group: the former represents the deeper segment of the core and is thus closer to the Wilson Group.

## **7.2 RELATION TO CLAREMONT AGE**

The presence of volcanic clasts from the Diamond Brook Formation places the upper-age of the Claremont conglomerate around  $348 \pm 3$  Ma (Table 2.2). The upper age bracket is consistent with the 320 Ma age imposed by the overlying Boss Point Formation. The discrepancy regarding the source of the sedimentary species might slightly affect the age: If the species is Byers Brook Formation, the age constraint of the Claremont conglomerate is changed to  $358 \pm 1$  Ma.

Furthermore, the tight constraint of this age-bracket is notable. Regarding the precision of ages, the current dating methods for conglomerate rocks are antithetic: Radiogenic geochronology is able to constrain the age of a sedimentary unit to within one million years, while stratigraphy constraints carry uncertainties of about 100 million years (Rasmussen, 2005). The age-bracketing method presented in this thesis offers an intermediate solution where a series of petrographic and geochemical analyses can be used to provide relatively tight age constraints (roughly 30 Ma).



### **7.3 POSSIBLE SOURCES OF ERROR**

The main sources of error are listed below:

1. High degree of weathering and alteration in the Claremont samples made petrographical descriptions difficult and increases the uncertainty of geochemical results.
2. Sampling bias is possible since clasts were preferentially selected based on size and visible compositional variation.
3. Geochemical error associated with calibrating multiple XRF analyses (both XRF runs for the Claremont as well as the calibration between the Claremont and DNR data) affects the comparative analysis and should be taken into consideration.
4. Conversion of element intensities measured by the XRF analyzer to elemental concentrations is done by calculation. This calculation is established by individual geoscientists for a particular XRF machine (human error).

## **CHAPTER 8: Conclusions**

### **8.1 CONCLUSION**

This thesis shows that it is possible to estimate the upper-age bracket of a conglomerate by identifying the clast species present. In total, three species are present in the Claremont conglomerate: felsic, mafic and sedimentary species. The felsic and mafic species correlate with the Byers Brook-Diamond Brook Formation rhyolites and basalts (respectively). The bimodal facies of the Fountain Lake Group is thus reflected in the conglomerate. The sedimentary species consists of siltstones and limestones and correlates with both the Wilson Brook Formation and Diamond Brook Formation. The source rocks of these species bracket the upper-age of the Claremont conglomerate to between 348-320 Ma.

Petrography, XRF geochemistry and hand sample comparison can thus be used to bracket the age of a conglomerate. Though the results are consistent across all methods, qualitative (petrography and hand sample comparison) methods were a valuable addition to XRF geochemistry to help determine the source rock of the clast species from potential sources. A multi-method approach is thus recommended to find the source rocks of conglomeratic clasts.

## 8.2 RECOMMENDATIONS

The following recommendations are suggested for future study of the Claremont conglomerate and/or use of XRF as a comparative tool:

1. Test the linearity of peak intensities to measure the error of XRF runs (Fralick et al., 1997).  
Perform a log-ratio calibration model (Weltje et al., 2008) for non-linearity of the relation between relative intensities and concentrations.
2. Investigate brines. Analysis of veins in Claremont could reveal source of Sr-enrichment and possibly link composition of these veins to brines in the Magdalen Basin.
3. Detailed logging of core might better characterize the vertical variation of the Claremont conglomerate and discern separate stages of evolution.
4. The Claremont conglomerate is also exposed north of Tatamagouche Bay. Examining outcrop there might lead to new insights regarding the clast species as well as provide information regarding lateral variability in this conglomerate. Further, geochemical data distal to the Cobequids might discriminated possible causes of Sr-enrichment.
5. Comparative analysis of the 2 peraluminous felsic samples (sub-species A) might yield an additional source for the Claremont conglomerate.

## REFERENCES

- Bradshaw, J.D. et al. (2012) Permo-Carboniferous conglomerates in the Trinity Peninsula Group at View Point, Antarctic Peninsula: sedimentology, geochronology and isotope evidence for provenance and tectonic setting in Gondwana; *Geol. Mag.*, v. 149, p.626-644. DOI: 10.1017/S001675681100080X
- Dunning, G.R., et. al. (2002) Chronology of Devonian to early Carboniferous rifting and igneous activity in southern Magdalen basin based on U-Pb (zircon) dating; *Can J. Earth Sci.*, v. 39, p. 1219-1237.
- Donohoe, H.V.Jr. and P.I. Wallace (1980). Structure and Stratigraphy of the Cobequid Highlands, Nova Scotia. GSC Field Trip Guidebook.
- Donohoe, H.V., Jr. and P.I. Wallace(1982) Geological map of the Cobequid Highlands, Colchester, Cumberland and Pictou Counties, NS; Nova Scotia Department of Natural Resources, Map ME 1982-9, scale 1:50 000.
- Grange, M. et al. (2010) Proterozoic events recorded in quartzite cobbles at Jack Hills, Western Australia: New constraints on sedimentation and source of >4 Ga zircons; *Earth and Planetary Science Letters*, v.292, p.158-169.
- Jutras, P. et al. (2015) Sedimentology of the lower Serpukhovian (upper Mississippian) Mabou Group in the Cumberland Basin of eastern Canada: tectonic, halokinetic and climatic implications; *Can. J. Earth Science*, v. 52, p. 1-19. DOI: [dx.doi.org/10.1139/cjes-2015-0062](https://doi.org/10.1139/cjes-2015-0062)
- Karner, G.D. et al. (1997) Tectonic significance of syn-rift sediment packages across the Gabon-Cabinda continental margin; *Marine and Petroleum Geology*, v. 14, n.7/8, p. 973-1000. PII: S0264-8172(97)00040-8
- Keppie, J.D. et al. (1997) Palaeozoic within-plate volcanic rocks in Nova Scotia (Canada) reinterpreted: isotopic constraints on magmatic source and palaeocontinental reconstructions; *Geological Magazine*, v. 134, iss. 04, p. 425-447.
- Keppie, J.D. and T.E. Krogh (1999) U-Pb chronology of Devonian Granites in the Meguma terrane of Nova Scotia, Canada: evidence for hotspot melting of a neoproterozoic source; *Journal of Geology*, v. 107, n. 5, p. 555-568.
- Kotkova, J. et al. (2007) Clasts of Varisxan high-grade rocks within Upper Viséan conglomerates —constraints on exhumation history from petrology and U-Pb chronology; *J. metamorphic Geol.*, v. 25, p. 781-801.

Lavoie, D. (1994) Lithology and preliminary paleoenvironmental interpretation of the Macumber and Pembroke formations (Windsor Group, early Carboniferous), Nova Scotia; *in* Current Research 1194-D; Geological Survey of Canada, p. 79-88.

MacHattie, T.G. (2010) Nature and Setting of Late Devonian-Early Carboniferous Rare Earth Element Mineralization in the Eastern Cobequid Highlands, NS; *in* Mineral Resources Branch, Report of Activities 2009; Nova Scotia Department of Natural Resources, Report ME 2011-1, p. 75-92.

MacHattie, T.G. and C.E. White (2012) Preliminary Geology of the Eastern Cobequid Highlands, Northern Mainland Nova Scotia; *in* Mineral Resources Branch, Report of Activities 2012; Nova Scotia Department of Natural Resources, Report ME 2013-001, p. 27-43.

MacHattie, T.G. (2013) An Update of Bedrock Mapping in the Eastern Cobequid Highlands, Northern Mainland Nova Scotia; *in* Mineral Resources Branch, Report of Activities 2013; Nova Scotia Department of Natural Resources, Report ME 2014-001, p. 145-156.

MacHattie, T.G. and G.A. O'Reilly (2008) Field and Geochemical Evidence for Contemporaneous Mafic Magmatism and Iron Oxide-Cooper-Gold (IOCG) Mineralization and Alteration along the Cobequid-Chedabucto Fault Zone; *in* Mineral Resources Branch, Report of Activities 2008; Nova Scotia Department of Natural Resources, Report ME 2009-1, p.71-83.

MacHattie T.G. and G.A. O'Reilly (2008) Timing of Iron Oxide-Copper-Gold (IOCG) Mineralization and Alteration along the Cobequid-Chedabucto Fault Zone; *in* Mineral Resources Branch, Report of Activities 2009; Nova Scotia Department of Natural Resources, Report ME 2009-1, p.63-69.

Manzotti, P. et al. (2015) Detrital zircon geochronology in blueschist-facies meta-conglomerates from the Western Alps: implications for the late Carboniferous to early Permian palaeogeography; *Int. J. Earth Science*, v. 104, p. 703-731.

Mitchell, R.H. (1990) A review of the compositional variation of amphiboles in alkaline plutonic complexes; *Lithos*, v. 26, p. 135-156.

Murphy, J.B., G. Pe-Piper, D.J.W. Piper, R.D. Nance and R. Doig (2001) Geology of the Eastern Cobequid Highlands, Nova Scotia. *GSC Bulletin*, 556: 1-61.

Murphy, J.B. (2002) Geochemistry of the Neoproterozoic metasedimentary Gamble Brook Formation, Avalon terrane, Nova Scotia: Evidence for a rifted-arc environment along the West Gondwanan margin of Rodinia; *Journal of Geology*, v. 110, n. 4, p. 407-419.

- Murphy, J.B. and J.D. Keppie (1998) Late Devonian palinspastic reconstruction of the Avalon-Meguma terrane boundary: implications for terrane accretion and basin development in the Appalachian orogen; *Tectonophysics*, v. 284, p. 221-231.
- Murphy, J.B. et al. (1999) Fault reactivation within Avalonia: plate margin to continental interior deformation; *Tectonophysics*, v. 305, p. 183-204.
- Murphy, J.B. and M.A. Hamilton (2000) Orogenesis and basin development: U-Pb detrital zircon age constraints on evolution of the late Paleozoic St. Marys basin, central mainland Nova Scotia; *Journal of Geology*, v.108, n.1, p. 53-71.
- Murphy, J.B. and J.D. Keppie (2005) The Acadian Orogeny in the Northern Appalachians; *Int. Geology Review*, v.47, n. 7, p. 663-687.
- Murphy, J.B. et al. (2011) Minas Fault Zone: late Paleozoic history of an intra-continental orogenic transform fault in the Canadian Appalachians; *Journ. of Structural Geology*, v. 33, p. 312-328.
- Nesse, W. D. (2012). *Introduction to mineralogy* (2nd ed.). New York: Oxford University Press.
- Olsen, P.E. and R.W. Schlische (1990) Transtensional arm of the early Mesozoic Fundy rift basin: Penecontemporaneous faulting and sedimentation; *Geology*, v. 18, p. 695-698.
- Papoutsas, A.D. and G. Pe-Piper (2013) The relationship between REE-Y-Nb-Th minerals and the evolution of an A-type granite, Wentworth Pluton, Nova Scotia; *American Mineralogist*, v. 98, p. 444-462.
- Papoutsas, A.D. (2015) The petrological evolution of the late Paleozoic A-type granites of the Cobequid Highlands, Canada; PhD thesis. Dalhousie University, Halifax, Nova Scotia, p. 208.
- Pearce J.A. and Cann, J. (1973) Tectonic setting of basic volcanic rocks investigated using trace elements analyses; *Earth and Planetary Science Letters*, v. 19, p. 290-300.
- Pearce, J.A., N.B.W. Harris and A.G. Tindle (1984) Trace element discrimination diagrams for the tectonic interpretation of granitic rocks; *J. Petrol.*, v. 25, p. 956-983.
- Pe-Piper, G. and D.J.W. Piper (2002) A synopsis of the geology of the Cobequid Highlands, Nova Scotia; *Atlantic Geology*, v. 38, p. 145-160.
- Pe-Piper, G. et al. (2004) Early Carboniferous deformation and mineralization in the Cobequid shear zone, Nova Scotia: an  $^{40}\text{Ar}/^{39}\text{Ar}$  geochronology study; *Can. J. Earth Science*, v. 41, p. 1425-1436.

Pe-Piper, G. and I. Koukouvelas (1994) Earliest Carboniferous plutonism, western Cobequid Highlands, Nova Scotia; *in* Current Research 1994-D; Geological Survey of Canada, p. 103-107.

Pe-Piper, G. (1988) Calcic amphiboles of mafic rocks of the Jeffers Brook plutonic complex, Nova Scotia, Canada; *American Mineralogist*, v. 73, p. 993-1006.

Pe-Piper, G. (1996) The Devonian-Carboniferous Wentworth plutonic complex (Folly lake & Hart Lake-Byers Lake plutons) of the central Cobequid Highlands, Nova Scotia; Geological Survey of Canada open file #3373, OSC92-02028-(004), 73p.

Piper, D.J.W. et al. (1996) The stratigraphy and geochemistry of late Devonian to early Carboniferous volcanic rocks of the northern Chignecto peninsula, Cobequid Highlands, Nova Scotia; *Atlantic Geology*, v.32, p. 32-52.

Piper, D.J.W. et al. (1993) Devonian-Carboniferous igneous intrusions and their deformation, Cobequid Highlands, Nova Scotia; *Atlantic Geology*, v. 29, p. 219-232.

Rudolph, R.S. and G. Pe-Piper (1999) Using whole rock geochemistry to locate the source of igneous erratics from drumlins on the Atlantic coast of Nova Scotia; *Boreas*, v. 28. p. 308-325.

Ryan, R. J and C. Boehner (1990) Cumberland Basin Geology Map: Tatamagouche and Malagash, Cumberland, Colchester and Pictou Counties. Nova Scotia Department of Mines and Energy, Map 90-14, scale 1: 50 000.

Satkoski, A.M. et al. (2010) Provenance of late Neoproterozoic and Cambrian sediments in Avalonia: Constraints from detrital zircon ages and Sm-Nd isotopic compositions in Southern New Brunswick, Canada; *Journal of Geology*, v. 118, n.2, p.187-200.

Skehan, J.W. (1997) Assembly and dispersal of supercontinents: the view from Avalon.; *Journal of Geodynamics*, v. 23, n.3/4, p. 237-262.

Stapinsky, M. et al. (2002) Groundwater resources assessment in the Carboniferous Maritimes Basin: preliminary results of the hydrogeological characterization, New Brunswick, Nova Scotia, and Prince Edward Island; Geological Survey of Canada, Current Research 2002-D8, 12p.

Waldron., J.W.F. et al. (2013) Evaporite tectonics and the late Paleozoic stratigraphic development of the Cumberland basin, Appalachians of Atlantic Canada; *GSA Bulletin*, May/June 2013; v. 125, no. 5/6, p. 945-960.

Winchester, J.A. and Floyd, P.A. (1977) Geochemical discrimination of different magma series and their differentiation products using immobile elements; *Chemical Geology*, v. 20, p. 325-343.



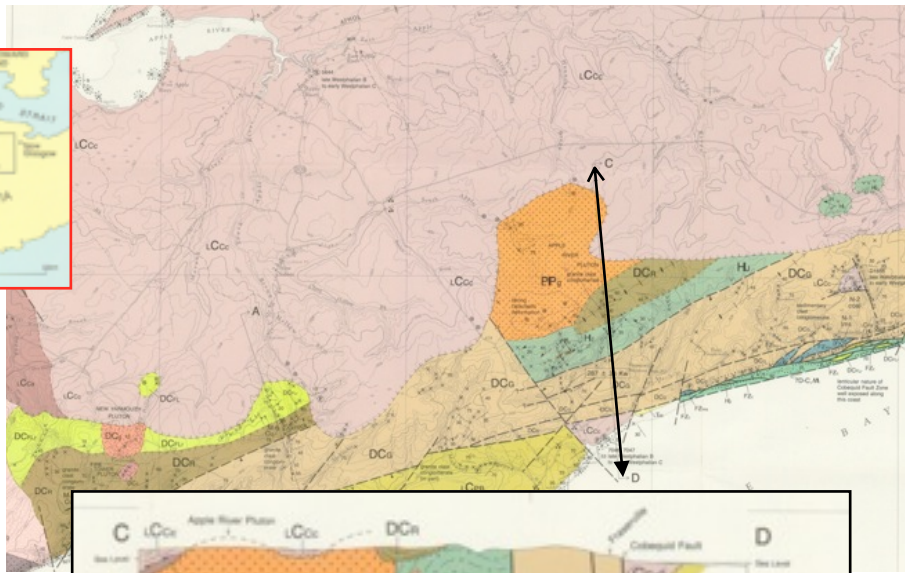
Withjack, M. O. et al. (1995) Tectonic evolution of the Fundy rift basin, Canada: Evidence of extension and shortening during passive margin development; *Tectonics*, v. 14, p. 390-405.

Zanoni, D. et al. (2010) Vestiges of lost tectonic units in conglomerate pebbles? A test in Permian sequences of the Southalpine Orobic Alps; *Geol. Mag.*, v. 147, p. 98-122.

# Appendix A: Geologic Maps of the Cobequid Highlands

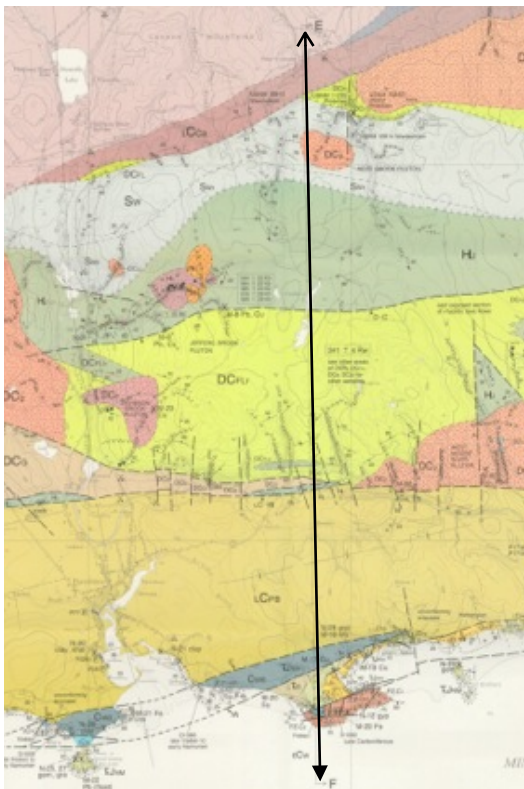
\*from Donohoe & Wallace (1982)

Reference Map:



(above) Western Cobequids (block 1 on reference map): conglomerate units include Rapid Brook Formation (DCR) and Cumberland Group (LCCa, b, c). (Legend follows)

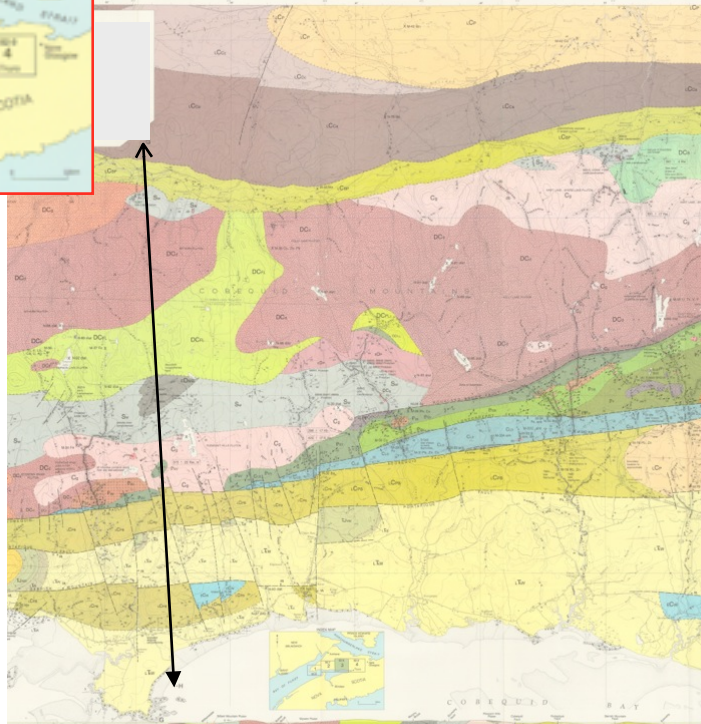
(below) Central-West Cobequids (block 2): Cumberland Group (LCCa, b, c) overlies Wilson Brook volcanics (Sw), faulted contact with Fountain Lake Group volcanics and agglomerate (DCFLr)



Reference Map:

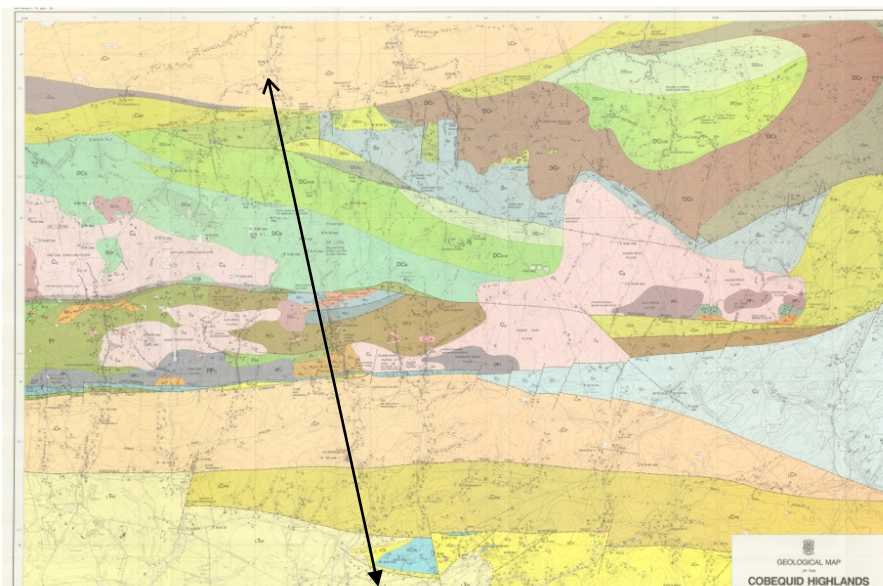


Following maps are from Donohoe & Wallace (1982)



(above) Central-East Cobequids (block 3): Cumberland Group (LCCb) and Boss Point Formation (LCBP) conglomerates, Wilson Formation (Sw) volcanics and conglomerate, Fountain Lake Group volcanics (DCFL) unconformably overlie Sw and Murphy Brook conglomerate (EDMB)

(below) Eastern Cobequids (block 4): Pictou (LCP) and Boss Point Formation (LCBP) conglomerates overlie Warwick Mountain volcanics (Hw), McKay Brook conglomerate\* (DCD-M) and Byers Brook volcanics (DCB), OSU-1,2 volcanics and Nuttby Formation conglomerate and volcanics (DCN) present.





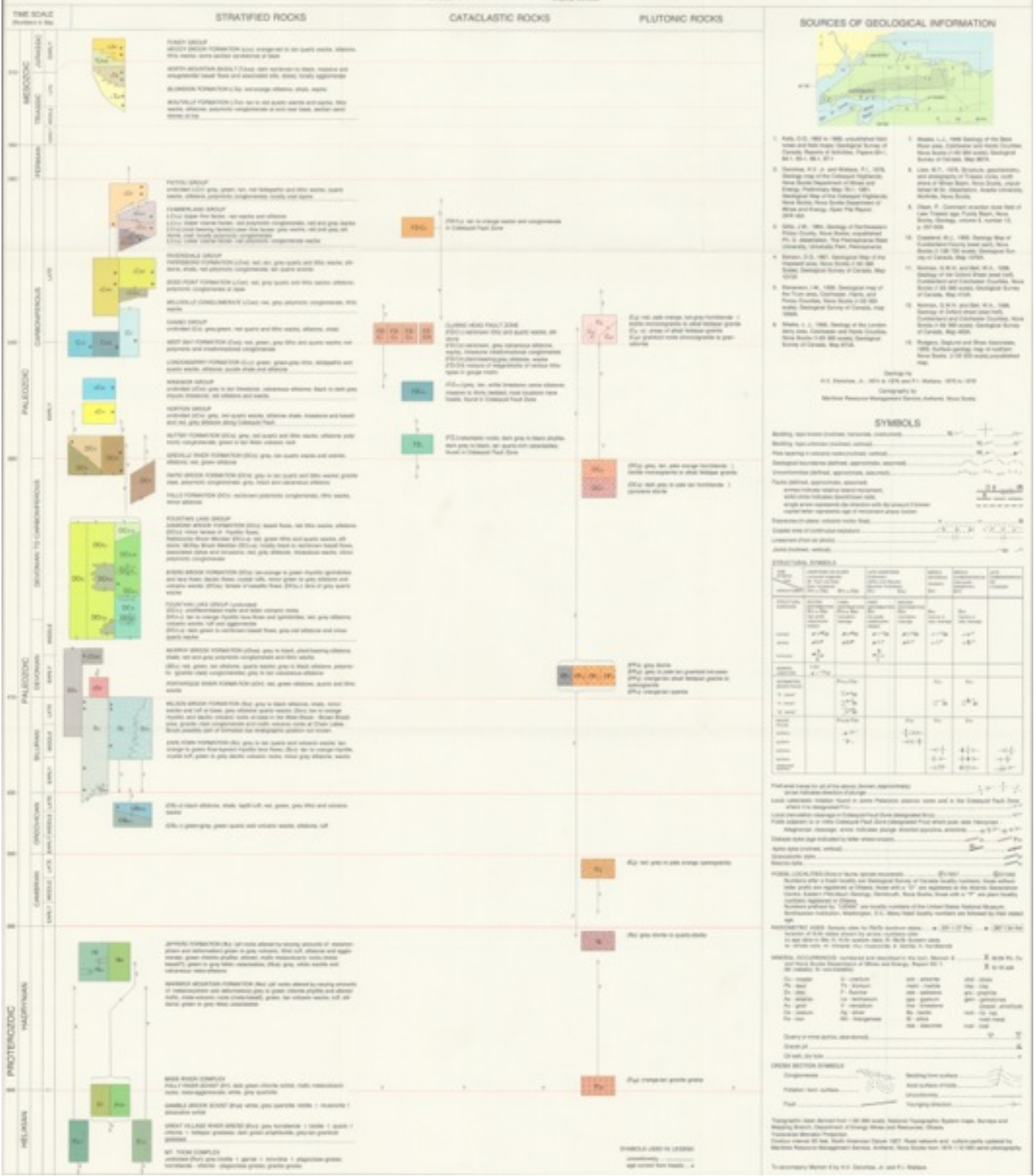


# LEGEND FOR THE GEOLOGICAL MAP OF THE COBEQUID HIGHLANDS

COLCHESTER, CUMBERLAND & PICTOU COUNTIES  
NOVA SCOTIA

H.V. Dawson, Jr. and P.J. Wallace

1982  
NOVA SCOTIA DEPARTMENT OF MINES AND ENERGY  
Nova Scotia Department of Mines and Energy  
Nova Scotia Department of Mines and Energy



## Appendix B: Petrographic Sample Descriptions

**Table 1B.** Petrographic description for each sample. Fine-grain size and considerable degree of weathering makes mineral identification difficult.

Group	Sample ID	Textures	Primary Minerals	Secondary Minerals
<b>SED</b>	<b>BM-003</b>	f.grained well-sorted cross-bedding	qtz plg musc oxides zr	chl
	<b>BM-3M</b>	f.grained parallel laminations	qtz plg musc oxides zr	chl
	<b>BM-4</b>	f.grained well-sorted carbonate patches	qtz plg musc oxides zr	ca glass?
	<b>2060c</b>	v.f. grained well-sorted parallel laminations mineral alignment (musc) kink bands	qtz plg musc oxides zr	chl
<b>FELSIC</b>	<b>1232a</b>	porphyritic hypocrystalline flow bands recrystallization spherulitic	qtz snd? plg Fe-oxides	glass ht
	<b>1232b</b>	porphyritic hypocrystalline flow bands granophyric	plg snd? agr Fe-oxides zr	glass ht
	<b>1170a</b> (Fig. 4.7)	porphyritic hypocrystalline compositional banding spherulite	flds plg opaque mineral	glass ca

	<b>1228</b>	porphyritic flow banded granophyric spherulitic	flds qtz plg oxides	
	<b>1237</b>	porphyritic graphic recrystallization	flds opaque mineral qtz px	ht chl ca (veins)
	<b>1255</b>	porphyritic hypocrystalline	flds plg opaque min	glass spt? ca (veins)
	<b>1279</b> (Fig. 4.6)	hypocrystalline poikilitic (plg) graphic resorption	flds qtz plg opaque mins minor px	spt?
<b>MAFIC</b>	<b>1819</b>	f. grained equigranular hyalopilitic poikilitic (plg)	plg px flds opaque mineral amph	glass ca chl
	<b>2234</b> (Fig. 4.9)	porphyritic vesicular poikilitic (plg) pilotaxitic	plg px opaque mineral	chl (amygdules) ht ca
	<b>2513</b>	v.f. grained equigranular pilotaxitic Fe-staining	plg opaque mineral bt amph minor px	ht ca
	<b>2549</b>	inequigranular holocrystalline poikilitic (plg) Fe-staining	plg opaque mineral cpx	chl
	<b>2567</b>	equigranular pilotaxitic bladed oxides pseudomorphism	plg opaque minerals flds amph (ept?)	chl ca
	<b>2567.5</b> (Fig. 4.10)	inequigranular kink bands (bt)	plg opaque mineral bt minor px	ht ept

## **Appendix C: Microprobe**

Microprobe analysis was completed to identify minerals in the Claremont clasts with particular interest for opaque minerals. Preliminary results show presence of ilmenite, sphene, biotite, muscovite, plagioclase and amphibole. The high degree of weathering and alterations in the clasts made scarce of fresh minerals in the Claremont samples. Based on these preliminary results, microprobe analysis was not pursued.

Point analyses were done on specific grains identified in thin section and prior to microprobe use and few other suspect grains. Result tables are presented below. Photos of BSE images of analyzed grains follow: analysis was done on the grain in cross hairs unless otherwise noted. Some additional pictures were taken for grains of interest (identified by WDS). WDS tables saved.

### **ANALYTICAL PARAMETERS:**

Microprobe: **JOEL 8200 Superprobe**

Accelerating voltage: 15 kV

Beam Current: 20 nA

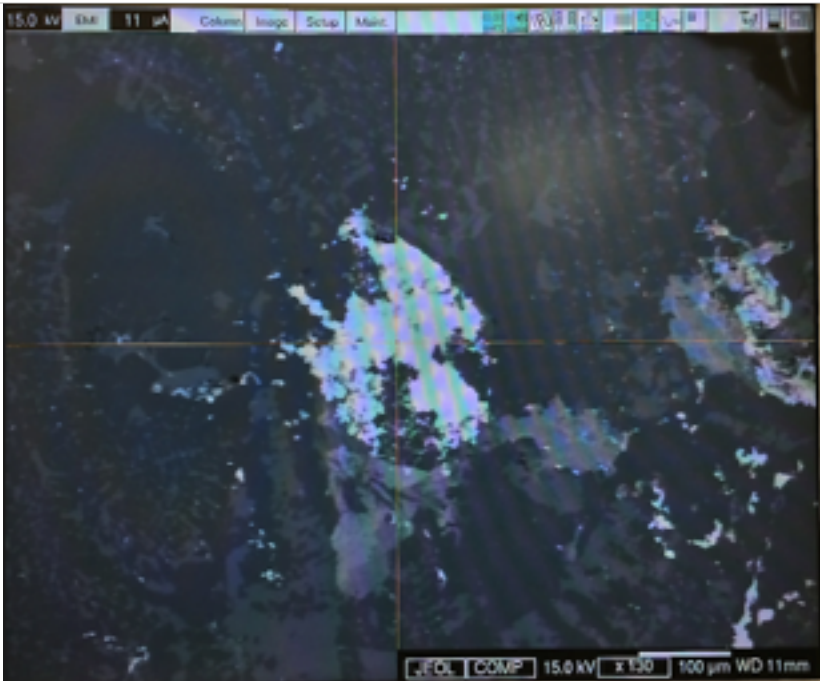
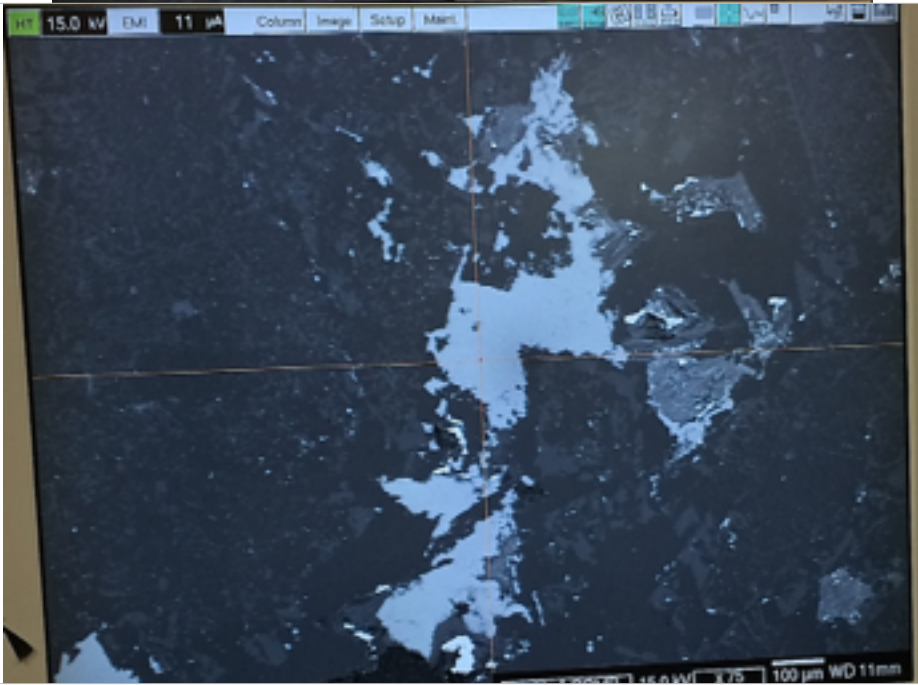
Counting Time: 20 s

Cation correction: 1 oxygen pfu

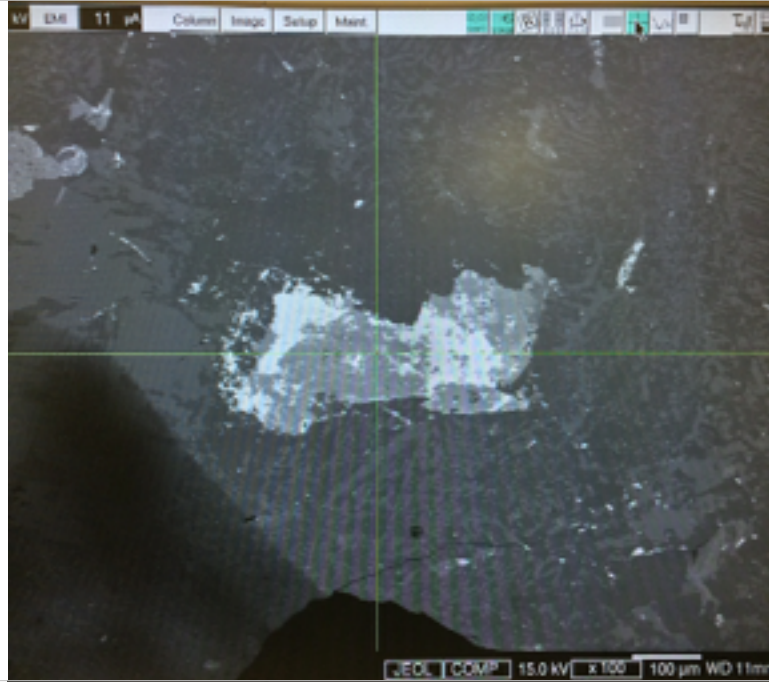
Correction method: ZAF

Standard: Block 53 (Al, Ca, Cr, Fe, K, Mg, Mn, Na, Si, Ti)

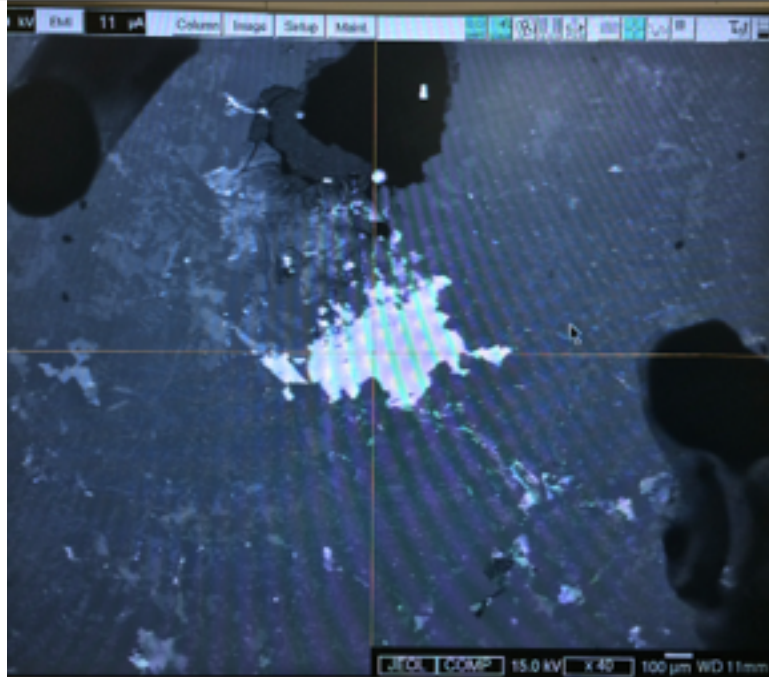


Sample	Probe No.	BSE Image of Analyzed Grain
1237	30, 31, 32	
	33, 34, 35	

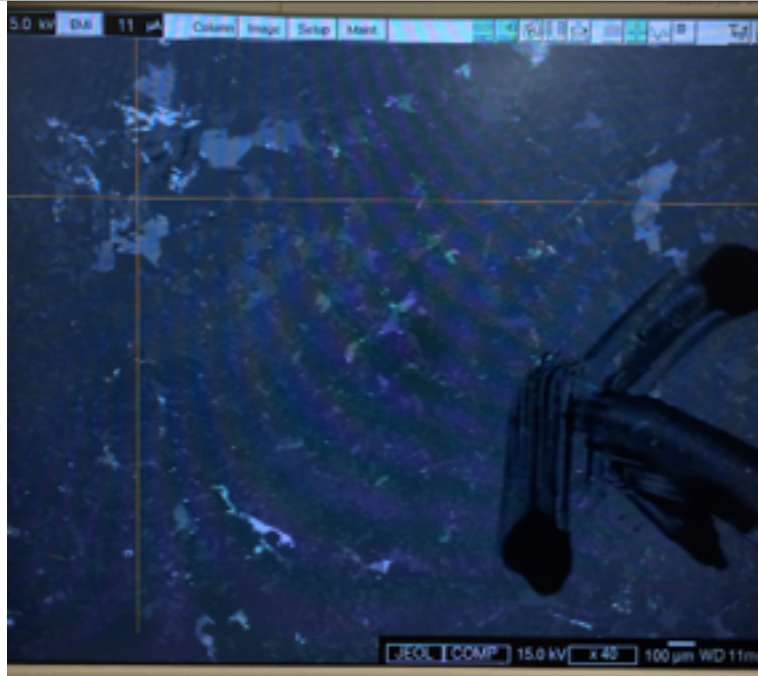
36, 37, 38



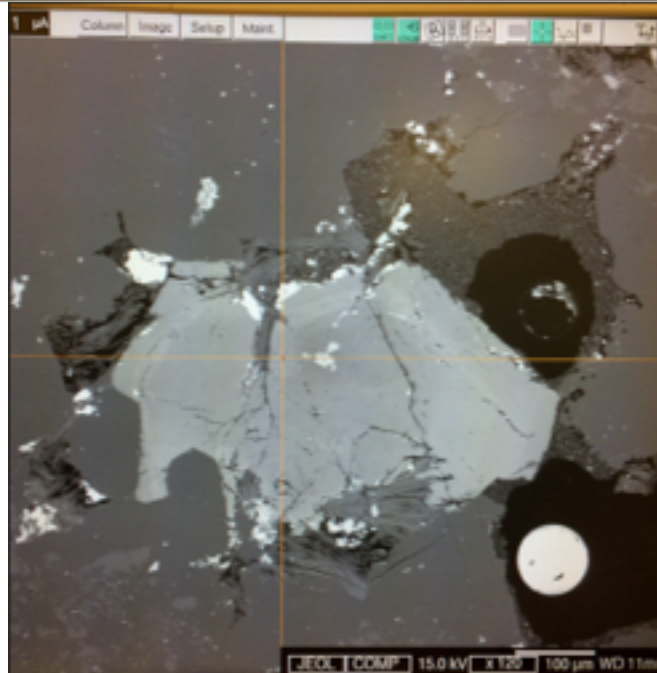
39, 40, 41



42, 43, 44



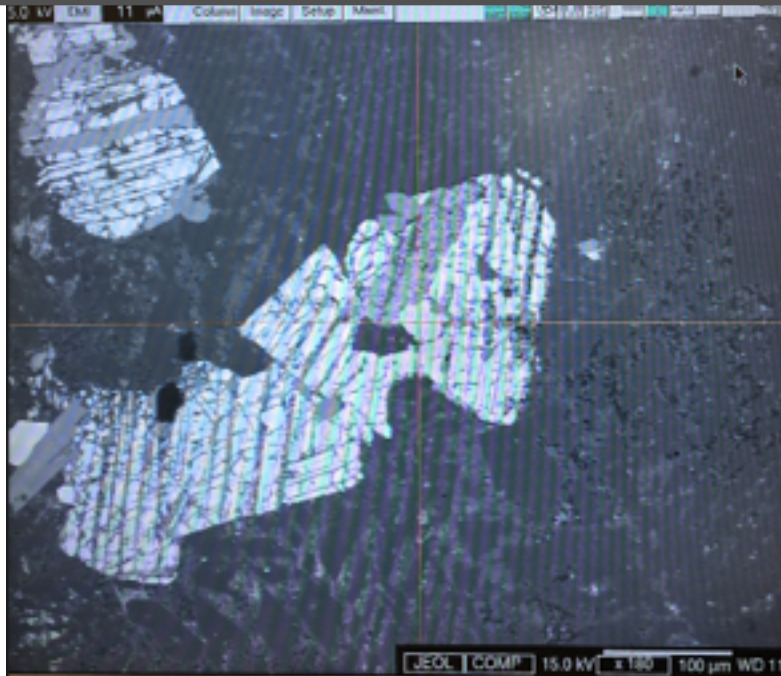
zoning  
(not  
analyzed)



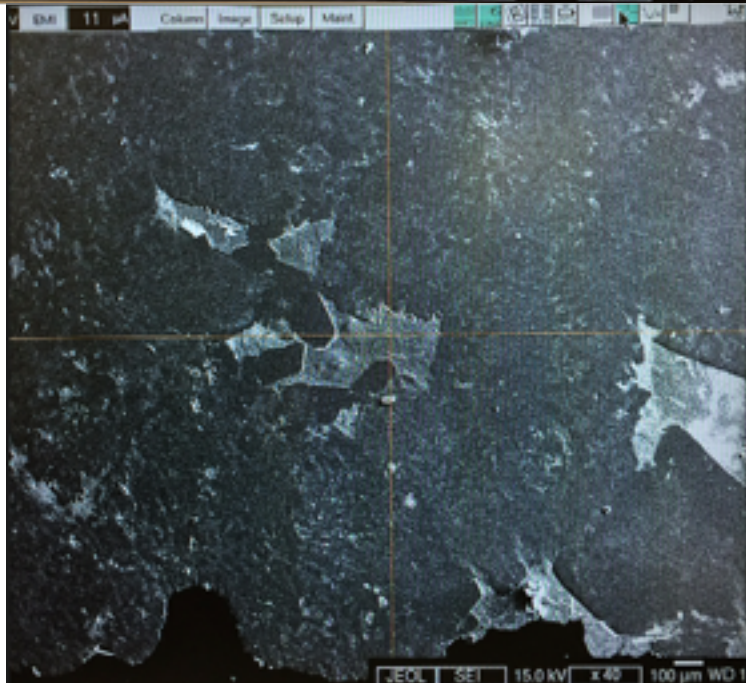


1279

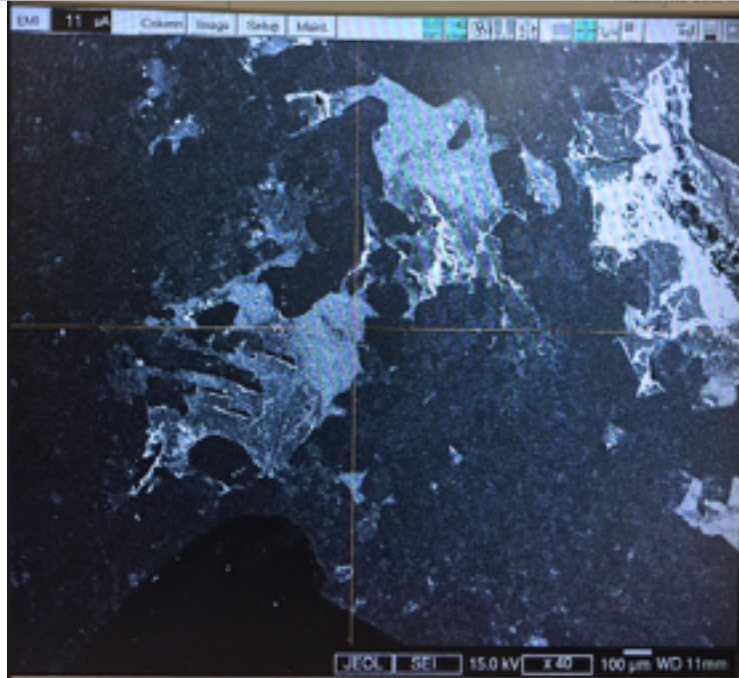
zircon  
(not  
analyzed)



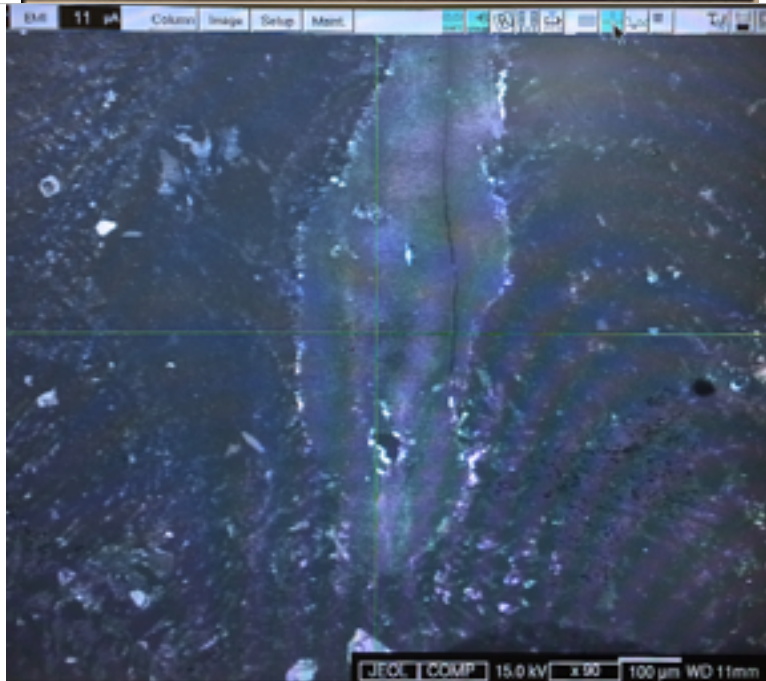
(not  
analyzed)



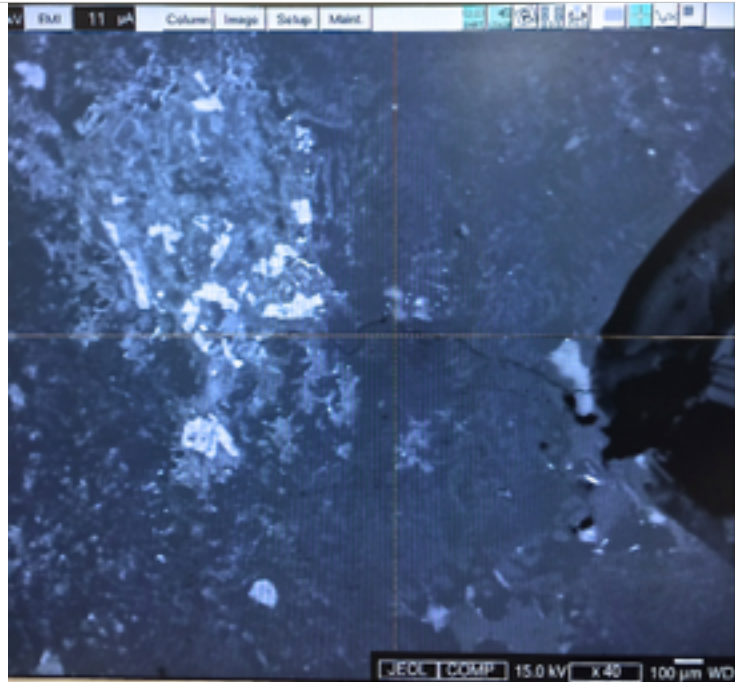
1279 65, 66, 67



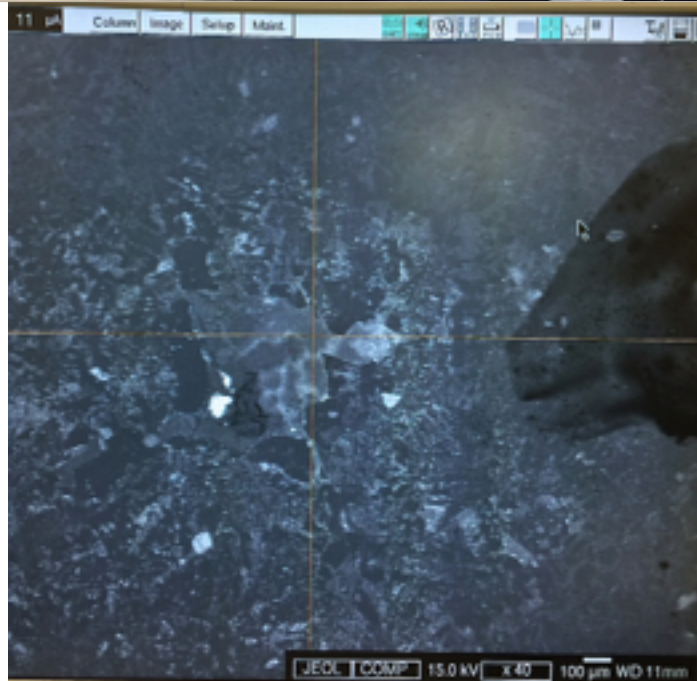
68, 69



3  
(analyzed  
light  
mineral)

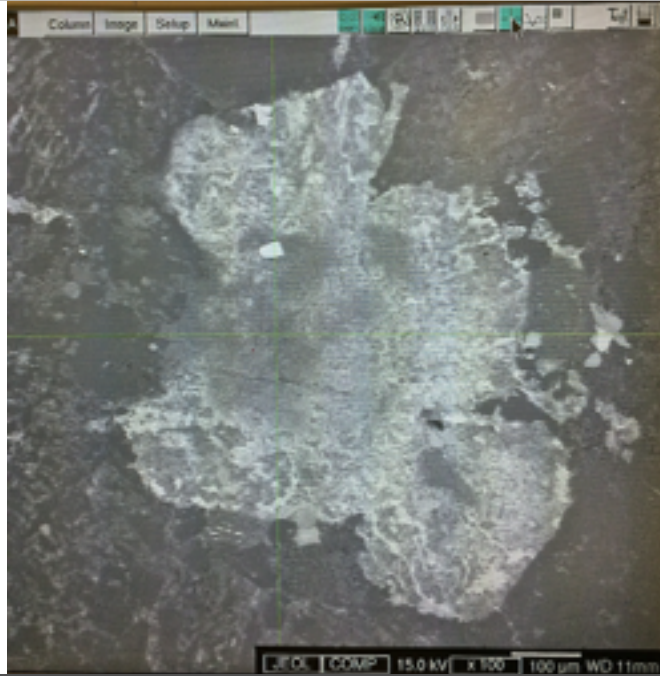


70, 71, 72

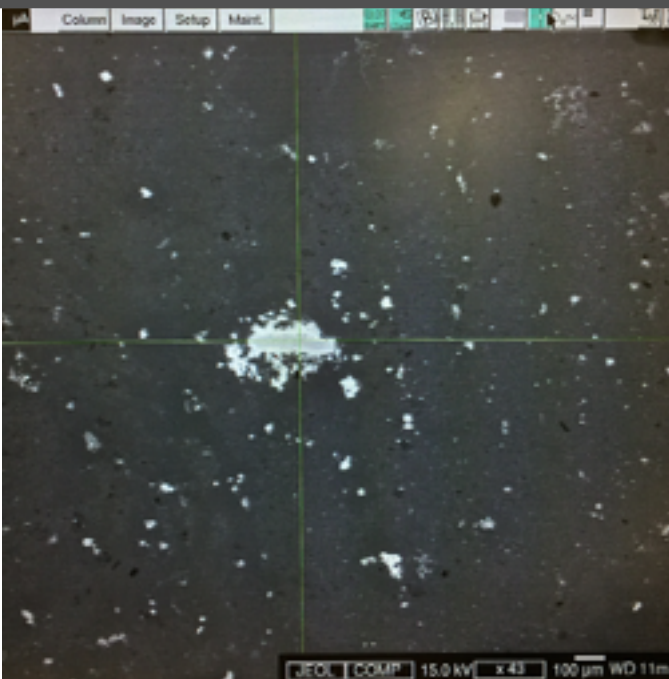




5  
(discarded)



1228 97, 98, 99



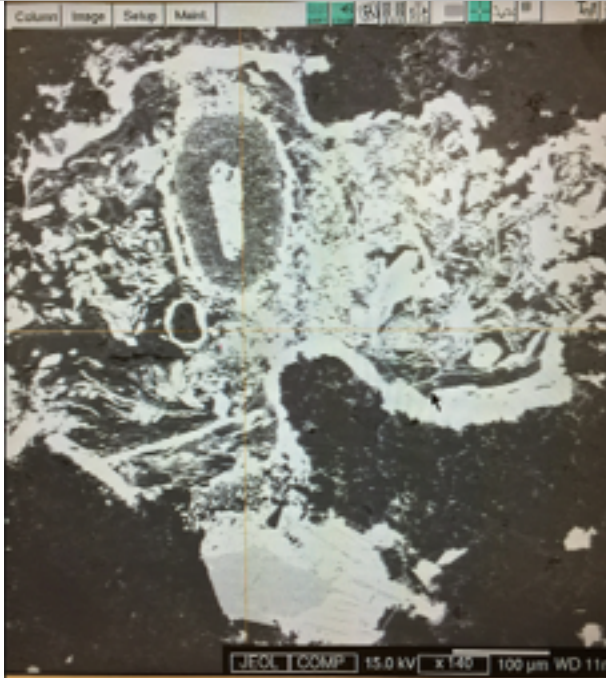


2

cryptocrystalline qtz?

points taken on light grain just above "JOEL" on information bar

100, 101



102, 103, 104



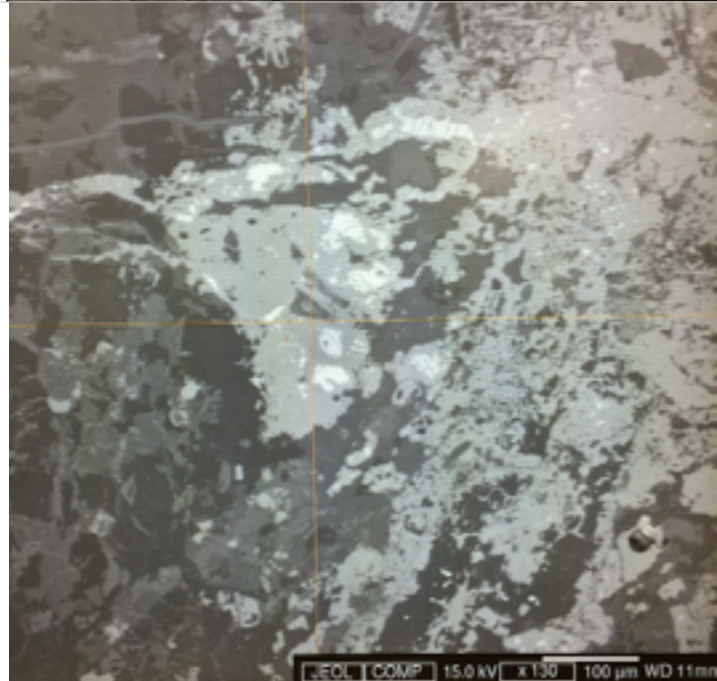
2567

reoccurring  
phenocryst  
(not  
analyzed)

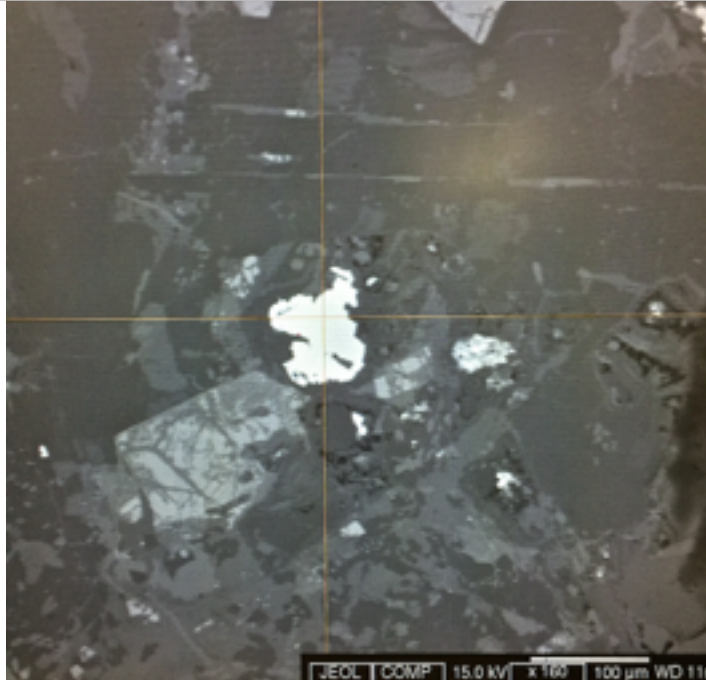


\*Analyzed  
light backed  
on grain  
under cross  
hairs

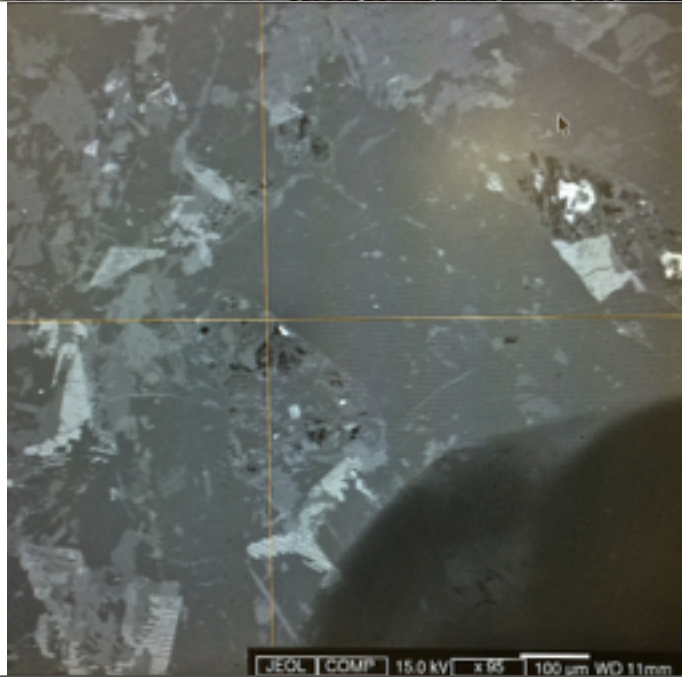
105, 106,  
107



111, 112,  
113

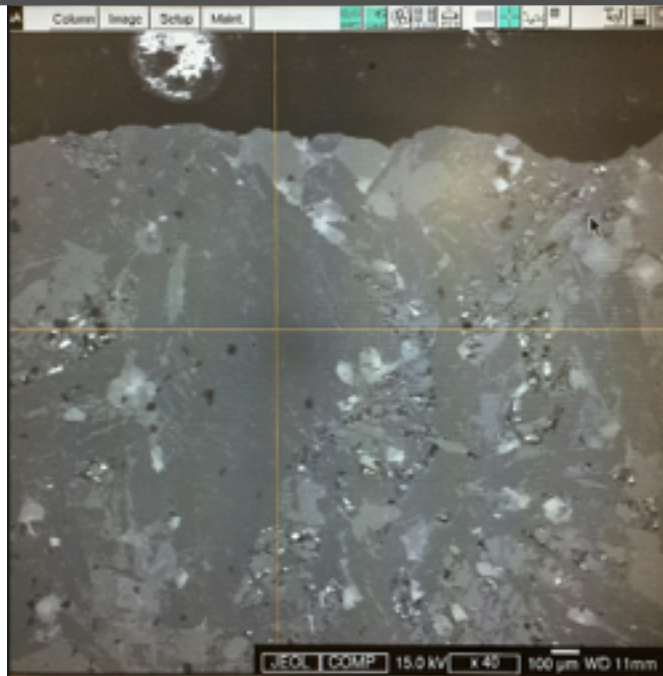


(discarded)

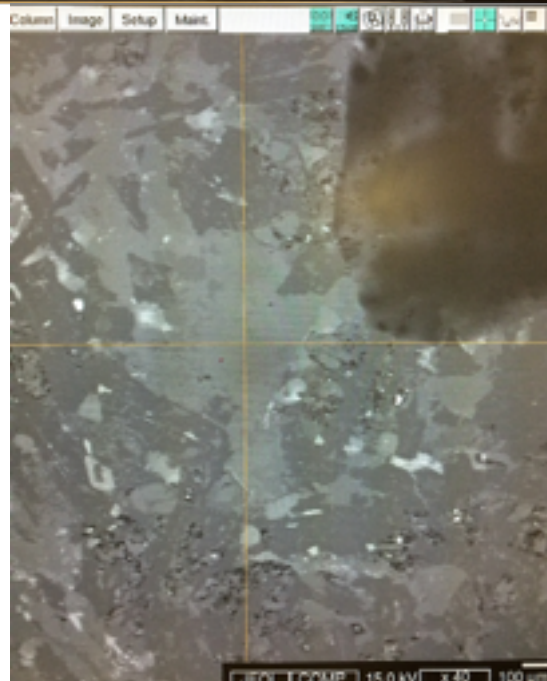


2234

124, 125,  
126

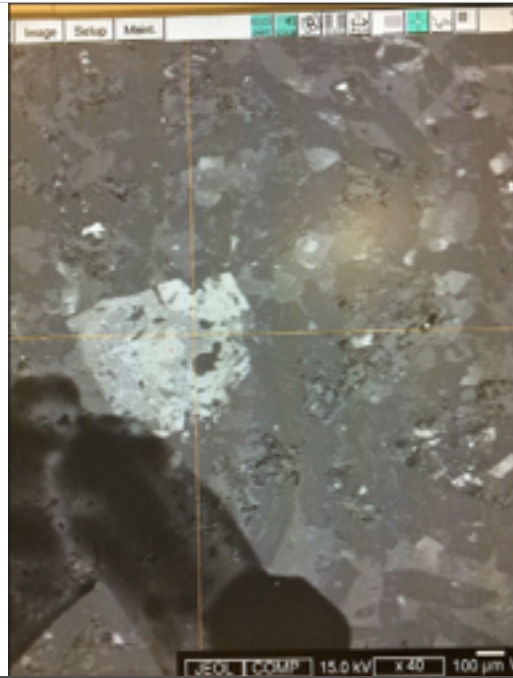


127-132





133, 134  
\*analyzed  
light patch  
in  
phenocryst



SAMPLE 1237		Fe-Oxide			Ilmenite			Titanite			Fe-oxide			Titanite		
MINERAL	1			2			3			4			5			
Grain #	1	2	3	4	5	6	7	8	9	10	11	12	13	14	15	
<b>No.</b>	30	31	32	33	34	35	36	37	38	39	40	41	42	43	44	
<b>SiO2</b>	0.14	0.62	0.72	0.80	0.37	0.16	22.03	29.37	29.66	0.43	0.33	0.48	29.90	29.71	30.23	
<b>Al2O3</b>	0.00	0.23	0.29	0.20	0.19	0.06	1.33	2.03	1.97	0.15	0.10	0.07	4.16	4.34	3.66	
<b>TiO2</b>	2.93	3.10	2.98	2.73	2.28	2.58	32.38	30.13	33.54	3.57	3.03	3.41	30.75	29.94	30.99	
<b>FeO</b>	85.20	83.67	83.22	84.02	84.57	85.30	17.72	3.64	2.15	84.22	85.56	84.98	0.99	1.22	1.06	
<b>MnO</b>	0.16	0.22	0.23	0.21	0.17	0.14	1.02	0.07	0.02	0.21	0.19	0.22	0.00	0.00	0.01	
<b>MgO</b>	0.00	0.00	0.00	0.00	0.00	0.00	0.00	0.00	0.00	0.00	0.00	0.00	0.00	0.00	0.00	
<b>CaO</b>	0.08	0.11	0.13	0.13	0.11	0.08	20.38	27.41	28.36	0.09	0.11	0.13	28.87	28.87	28.77	
<b>Na2O</b>	0.00	0.04	0.03	0.01	0.00	0.00	0.07	0.09	0.03	0.01	0.03	0.02	0.00	0.00	0.00	
<b>K2O</b>	0.07	0.06	0.07	0.07	0.08	0.07	0.06	0.03	0.03	0.07	0.08	0.06	0.03	0.04	0.01	
<b>Cr2O3</b>	0.23	0.21	0.23	0.20	0.23	0.22	0.11	0.07	0.05	0.26	0.25	0.21	0.00	0.00	0.00	
<b>Total</b>	88.80	88.25	87.89	88.37	87.99	88.60	95.11	92.85	95.80	88.99	89.68	89.57	94.70	94.12	94.73	
<b>Si</b>	0.00	0.01	0.01	0.01	0.00	0.00	0.17	0.21	0.20	0.01	0.00	0.01	0.21	0.21	0.21	
<b>Al</b>	0.00	0.00	0.00	0.00	0.00	0.00	0.01	0.02	0.02	0.00	0.00	0.00	0.03	0.04	0.03	
<b>Ti</b>	0.03	0.03	0.03	0.03	0.02	0.03	0.18	0.16	0.17	0.03	0.03	0.03	0.16	0.16	0.16	
<b>Fe</b>	0.93	0.91	0.91	0.91	0.93	0.94	0.11	0.02	0.01	0.91	0.92	0.91	0.01	0.01	0.01	
<b>Mn</b>	0.00	0.00	0.00	0.00	0.00	0.00	0.01	0.00	0.00	0.00	0.00	0.00	0.00	0.00	0.00	
<b>Mg</b>	0.00	0.00	0.00	0.00	0.00	0.00	0.00	0.00	0.00	0.00	0.00	0.00	0.00	0.00	0.00	
<b>Ca</b>	0.00	0.00	0.00	0.00	0.00	0.00	0.16	0.21	0.21	0.00	0.00	0.00	0.21	0.21	0.21	
<b>Na</b>	0.00	0.00	0.00	0.00	0.00	0.00	0.00	0.00	0.00	0.00	0.00	0.00	0.00	0.00	0.00	
<b>K</b>	0.00	0.00	0.00	0.00	0.00	0.00	0.00	0.00	0.00	0.00	0.00	0.00	0.00	0.00	0.00	
<b>Cr</b>	0.00	0.00	0.00	0.00	0.00	0.00	0.00	0.00	0.00	0.00	0.00	0.00	0.00	0.00	0.00	
<b>Total</b>	0.97	0.96	0.96	0.96	0.97	0.97	0.65	0.62	0.62	0.96	0.97	0.96	0.62	0.62	0.62	

SAMPLE MINERAL Grain # No.	1279								
	Biotite (altered)			Biotite (altered)		Muscovite			
	2			3		4			
	65	66	67	68	69	70	71	72	
<b>SiO2</b>	36.06	36.27	34.67	5.45	20.15	50.28	48.51	50.56	
<b>Al2O3</b>	20.05	20.45	20.21	3.06	12.48	29.68	28.83	29.63	
<b>TiO2</b>	0.00	0.00	0.05	0.89	0.67	0.00	0.00	0.00	
<b>FeO</b>	20.56	18.57	25.97	76.88	50.76	3.17	2.61	2.63	
<b>MnO</b>	0.37	0.33	0.36	0.18	0.39	0.00	0.00	0.00	
<b>MgO</b>	7.55	7.05	7.44	0.85	4.95	1.32	1.17	1.42	
<b>CaO</b>	0.91	1.08	0.79	0.16	0.30	1.05	0.75	0.96	
<b>Na2O</b>	0.05	0.04	0.06	0.14	0.04	0.05	0.07	0.05	
<b>K2O</b>	2.00	2.26	2.01	0.27	1.07	6.86	6.78	7.00	
<b>Cr2O3</b>	0.00	0.00	0.00	0.08	0.00	0.00	0.00	0.00	
<b>Total</b>	87.54	86.04	91.56	87.96	90.80	92.40	88.73	92.25	
<b>Si</b>	0.26	0.26	0.25	0.07	0.18	0.31	0.31	0.31	
<b>Al</b>	0.17	0.18	0.17	0.04	0.13	0.21	0.22	0.21	
<b>Ti</b>	0.00	0.00	0.00	0.01	0.00	0.00	0.00	0.00	
<b>Fe</b>	0.12	0.11	0.15	0.77	0.37	0.02	0.01	0.01	
<b>Mn</b>	0.00	0.00	0.00	0.00	0.00	0.00	0.00	0.00	
<b>Mg</b>	0.08	0.08	0.08	0.02	0.06	0.01	0.01	0.01	
<b>Ca</b>	0.01	0.01	0.01	0.00	0.00	0.01	0.01	0.01	
<b>Na</b>	0.00	0.00	0.00	0.00	0.00	0.00	0.00	0.00	
<b>K</b>	0.02	0.02	0.02	0.00	0.01	0.05	0.06	0.05	
<b>Cr</b>	0.00	0.00	0.00	0.00	0.00	0.00	0.00	0.00	
<b>Total</b>	0.66	0.66	0.68	0.91	0.76	0.61	0.61	0.61	



<b>SAMPLE</b>		<b>1228</b>						
<b>MINERAL</b>	<b>Ti-Fe Oxide (ilmenite)</b>			<b>Fe Oxide</b>		<b>Fe-Ti Oxide</b>		
<b>Grain #</b>	<b>1</b>			<b>2</b>		<b>3</b>		
<b>No.</b>	97	98	99	100	101	102	103	104
<b>SiO2</b>	0.19	0.08	0.12	85.42	95.00	1.46	1.55	1.54
<b>Al2O3</b>	0.27	0.09	0.23	0.07	0.79	0.68	0.79	0.71
<b>TiO2</b>	15.21	50.22	10.55	0.19	0.04	2.09	2.23	2.23
<b>FeO</b>	73.33	41.11	77.14	1.81	0.41	82.22	81.91	81.62
<b>MnO</b>	0.73	1.09	1.28	0.02	0.00	0.35	0.37	0.33
<b>MgO</b>	0.00	0.00	0.00	0.00	0.01	0.00	0.00	0.00
<b>CaO</b>	0.06	0.04	0.06	0.00	0.02	0.17	0.18	0.18
<b>Na2O</b>	0.05	0.02	0.01	0.00	0.07	0.04	0.05	0.06
<b>K2O</b>	0.09	0.07	0.08	0.02	0.19	0.10	0.10	0.10
<b>Cr2O3</b>	0.19	0.18	0.24	0.00	0.00	0.23	0.26	0.25
<b>Total</b>	90.12	92.90	89.72	87.53	96.53	87.34	87.44	87.01
<b>Si</b>	0.00	0.00	0.00	0.49	0.49	0.02	0.02	0.02
<b>Al</b>	0.00	0.00	0.00	0.00	0.00	0.01	0.01	0.01
<b>Ti</b>	0.13	0.34	0.10	0.00	0.00	0.02	0.02	0.02
<b>Fe</b>	0.71	0.31	0.78	0.01	0.00	0.89	0.89	0.89
<b>Mn</b>	0.01	0.01	0.01	0.00	0.00	0.00	0.00	0.00
<b>Mg</b>	0.00	0.00	0.00	0.00	0.00	0.00	0.00	0.00
<b>Ca</b>	0.00	0.00	0.00	0.00	0.00	0.00	0.00	0.00
<b>Na</b>	0.00	0.00	0.00	0.00	0.00	0.00	0.00	0.00
<b>K</b>	0.00	0.00	0.00	0.00	0.00	0.00	0.00	0.00
<b>Cr</b>	0.00	0.00	0.00	0.00	0.00	0.00	0.00	0.00
<b>Total</b>	0.86	0.66	0.90	0.50	0.50	0.96	0.95	0.95

SAMPLE MINERAL Grain #	2567			Albite		
	Fe-Oxide					
No.	1	106	107	3	112	113
<b>SiO2</b>	0.83	2.08	2.04	67.17	67.00	67.45
<b>Al2O3</b>	0.31	0.45	0.61	19.87	20.25	19.94
<b>TiO2</b>	0.63	0.45	0.06	0.00	0.00	0.00
<b>FeO</b>	64.56	81.07	79.44	0.00	0.00	0.06
<b>MnO</b>	0.30	0.31	0.05	0.00	0.00	0.00
<b>MgO</b>	0.02	0.01	0.00	0.00	0.00	0.00
<b>CaO</b>	1.07	0.52	0.31	0.66	0.82	0.74
<b>Na2O</b>	0.05	0.05	0.00	11.32	10.67	11.37
<b>K2O</b>	0.08	0.07	0.06	0.04	0.09	0.01
<b>Cr2O3</b>	0.23	0.24	0.03	0.00	0.00	0.00
<b>Total</b>	68.08	85.24	82.59	99.05	98.83	99.57
<b>Si</b>	0.01	0.03	0.03	0.37	0.37	0.37
<b>Al</b>	0.01	0.01	0.01	0.13	0.13	0.13
<b>Ti</b>	0.01	0.00	0.00	0.00	0.00	0.00
<b>Fe</b>	0.92	0.91	0.92	0.00	0.00	0.00
<b>Mn</b>	0.00	0.00	0.00	0.00	0.00	0.00
<b>Mg</b>	0.00	0.00	0.00	0.00	0.00	0.00
<b>Ca</b>	0.02	0.01	0.00	0.00	0.00	0.00
<b>Na</b>	0.00	0.00	0.00	0.12	0.11	0.12
<b>K</b>	0.00	0.00	0.00	0.00	0.00	0.00
<b>Cr</b>	0.00	0.00	0.00	0.00	0.00	0.00
<b>Total</b>	0.97	0.96	0.97	0.63	0.62	0.63

<b>SAMPLE 2234</b>		<b>Chlorite?</b>			<b>Amphibole pseudomorph</b>						<b>Fe-Oxide</b>	
<b>MINERAL</b>												
<b>Grain #</b>	<b>1</b>			<b>2</b>						<b>3</b>		
<b>No.</b>	124	125	126	127	128	129	130	131	132	133	134	
<b>SiO2</b>	35.99	66.75	65.92	28.04	27.43	27.74	27.05	37.22	26.13	3.74	3.00	
<b>Al2O3</b>	21.64	20.48	20.59	16.22	16.22	16.20	18.28	22.94	17.93	1.38	0.81	
<b>TiO2</b>	0.00	0.00	0.00	0.00	0.00	0.00	0.00	0.08	0.01	0.52	0.35	
<b>FeO</b>	11.79	0.08	0.09	24.90	24.55	24.52	27.21	11.67	28.46	76.63	78.76	
<b>MnO</b>	1.22	0.00	0.00	0.34	0.31	0.30	0.46	0.11	0.41	0.41	0.36	
<b>MgO</b>	17.38	0.23	0.21	16.47	16.33	16.33	13.22	0.08	12.69	0.53	0.11	
<b>CaO</b>	0.35	0.89	1.10	0.07	0.05	0.05	0.13	23.68	0.03	0.49	0.41	
<b>Na2O</b>	0.63	8.26	8.90	0.01	0.01	0.01	0.01	0.01	0.01	0.08	0.06	
<b>K2O</b>	1.01	0.53	0.51	0.03	0.03	0.03	0.03	0.02	0.02	0.07	0.10	
<b>Cr2O3</b>	0.00	0.00	0.00	0.02	0.00	0.00	0.00	0.00	0.02	0.22	0.22	
<b>Total</b>	90.01	97.21	97.31	86.10	84.93	85.19	86.38	95.82	85.70	84.04	84.17	
<b>Si</b>	0.24	0.37	0.37	0.21	0.21	0.21	0.21	0.25	0.21	0.05	0.04	
<b>Al</b>	0.17	0.13	0.14	0.15	0.15	0.15	0.17	0.18	0.17	0.02	0.01	
<b>Ti</b>	0.00	0.00	0.00	0.00	0.00	0.00	0.00	0.00	0.00	0.01	0.00	
<b>Fe</b>	0.07	0.00	0.00	0.16	0.16	0.16	0.18	0.06	0.19	0.83	0.88	
<b>Mn</b>	0.01	0.00	0.00	0.00	0.00	0.00	0.00	0.00	0.00	0.00	0.00	
<b>Mg</b>	0.17	0.00	0.00	0.19	0.19	0.19	0.15	0.00	0.15	0.01	0.00	
<b>Ca</b>	0.00	0.01	0.01	0.00	0.00	0.00	0.00	0.17	0.00	0.01	0.01	
<b>Na</b>	0.01	0.09	0.10	0.00	0.00	0.00	0.00	0.00	0.00	0.00	0.00	
<b>K</b>	0.01	0.00	0.00	0.00	0.00	0.00	0.00	0.00	0.00	0.00	0.00	
<b>Cr</b>	0.00	0.00	0.00	0.00	0.00	0.00	0.00	0.00	0.00	0.00	0.00	
<b>Total</b>	0.68	0.61	0.61	0.71	0.71	0.71	0.71	0.66	0.71	0.94	0.95	

## Appendix C: XRF Results and Error

The portable XRF analyzer was used in this thesis for comparative geochemistry. Three to six points were taken on each clast based on sample homogeneity. Homogeneity was determined by tracing the consistency of three elements for which the instrumental deviation was lowest (Zr, Zn and Ag) during analysis. The mean and standard deviation were then calculated. Elements that deviated less than 10% from the mean were deemed significant and used for geochemical analysis. Samples were selected for the re-run based on standard deviation results of the first run.

The rhyolite standard was used to calibrate both Claremont XRF runs. Standard deviation shows the following elements are comparable between runs: Cl, K, V, Cr, Mn, Fe, Ni, Cu, As, Rb, Sr, Y, Zr, Ba. These elements are shaded in the table below. The standard deviation between the Claremont analyses and MacHattie's results is notably variable. Further statistics are recommended to assess this relationship. A correction calculation was applied by T. MacHattie to the Claremont samples (T. MacHattie, pers. comm.).

The mean results and standard deviation for each sample are presented in below. The mean of both runs is used for elements that were analyzed a second time. The number of point analyses is noted beside the run number (n=x). Elements that are lightly shaded (green in colour) have good standard deviation (<10%) while darkly shaded elements are discarded due to deviation >30%.

**a09-tm-165a***\*good elements (<10% stdev) for Claremont analysis are shaded*

<b>Element</b>	<b>FIRST RUN</b>	<b>RERUN</b>	<b>StDev between runs</b>	<b>StDev (%)</b>	<b>MacHattie</b>	<b>% dev to 1st run</b>	<b>% dev to rerun</b>
<b>Cl</b>	765	753	9	1.1	1002	18.9	20.1
<b>K</b>	55585	53941	1163	2.1	53708	2.4	0.3
<b>Ca</b>	965	1425	326	27.2	963	0.1	27.4
<b>Ti</b>	840	1051	149	15.8	841	0.0	15.7
<b>V</b>	66	66	0	0.0	65	1.1	1.1
<b>Cr</b>	90	85	4	4.3	96	4.2	8.5
<b>Mn</b>	502	521	13	2.6	595	11.9	9.4
<b>Fe</b>	27855	28328	334	1.2	33558	13.1	12.0
<b>Ni</b>	43	41	1	3.4			
<b>Cu</b>	130	129	1	0.5	43	71.1	70.7
<b>Zn</b>	20	17	2	12.2	150	108.1	112.9
<b>As</b>	386	379	5	1.3	5	138.2	138.1
<b>Rb</b>	424	436	8	1.9	348	14.0	15.9
<b>Sr</b>	2239	2242	2	0.1	15	139.5	139.5
<b>Y</b>	185	175	7	3.9	418	54.6	57.9
<b>Zr</b>	64	64	0	0.4	2101	133.1	133.1
<b>Nb</b>		28		0.0	149		96.7
<b>Ag</b>		45		0.0			
<b>Sn</b>	180	370	135	48.9	19	114.4	127.6
<b>Ba</b>	551	568	12	2.2	2	140.4	140.4
<b>Ce</b>		1106		0.0	529		49.9
<b>Pr</b>	23			0.0	61	63.5	
<b>Nd</b>		8		0.0	201		130.1
<b>Pb</b>		26		0.0	16		32.8
<b>Th</b>				0.0	41		

Rhyolite standard a09-tm-165a is used to calibrate both Claremont sample runs. Elements with less than 10% standard deviation are considered good for geochemical analysis. The standard deviation between the Claremont and MacHattie's results are calculated for each of the Claremont runs. Bolded elements are preferred for comparative geochemistry (show less than 10% deviation for both the 1st and 2nd Claremont run).

## Mean Results and Standard Deviation per Sample

<b>2234.0</b>	<b>Rerun</b>	<b>n=3</b>	<b>Initial Run</b>	<b>n=3</b>	<b>TOTAL</b>		
<b>Element</b>	<b>avg</b>	<b>stdev</b>	<b>avg</b>	<b>stdev</b>	<b>MEAN</b>	<b>STDEV</b>	<b>% dev mean</b>
P	0	0	0	0	0	0.0	0.0
S	0	0	1641	112	820	1160.0	141.4
Cl	1706	167	1556	161	1631	106.1	6.5
K	8983	501	7721	400	8352	892.1	10.7
Ca	63703	5606	57968	5505	60836	4055.3	6.7
Ti	11170	1354	10218	35	10694	672.9	6.3
V	164	15	146	12	155	12.5	8.1
Cr	179	36	163	6	171	10.8	6.3
Mn	1874	160	1873	29	1874	0.7	0.0
Fe	103094	20890	85214	3053	94154	12643.3	13.4
Ni	31	3	29	3	30	1.9	6.3
Cu	25	3	18	3	21	4.9	23.4
Zn	98	15	88	2	93	6.6	7.1
As	17	2	14	2	16	2.0	12.8
Rb	23	1	20	2	21	2.0	9.2
Sr	616	57	600	5	608	11.1	1.8
Y	37	4	30	1	33	5.3	16.0
Zr	107	13	93	3	100	9.9	9.9
Nb	13	2	11	2	12	1.4	11.2
Ag	68	5	75	4	71	4.9	7.0
Cd	0	0	0	0	0	0.0	0.0
Sn	13	2	0	0	7	9.4	141.4
Sb	0	0	0	0	0	0.0	0.0
Ba	442	12	426	26	434	11.1	2.6
La	0	0	0	0	0	0.0	0.0
Ce	0	0	89	0	45	62.9	141.4
Pr	132	20	174	2	153	29.5	19.2
Nd	240	69	341	71	291	71.4	24.6
Sm	0	0	0	0	0	0.0	0.0
W	0	0	0	0	0	0.0	0.0
Hg	0	0	9	1	4	6.0	141.4

Pb	0	0	0	0	0	0.0	0.0
Bi	0	0	0	0	0	0.0	0.0
Th	0	0	0	0	0	0.0	0.0
U			0	0	0		0.0
<b>2513.0</b>	<b>Rerun</b>		<b>Initial Run</b>	<b>n=3</b>	<b>TOTAL</b>		
<b>Element</b>	<b>avg</b>	<b>stdev</b>	<b>avg</b>	<b>stdev</b>	<b>MEAN</b>	<b>STDEV</b>	<b>% dev mean</b>
P			0	0	0	0.0	0.0
S			1472	0	1472	0.0	0.0
Cl			1079	148	1079	148.4	13.8
K			4672	559	4672	558.9	12.0
Ca			36182	282	36182	281.8	0.8
Ti			20644	357	20644	357.4	1.7
V			216	12	216	11.6	5.4
Cr			0	0	0	0.0	0.0
Mn			1913	85	1913	85.3	4.5
Fe			115533	9917	115533	9917.5	8.6
Ni			0	0	0	0.0	0.0
Cu			0	0	0	0.0	0.0
Zn			133	5	133	5.3	4.0
As			23	2	23	1.5	6.5
Rb			14	1	14	1.0	7.2
Sr			498	7	498	6.8	1.4
Y			62	4	62	4.4	7.0
Zr			200	4	200	4.4	2.2
Nb			25	2	25	1.9	7.4
Ag			93	11	93	10.6	11.4
Cd			0	0	0	0.0	0.0
Sn			16	2	16	2.0	12.5
Sb			0	0	0	0.0	0.0
Ba			278	33	278	33.3	12.0
La			0	0	0	0.0	0.0
Ce			86	4	86	4.2	4.8



Pr			167	53	167	52.8	31.6
Nd			345	16	345	16.2	4.7
Sm			0	0	0	0.0	0.0
W			0	0	0	0.0	0.0
Hg			11	0	11	0.0	0.0
Pb			13	1	13	0.6	4.6
Bi			0	0	0	0.0	0.0
Th			0	0	0	0.0	0.0
U			0	0	0	0.0	0.0
<b>2549.0</b>	<b>Rerun</b>	<b>n=3</b>	<b>Initial Run</b>	<b>n=5</b>	<b>TOTAL</b>		
<b>Element</b>	<b>avg</b>	<b>stdev</b>	<b>avg</b>	<b>stdev</b>	<b>MEAN</b>	<b>STDEV</b>	<b>% dev mean</b>
P	0	0	0	0	0	0.0	0.0
S	0	0	1303	48	652	921.4	141.4
Cl	1245	72	859	186	1052	272.8	25.9
K	10583	931	9523	986	10053	749.4	7.5
Ca	55875	4272	53340	4748	54607	1792.3	3.3
Ti	5822	859	6211	1664	6017	275.1	4.6
V	94	7	81	9	88	9.0	10.3
Cr	219	56	183	35	201	25.1	12.5
Mn	1607	104	1622	41	1614	10.8	0.7
Fe	43289	5107	50049	12697	46669	4779.5	10.2
Ni	30	3	21	2	25	6.5	26.0
Cu	24	5	23	6	24	0.5	2.2
Zn	68	5	68	5	68	0.0	0.0
As	14	1	15	3	15	0.7	4.9
Rb	31	1	28	3	30	2.4	8.1
Sr	858	89	961	39	909	73.0	8.0
Y	20	2	15	1	17	3.7	21.6
Zr	56	8	49	9	52	5.4	10.4
Nb	7	1	5	1	6	0.9	15.0
Ag	60	7	55	4	57	3.7	6.5
Cd	0	0	0	0	0	0.0	0.0
Sn	11	1	12	3	11	1.1	9.4

Sb	0	0	0	0	0	0.0	0.0
Ba	591	80	491	50	541	70.9	13.1
La	0	0	0	0	0	0.0	0.0
Ce	80	0	0	0	40	56.6	141.4
Pr	182	29	157	18	169	17.3	10.2
Nd	340	103	285	62	313	38.7	12.4
Sm	0	0	0	0	0	0.0	0.0
W	0	0	0	0	0	0.0	0.0
Hg	0	0	8	1	4	5.7	141.4
Pb	0	0	0	0	0	0.0	0.0
Bi	0	0	0	0	0	0.0	0.0
Th	0	0	0	0	0	0.0	0.0
U			0	0	0		0.0
<b>2567.0</b>	<b>Rerun</b>		<b>Initial Run</b>	<b>n=3</b>	<b>TOTAL</b>		
<b>Element</b>	<b>avg</b>	<b>stdev</b>	<b>avg</b>	<b>stdev</b>	<b>MEAN</b>	<b>STDEV</b>	<b>% dev mean</b>
P			0	0	0	0.0	0.0
S			0	0	0	0.0	0.0
Cl			1033	265	1033	264.7	25.6
K			7291	374	7291	374.3	5.1
Ca			61403	3697	61403	3696.6	6.0
Ti			11124	559	11124	558.7	5.0
V			137	4	137	4.0	3.0
Cr			185	44	185	44.1	23.9
Mn			2682	65	2682	65.2	2.4
Fe			76560	7689	76560	7689.3	10.0
Ni			39	0	39	0.0	0.0
Cu			11	0	11	0.0	0.0
Zn			121	9	121	8.7	7.2
As			13	2	13	2.5	18.6
Rb			21	1	21	1.2	5.5
Sr			695	43	695	42.5	6.1
Y			36	1	36	1.4	3.9
Zr			114	8	114	8.0	7.0

Nb			12	1	12	0.6	5.2
Ag			60	8	60	8.1	13.5
Cd			0	0	0	0.0	0.0
Sn			14	0	14	0.0	0.0
Sb			0	0	0	0.0	0.0
Ba			360	10	360	10.0	2.8
La			0	0	0	0.0	0.0
Ce			0	0	0	0.0	0.0
Pr			99	8	99	7.5	7.6
Nd			193	60	193	60.5	31.3
Sm			0	0	0	0.0	0.0
W			0	0	0	0.0	0.0
Hg			9	1	9	0.7	8.3
Pb			0	0	0	0.0	0.0
Bi			0	0	0	0.0	0.0
Th			0	0	0	0.0	0.0
U			0	0	0	0.0	0.0
<b>2567.5</b>	<b>Rerun</b>		<b>Initial Run</b>	<b>n=3</b>	<b>TOTAL</b>		
<b>Element</b>	<b>avg</b>	<b>stdev</b>	<b>avg</b>	<b>stdev</b>	<b>MEAN</b>	<b>STDEV</b>	<b>% dev mean</b>
P			11131	0	11131	0.0	0.0
S			2741	0	2741	0.0	0.0
Cl			902	325	902	324.9	36.0
K			2336	11	2336	10.8	0.5
Ca			68563	1094	68563	1094.0	1.6
Ti			20301	538	20301	537.9	2.6
V			296	36	296	36.1	12.2
Cr			26	0	26	0.0	0.0
Mn			2297	80	2297	79.7	3.5
Fe			103891	1082	103891	1082.3	1.0
Ni			0	0	0	0.0	0.0
Cu			262	273	262	273.2	104.3
Zn			116	1	116	0.6	0.5
As			19	1	19	1.0	5.2

Rb			9	2	9	1.6	18.9
Sr			1027	10	1027	10.4	1.0
Y			59	2	59	2.1	3.5
Zr			172	1	172	1.2	0.7
Nb			20	0	20	0.3	1.3
Ag			115	18	115	17.7	15.4
Cd			0	0	0	0.0	0.0
Sn			15	3	15	3.0	20.0
Sb			0	0	0	0.0	0.0
Ba			2578	561	2578	561.5	21.8
La			0	0	0	0.0	0.0
Ce			0	0	0	0.0	0.0
Pr			83	2	83	2.1	2.6
Nd			196	48	196	47.7	24.3
Sm			0	0	0	0.0	0.0
W			0	0	0	0.0	0.0
Hg			14	2	14	2.1	14.5
Pb			0	0	0	0.0	0.0
Bi			0	0	0	0.0	0.0
Th			0	0	0	0.0	0.0
U			0	0	0	0.0	0.0
<b>BM-003</b>	<b>Rerun</b>	<b>n=3</b>	<b>Initial Run</b>	<b>n=3</b>	<b>TOTAL</b>		
<b>Element</b>	<b>avg</b>	<b>stdev</b>	<b>avg</b>	<b>stdev</b>	<b>MEAN</b>	<b>STDEV</b>	<b>% dev mean</b>
P	0	0	0	0	0	0.0	0.0
S	0	0	832	0	416	588.3	141.4
Cl	0	0	0	0	0	0.0	0.0
K	8872	2130	8299	1529	8585	404.9	4.7
Ca	20671	6793	23326	5422	21999	1877.1	8.5
Ti	4252	389	4350	410	4301	69.5	1.6
V	52	8	50	14	51	1.4	2.8
Cr	76	10	89	6	83	9.4	11.4
Mn	386	71	420	52	403	24.3	6.0
Fe	22772	5988	20760	3928	21766	1423.2	6.5



V			65	3	65	3.1	4.7
Cr			43	7	43	6.6	15.2
Mn			447	18	447	18.1	4.1
Fe			49749	78	49749	78.4	0.2
Ni			32	3	32	3.1	9.6
Cu			13	3	13	3.2	24.1
Zn			84	4	84	3.6	4.3
As			10	2	10	1.5	15.6
Rb			24	1	24	1.4	5.9
Sr			66	2	66	1.7	2.6
Y			51	1	51	1.1	2.2
Zr			244	21	244	20.8	8.5
Nb			16	2	16	2.4	15.0
Ag			58	5	58	5.1	8.9
Cd			0	0	0	0.0	0.0
Sn			10	0	10	0.0	0.0
Sb			0	0	0	0.0	0.0
Ba			170	1	170	0.6	0.3
La			0	0	0	0.0	0.0
Ce			104	9	104	8.7	8.3
Pr			241	27	241	27.1	11.2
Nd			496	88	496	87.7	17.7
Sm			0	0	0	0.0	0.0
W			0	0	0	0.0	0.0
Hg			0	0	0	0.0	0.0
Pb			0	0	0	0.0	0.0
Bi			0	0	0	0.0	0.0
Th			17	2	17	2.1	12.0
U			0	0	0	0.0	0.0
<b>BM-2M</b>	<b>Rerun</b>		<b>Initial Run</b>	<b>n=3</b>	<b>TOTAL</b>		
<b>Element</b>	<b>avg</b>	<b>stdev</b>	<b>avg</b>	<b>stdev</b>	<b>MEAN</b>	<b>STDEV</b>	<b>% dev mean</b>
P			0	0	0	0.0	0.0
S			0	0	0	0.0	0.0

Cl			0	0	0	0.0	0.0
K			13450	166	13450	165.8	1.2
Ca			59609	1007	59609	1006.8	1.7
Ti			3192	66	3192	65.7	2.1
V			48	1	48	1.2	2.4
Cr			69	4	69	4.4	6.3
Mn			777	18	777	17.7	2.3
Fe			21255	975	21255	974.5	4.6
Ni			33	4	33	3.5	10.5
Cu			16	2	16	1.7	10.8
Zn			55	4	55	3.6	6.6
As			9	0	9	0.2	2.6
Rb			54	2	54	1.7	3.2
Sr			289	8	289	8.4	2.9
Y			49	3	49	3.0	6.1
Zr			175	4	175	4.0	2.3
Nb			11	0	11	0.3	2.7
Ag			54	7	54	6.6	12.1
Cd			0	0	0	0.0	0.0
Sn			0	0	0	0.0	0.0
Sb			0	0	0	0.0	0.0
Ba			227	14	227	13.8	6.1
La			0	0	0	0.0	0.0
Ce			106	25	106	24.5	23.2
Pr			291	35	291	35.4	12.2
Nd			525	51	525	51.4	9.8
Sm			0	0	0	0.0	0.0
W			0	0	0	0.0	0.0
Hg			7	0	7	0.0	0.0
Pb			0	0	0	0.0	0.0
Bi			0	0	0	0.0	0.0
Th			12	2	12	1.5	12.4
U			0	0	0	0.0	0.0



<b>BM-4M</b>	<b>Rerun</b>	<b>n=3</b>	<b>Initial Run</b>	<b>n=3</b>	<b>TOTAL</b>		
<b>Element</b>	<b>avg</b>	<b>stdev</b>	<b>avg</b>	<b>stdev</b>	<b>MEAN</b>	<b>STDEV</b>	<b>% dev mean</b>
P	0	0	0	0	0	0.0	0.0
S	0	0	0	0	0	0.0	0.0
Cl	1151	168	0	0	576	814.1	141.4
K	12870	1423	15759	1995	14315	2042.8	14.3
Ca	266147	46453	35140	19459	150643	163346.9	108.4
Ti	2587	276	3550	132	3069	680.7	22.2
V	62	3	58	3	60	2.6	4.3
Cr	70	2	57	10	64	9.4	14.8
Mn	1856	328	816	174	1336	735.6	55.1
Fe	15890	1259	29699	3229	22794	9764.7	42.8
Ni	46	3	42	4	44	3.1	6.9
Cu	17	2	13	2	15	2.4	15.7
Zn	167	9	68	5	118	70.0	59.6
As	38	5	8	1	23	20.9	90.8
Rb	64	9	76	11	70	8.7	12.4
Sr	211	22	114	15	162	68.7	42.3
Y	47	2	23	1	35	16.8	47.7
Zr	126	9	145	5	136	13.9	10.3
Nb	11	1	12	1	11	0.8	7.4
Ag	51	6	43	3	47	5.7	12.1
Cd	0	0	0	0	0	0.0	0.0
Sn	10	0	0	0	5	7.1	141.4
Sb	0	0	0	0	0	0.0	0.0
Ba	310	19	322	36	316	8.5	2.7
La	0	0	0	0	0	0.0	0.0
Ce	164	22	0	0	82	116.0	141.4
Pr	293	49	187	29	240	74.7	31.1
Nd	573	77	363	12	468	149.0	31.8
Sm	0	0	0	0	0	0.0	0.0
W	0	0	0	0	0	0.0	0.0
Hg	0	0	6	0	3	4.2	141.4
Pb	10	0	7	2	8	2.0	24.4
Bi	0	0	0	0	0	0.0	0.0

Th	11	3	12	3	11	0.9	8.3
U			0	0	0		0.0
<b>1170a</b>	<b>Rerun</b>	<b>n=3</b>	<b>Initial Run</b>		<b>TOTAL</b>		
<b>Element</b>	<b>avg</b>	<b>stdev</b>	<b>avg</b>	<b>stdev</b>	<b>MEAN</b>	<b>STDEV</b>	<b>% dev mean</b>
P	0	0			0	0.0	141.4
S	0	0			0	0.0	141.4
Cl	2102	504			2102	504.3	52.5
K	35876	1544			35876	1544.1	10.9
Ca	17131	17524			17131	17523.9	26.6
Ti	1078	41			1078	40.6	20.7
V	31	10			31	9.8	5.8
Cr	29	9			29	8.6	1.9
Mn	451	241			451	241.4	32.0
Fe	10408	3646			10408	3646.4	48.0
Ni	13	2			13	1.9	4.9
Cu	21	3			21	3.1	7.3
Zn	96	20			96	20.5	47.1
As	12	1			12	0.7	8.7
Rb	216	11			216	10.6	12.3
Sr	53	5			53	5.4	19.7
Y	176	17			176	16.6	2.0
Zr	1037	102			1037	102.1	3.4
Nb	72	5			72	4.5	4.2
Ag	37	6			37	6.0	20.8
Cd	0	0			0	0.0	0.0
Sn	11	1			11	0.5	24.7
Sb	0	0			0	0.0	0.0
Ba	68	8			68	8.3	8.0
La	0	0			0	0.0	0.0
Ce	110	36			110	35.9	13.0
Pr	315	34			315	33.7	26.7
Nd	587	38			587	38.1	26.1
Sm	0	0			0	0.0	0.0

W	0	0			0	0.0	0.0
Hg	0	0			0	0.0	0.0
Pb	380	110			380	110.0	24.3
Bi	0	0			0	0.0	0.0
Th	24	6			24	6.5	18.6
U							0.0
<b>1228.0</b>	<b>Rerun</b>	<b>n=3</b>	<b>Initial Run</b>	<b>n=3</b>	<b>TOTAL</b>		
<b>Element</b>	<b>avg</b>	<b>stdev</b>	<b>avg</b>	<b>stdev</b>	<b>MEAN</b>	<b>STDEV</b>	<b>% dev mean</b>
P	0	0	0	0	0	0.0	0.0
S	0	0	620	0	310	438.4	141.4
Cl	7616	3855	266	0	3941	5197.5	131.9
K	14045	4292	13862	550	13954	129.4	0.9
Ca	758	590	525	73	642	164.8	25.7
Ti	1220	602	501	31	861	508.4	59.1
V	22	5	18	2	20	3.3	16.2
Cr	0	0	0	0	0	0.0	0.0
Mn	92	13	71	2	81	14.6	18.0
Fe	13207	2497	13244	471	13225	26.2	0.2
Ni			0	0	0		0.0
Cu	13	3	13	4	13	0.1	0.9
Zn	93	6	85	7	89	5.7	6.4
As	10	1	10	1	10	0.1	1.4
Rb	89	8	83	4	86	4.1	4.7
Sr	66	2	68	2	67	1.6	2.4
Y	49	9	44	5	46	3.1	6.6
Zr	294	25	298	3	296	3.1	1.0
Nb	90	10	84	1	87	4.6	5.3
Ag	21	3	26	5	24	3.5	15.0
Cd	0	0	0	0	0	0.0	0.0
Sn	0	0	0	0	0	0.0	0.0
Sb	0	0	0	0	0	0.0	0.0
Ba	71	5	48	2	59	16.0	27.0

La	0	0	0	0	0	0.0	0.0
Ce	0	0	0	0	0	0.0	0.0
Pr	181	30	208	22	195	19.1	9.8
Nd	293	66	380	31	336	61.3	18.2
Sm	0	0	0	0	0	0.0	0.0
W	0	0	0	0	0	0.0	0.0
Hg	0	0	0	0	0	0.0	0.0
Pb	5	0	0	0	3	3.6	141.4
Bi	0	0	0	0	0	0.0	0.0
Th	20	2	22	3	21	1.6	7.9
U			0	0	0		0.0
<b>1232a</b>	<b>Rerun</b>	<b>n=3</b>	<b>Initial Run</b>	<b>n=4</b>	<b>TOTAL</b>		
<b>Element</b>	<b>avg</b>	<b>stdev</b>	<b>avg</b>	<b>stdev</b>	<b>MEAN</b>	<b>STDEV</b>	<b>% dev mean</b>
P	0	0	0	0	0	0.0	0.0
S	0	0	0	0	0	0.0	0.0
Cl	1821	130	6412	4384	4116	3246.2	78.9
K	29711	1899	26216	2722	27963	2471.7	8.8
Ca	1049	208	567	182	808	341.2	42.2
Ti	608	99	496	76	552	79.3	14.4
V	18	1	17	5	18	0.7	4.0
Cr	0	0	7	0	4	4.9	141.4
Mn	126	14	118	27	122	5.8	4.8
Fe	10679	2291	10126	2412	10403	391.1	3.8
Ni	12	1	13	0	13	0.7	5.7
Cu	38	14	31	22	34	5.1	14.9
Zn	63	6	60	16	61	1.7	2.8
As	10	3	9	1	10	0.7	6.8
Rb	126	5	121	10	123	3.5	2.8
Sr	58	6	52	5	55	4.4	8.0
Y	81	17	73	22	77	5.3	6.9
Zr	238	49	216	46	227	15.8	7.0
Nb	81	20	78	11	80	2.1	2.7
Ag	23	6	19	10	21	3.2	15.3

Cd	0	0	0	0	0	0.0	0.0
Sn	14	3	11	1	13	2.4	18.6
Sb	0	0	0	0	0	0.0	0.0
Ba	80	15	80	5	80	0.1	0.1
La	0	0	0	0	0	0.0	0.0
Ce	0	0	0	0	0	0.0	0.0
Pr	216	15	157	60	186	42.3	22.7
Nd	371	24	304	103	338	47.8	14.2
Sm	0	0	0	0	0	0.0	0.0
W	0	0	0	0	0	0.0	0.0
Hg	0	0	0	0	0	0.0	0.0
Pb	7	1	9	0	8	1.3	17.8
Bi	0	0	0	0	0	0.0	0.0
Th	22	9	23	4	22	0.8	3.4
U			0	0	0		0.0

--	--	--	--	--	--	--	--

<b>1232b</b>	<b>Rerun</b>		<b>Initial Run</b>	<b>n=4</b>	<b>TOTAL</b>		
<b>Element</b>	<b>avg</b>	<b>stdev</b>	<b>avg</b>	<b>stdev</b>	<b>MEAN</b>	<b>STDEV</b>	<b>% dev mean</b>
P			0	0	0	0.0	0.0
S			0	0	0	0.0	0.0
Cl			33236	2718	33236	2717.9	8.2
K			13937	761	13937	761.2	5.5
Ca			543	96	543	95.8	17.6
Ti			589	17	589	17.3	2.9
V			18	2	18	1.7	9.3
Cr			0	0	0	0.0	0.0
Mn			153	9	153	9.1	5.9
Fe			14796	1404	14796	1403.6	9.5
Ni			0	0	0	0.0	0.0
Cu			14	5	14	4.6	32.7
Zn			60	2	60	1.5	2.5
As			10	0	10	0.3	3.0
Rb			100	1	100	0.7	0.7
Sr			118	4	118	3.8	3.3

Y			44	2	44	2.5	5.6
Zr			272	8	272	8.4	3.1
Nb			77	7	77	6.8	8.8
Ag			35	3	35	2.6	7.6
Cd			0	0	0	0.0	0.0
Sn			13	2	13	2.1	17.0
Sb			0	0	0	0.0	0.0
Ba			169	6	169	6.2	3.7
La			48	0	48	0.0	0.0
Ce			0	0	0	0.0	0.0
Pr			200	17	200	17.2	8.6
Nd			394	27	394	27.2	6.9
Sm			0	0	0	0.0	0.0
W			0	0	0	0.0	0.0
Hg			7	0	7	0.0	0.0
Pb			14	3	14	3.0	21.1
Bi			0	0	0	0.0	0.0
Th			20	1	20	1.0	5.0
U			0	0	0	0.0	0.0

--	--	--	--	--	--	--	--

<b>1237.0</b>	<b>Rerun</b>	<b>n=3</b>	<b>Initial Run</b>	<b>n=6</b>	<b>TOTAL</b>		
<b>Element</b>	<b>avg</b>	<b>stdev</b>	<b>avg</b>	<b>stdev</b>	<b>MEAN</b>	<b>STDEV</b>	<b>% dev mean</b>
P	0	0	4758	156	2379	3364.4	141.4
S	0	0	801	0	401	566.4	141.4
Cl	420	32	1201	129	810	552.0	68.1
K	29735	1055	29235	1763	29485	354.0	1.2
Ca	729	203	833	260	781	73.2	9.4
Ti	672	61	667	106	669	3.4	0.5
V	41	3	30	6	35	7.8	22.2
Cr	22	3	23	8	22	0.9	4.3
Mn	104	3	118	8	111	9.7	8.7
Fe	19441	2493	20164	2910	19802	511.4	2.6
Ni	16	4	15	3	16	0.5	3.0
Cu	21	5	15	3	18	4.2	23.6

Zn	72	7	75	11	74	2.4	3.2
As	12	1	11	2	11	0.4	3.1
Rb	171	7	170	11	171	0.9	0.5
Sr	24	0	25	3	25	1.3	5.3
Y	201	6	199	13	200	1.8	0.9
Zr	829	11	829	39	829	0.1	0.0
Nb	90	11	82	19	86	5.2	6.0
Ag	28	5	35	7	32	4.9	15.4
Cd	0	0	0	0	0	0.0	0.0
Sn	15	4	13	2	14	1.6	11.2
Sb	0	0	0	0	0	0.0	0.0
Ba	40	1	44	7	42	3.1	7.3
La	0	0	0	0	0	0.0	0.0
Ce	77	9	76	8	76	0.6	0.8
Pr	299	33	337	17	318	26.8	8.4
Nd	578	6	618	53	598	28.3	4.7
Sm	0	0	0	0	0	0.0	0.0
W	0	0	0	0	0	0.0	0.0
Hg	0	0	7	1	4	5.2	141.4
Pb	0	0	0	0	0	0.0	0.0
Bi	0	0	0	0	0	0.0	0.0
Th	24	1	19	2	22	3.4	15.8
U			0	0	0		0.0
<b>1279.0</b>	<b>Rerun</b>	<b>n=3</b>	<b>Initial Run</b>	<b>n=3</b>	<b>TOTAL</b>		
<b>Element</b>	<b>avg</b>	<b>stdev</b>	<b>avg</b>	<b>stdev</b>	<b>MEAN</b>	<b>STDEV</b>	<b>% dev mean</b>
P	0	0	0	0	0	0.0	0.0
S	0	0	0	0	0	0.0	0.0
Cl	6609	2401	1573	468	4091	3561.0	87.0
K	22609	4334	27910	853	25260	3748.4	14.8
Ca	956	122	1543	185	1250	414.6	33.2
Ti	1248	174	2289	366	1769	736.1	41.6
V	59	5	59	10	59	0.2	0.4
Cr	31	8	21	7	26	6.8	26.5



Mn	170	10	264	53	217	66.5	30.6
Fe	11782	922	24966	4794	18374	9323.0	50.7
Ni	12	1	13	1	12	0.7	5.9
Cu	15	2	25	5	20	7.1	36.0
Zn	106	3	119	10	113	9.7	8.6
As	14	3	14	2	14	0.1	0.9
Rb	150	5	144	0	147	4.0	2.7
Sr	94	6	94	3	94	0.4	0.5
Y	54	5	53	2	53	1.2	2.3
Zr	350	6	385	4	368	25.0	6.8
Nb	51	3	52	3	52	0.4	0.7
Ag	21	5	44	5	32	16.6	51.5
Cd	0	0	0	0	0	0.0	0.0
Sn	10	0	12	1	11	1.2	10.9
Sb	0	0	0	0	0	0.0	0.0
Ba	448	3	425	8	437	16.5	3.8
La	0	0	0	0	0	0.0	0.0
Ce	104	4	99	10	101	3.3	3.3
Pr	114	34	192	27	153	55.4	36.2
Nd	227	110	416	59	322	133.6	41.5
Sm	0	0	0	0	0	0.0	0.0
W	0	0	0	0	0	0.0	0.0
Hg	0	0	6	0	3	4.3	141.4
Pb	7	1	11	0	9	2.7	31.0
Bi	0	0	0	0	0	0.0	0.0
Th	22	5	21	7	22	0.7	3.2
U			0	0	0		0.0
<b>1819.0</b>	<b>Rerun</b>		<b>Initial Run</b>	<b>n=3</b>	<b>TOTAL</b>		
<b>Element</b>	<b>avg</b>	<b>stdev</b>	<b>avg</b>	<b>stdev</b>	<b>MEAN</b>	<b>STDEV</b>	<b>% dev mean</b>
P			0	0	0	0.0	0.0
S			0	0	0	0.0	0.0
Cl			5819	190	5819	189.6	3.3
K			3330	85	3330	84.9	2.5

Ca			56610	3626	56610	3625.8	6.4
Ti			17598	80	17598	79.8	0.5
V			191	2	191	2.0	1.0
Cr			0	0	0	0.0	0.0
Mn			1655	42	1655	41.9	2.5
Fe			95963	4310	95963	4309.8	4.5
Ni			0	0	0	0.0	0.0
Cu			18	5	18	4.9	28.3
Zn			96	3	96	2.6	2.8
As			16	2	16	1.8	11.6
Rb			8	2	8	2.0	24.9
Sr			513	8	513	7.8	1.5
Y			49	4	49	3.8	7.8
Zr			164	8	164	7.6	4.7
Nb			22	2	22	1.6	7.4
Ag			85	7	85	7.2	8.5
Cd			0	0	0	0.0	0.0
Sn			16	0	16	0.0	0.0
Sb			0	0	0	0.0	0.0
Ba			238	13	238	13.3	5.6
La			0	0	0	0.0	0.0
Ce			102	4	102	4.4	4.3
Pr			186	27	186	27.2	14.6
Nd			412	25	412	24.8	6.0
Sm			0	0	0	0.0	0.0
W			0	0	0	0.0	0.0
Hg			12	3	12	3.1	26.2
Pb			0	0	0	0.0	0.0
Bi			0	0	0	0.0	0.0
Th			0	0	0	0.0	0.0
U			0	0	0	0.0	0.0
<b>2060c</b>	<b>Rerun</b>		<b>Initial Run</b>	<b>n=3</b>	<b>TOTAL</b>		
<b>Element</b>	<b>avg</b>	<b>stdev</b>	<b>avg</b>	<b>stdev</b>	<b>MEAN</b>	<b>STDEV</b>	<b>% dev mean</b>
P			0	0	0	0.0	0.0

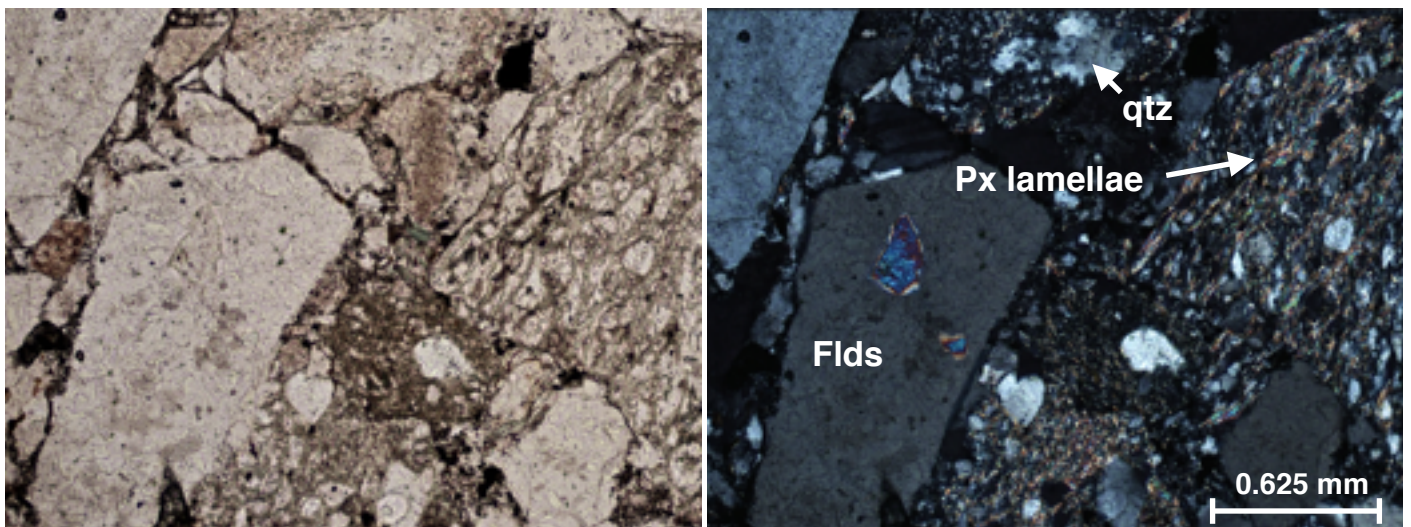
S			0	0	0	0.0	0.0
Cl			360	0	360	0.0	3.3
K			14364	847	14364	847.1	2.5
Ca			29757	14500	29757	14499.9	6.4
Ti			4155	200	4155	200.1	0.5
V			68	4	68	4.2	1.0
Cr			58	2	58	2.1	0.0
Mn			608	57	608	57.3	2.5
Fe			34466	981	34466	981.5	4.5
Ni			38	5	38	4.9	0.0
Cu			18	2	18	2.1	28.3
Zn			73	2	73	2.1	2.8
As			9	0	9	0.4	11.6
Rb			73	1	73	0.9	24.9
Sr			85	2	85	1.8	1.5
Y			26	1	26	1.4	7.8
Zr			139	2	139	2.1	4.7
Nb			14	1	14	1.3	7.4
Ag			55	3	55	2.8	8.5
Cd			0	0	0	0.0	0.0
Sn			0	0	0	0.0	0.0
Sb			0	0	0	0.0	0.0
Ba			311	12	311	12.0	5.6
La			0	0	0	0.0	0.0
Ce			0	0	0	0.0	4.3
Pr			247	14	247	14.1	14.6
Nd			433	45	433	45.3	6.0
Sm			0	0	0	0.0	0.0
W			0	0	0	0.0	0.0
Hg			0	0	0	0.0	26.2
Pb			0	0	0	0.0	0.0
Bi			0	0	0	0.0	0.0
Th			11	0	11	0.0	0.0
U			0	0	0	0.0	0.0

## Appendix E: Anomalous Samples

Four Claremont samples were deemed anomalous and excluded from the results and discussion of this thesis. Reasons for exclusion and XRF results are presented below. All anomalous samples were collected from the core randomly.

**Sample 1315.5** was excluded due to poor geochemical results (despite XRF rerun). The hand sample of the clast is highly weathered.

**Sample 1180.5** was excluded due to considerable geochemical deviation from the rest of the Claremont clasts. This clast is composed of lithic fragments.

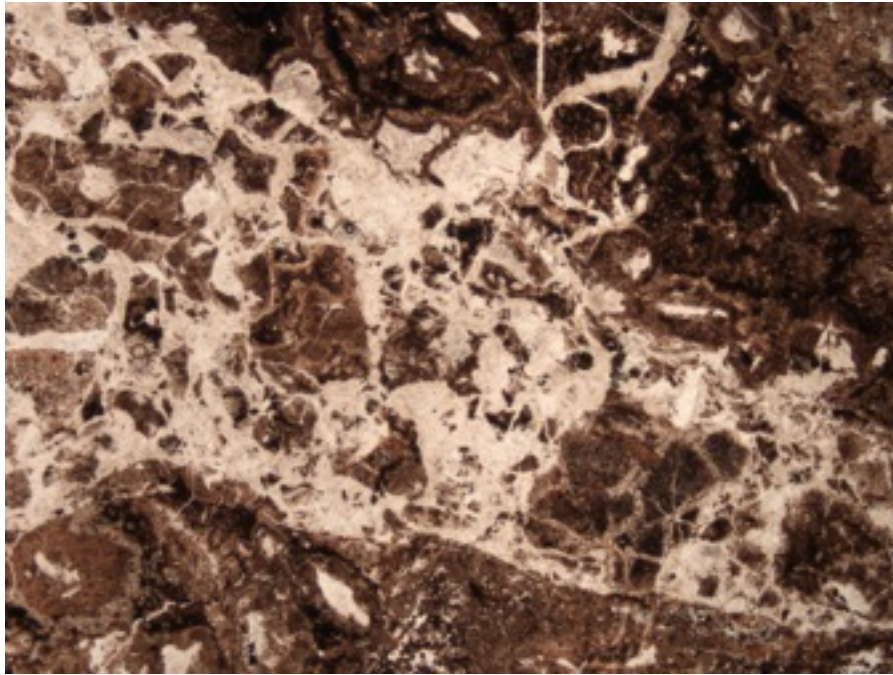


Sample 1180.5: Px lamellae in basalt fragments, recrystallized qtz, px inclusions in flds. (PPL, XPL)

**Sample 2236.5** was excluded because of anomalous petrography. The clast is extremely altered.

Petrography for this clast is unique. It is suspect dyke material (T. MacHattie, pers. comm.).

**Sample 1256.2** was excluded due to high alteration revealed by petrography.



Sample 1256.2a: highly altered, brecciated clast. PPL. FOV: 10.5 mm.

### Petrography of Anomalous Samples

<b>1180.5</b>	lithic fragments foliated clasts recrystallization (qtz) <i>lithic arenite?</i>	qtz microcline plg oxides amphibole	chl ht
<b>1256.2</b>	brecciated spherulite <i>*highly altered</i>	plg flds bt qtz oxides	ht spt?
<b>1315.5</b>	inequigranular interlocking skeletal structure (opaque) <i>*highly weathered</i>	plg bt px hb opaque mineral	ca
<b>2236.5</b>	porphyritic phenocryst clusters sericitization pseudomorphism	plg opaque (mgt?) qtz bt apatite	glass chl ser

